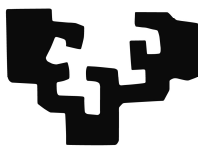


eman ta zabal zazu



Universidad  
del País Vasco

Euskal Herriko  
Unibertsitatea

**“Novel strategies for the preparation of  $^{13}\text{N}$ -  
labelled compounds: Synthesis of  $^{13}\text{N}$ -labelled  
Aromatic azides, triazoles and tetrazoles”**

PhD Thesis

**SAMEER JOSHI**

**San Sebastian,**

**March 2017**





eman ta zabal zazu



Universidad  
del País Vasco

Euskal Herriko  
Unibertsitatea

# **“Novel strategies for the preparation of $^{13}\text{N}$ -labelled compounds: Synthesis of $^{13}\text{N}$ -labelled Aromatic azides, triazoles and tetrazoles”**

A Dissertation Submitted to the Department of Organic Chemistry  
Of University of the Basque Country (UPV/EHU),  
For the degree of DOCTOR OF PHILOSOPHY

By

**SAMEER JOSHI**

Thesis Supervisor: Dr. Jordi Llop Roig  
University Tutor: Prof. Esther Lete

Donostia-San Sebastian, Spain

2017



*This thesis has been carried out in the Radiochemistry and Nuclear Imaging Laboratory of the Centro de Investigación Cooperativa en Biomateriales (CIC biomaGUNE). The research was financially supported by the project RADIOMI (EU FP7-PEOPLE-2012-ITN-RADIOMI).*



First of all, I would like to express my thanks to Professor Dr. Manuel Martin Lomas and Professor Dr. Luis Liz Marzan, former and current scientific directors of CIC biomaGUNE, respectively, for giving me the opportunity to develop the experimental work of this PhD in the outstanding facilities of the Centre. Thanks for the precious opportunity to get familiar with such an amount of diverse equipment in a multi-disciplinary, multi-cultural environment.

I express my deep sense of gratitude to my research supervisor Dr. Jordi Llop, for giving me such a wonderful opportunity to carry out PhD thesis under his supervision, teaching me many things about this fascinating field. Thanks for his continuous support throughout my doctoral studies and related research, for his patience, motivation, and immense knowledge. His guidance helped me in all the time of research and writing of this thesis. I could not have imagined having a better advisor and mentor for my PhD study, who directed me in the right path while giving the freedom to explore on my own. Apart from research, he is very nice human being. He is a role model for many students including me. I would love to be as good as him or somehow close to him in the future. I will remember all my life his special words in the lab for motivating students saying "EXCELLENT". As a result, there is always a positive energy inside the lab.

Besides my advisor, I am especially grateful to Dr. Vanessa Gomez for her continuous support from the beginning of my stay here. Also thanks for her encouraging words and help during the experimental work in the lab.

I am indebted to my tutor Prof. Dr. Esther Lete from the University of Basque country, Spain.

I take this moment to shower my words of gratitude to all my past and present colleagues in the group, Zurine, Carlos, Maria, Enrique, Vijay, Mikel Errasti, Mikel Gonzalez, Aitor, Larraitz, Beatriz, Kiran, Jaya, Eunice, Luis, Victor, Luka, Unai, Xabier, Olatz, Angel, Krishna, and Marcos for tremendous support in radiochemistry lab as well as for wonderful moments outside the laboratory, during my stay in San Sebastian. Thanks to all for cheering me and helping me all the time. I will never forget personal hospitality during my stay in San Sebastian.

The past three years I spent here, are certainly the best days in my life, I never felt away from home and each & every one of you are the reason for that, Thank you all.

I thank Dr. Javier Calvo Martinez for his support and fruitful discussion regarding the mass spectrometry and also Dr. Daniel Padro and Sandra Plaza for their help in NMR studies.

I wish to thank Eneko San Sebastian and Boguslaw Szczupak for keeping the PET-CT and other imaging instruments running.

I thank to Dr. Torsten Reese and Egoitz. Also thanks to people of animal lab, Ainhoa and Ander for their support during animal studies. I would also like to thank Abraham for his support. I thank to Nerea, Begoña, Anna and Julie for their help in microwave studies.

I would also like to thank all the people of administration, maintenance and other supporting departments. It's my pleasure to thank all the people at CIC biomaGUNE for their great hospitality, always being friendly and creating a nice atmosphere in the institute.

I would like to thank Prof. Clara Vinas, Prof. Francesc Teixidor and Dr. Jacek Koziarowski for their fruitful discussions during conducting experimental work, and Prof. Fernando Cossio and Dr. Abel De Cozar for their collaborative work on computational studies for the preparation of azide.

I am also grateful to many supervisors in the past, Dr. Jyoti Salvekar, Dr. Rajashree Kashalkar, Dr. Date from Sir Parashurambhau College, Pune, India. I would like to give my sincere thanks to Dr. Ramesh Joshi, Dr. Rohini Joshi and Dr. Shashikant Joshi from National chemical laboratory (NCL), Pune, India for their guidance, encouragement, and unfailing support.

I would like to give my sincere thanks to Dr. Chandrashekhar V. Rode for his precious support, guidance, and motivation along with Dr. Rasika Mane for their collaborative work on tetrazole.

I wish to express my sincere thanks to all of my colleagues from previous lab of NCL and Sai Lifesciences, Pune, India. Especially thanks to Sanjay, Sachin, Suhas, Dharmendra, Amit, Chetana, Laxman and Mukulesh.

My sincere thanks also goes to Prof. Dr. Antony Gee, Prof. Dr. Olof Solin, Prof. Dr. Albert Windhorst, Dr. Pal Mikecz, Dr. Didier Le Bars, Dr. Davide Camporese, Prof. Dr. Christer Halldin, Prof. Dr. Andre Luxen, Prof. Dr. Victor Pike and Dr. Sajinder Luthra for the stimulating discussion and also their insightful comments and encouragement, but also for the hard questions which incited me to widen my research from various perspectives.

In particular, I am grateful to Prof. Dr. Veronique Gouverneur for enlightening me the first glance of research and accepting me as a visiting student for two months collaborative work in University of Oxford. Many thanks to Dr. Pavlina Schmitz for her help and valuable support during past three years. Thanks to Dr. Sean Preshlock for his support in Oxford.



I thank my project fellows Lukas, Gregor, Yanlan, Francesco, Carlotta, Thomas, Anna, Ulrike, Aleksandra, Ana, Ture, Ermal, Nagesh, Dr. Anna and Dr. Giulia for their productive discussions and memorable days during meetings, seminars, school and conference.

I would also like to thank all the people of administration, maintenance and others from La Salle residence including Paola, Keppa, Aitor, Nickolas, Begoña and Manuel during my stay in San Sebastian. I would like to thank Nickolas, Paolin, Aiccha, Luca, Karen, Jakub, Mauricio, Ignacio, Manuel, Carlos, Oscar, Vladimir and Fathi for nice memorable days. I also take this opportunity to thank my entire Indian community that I met here in Donostia. Musthafa, Subir, Manoj, Ameen, Mohan-Shanthi, Sudam-Pallavi, Ravi-Garima. I feel very fortunate to meet them all here.

This is the time to thank my Indian friends, who supported me throughout these days from India, Kiran, Vishal, Sukruta, Ashutosh, Dheeraj, Vaibhav, Sagar and all my PG and Bachelor friends. I would like to thank all my well-wishers, my teachers, my friends, colleagues. Special thanks to my sister Madhura and her husband Nilesh for their continuous support.

Last but not the least; I take the opportunity to thank to my mother **Aai** and father **Baba** for supporting me spiritually throughout writing this thesis and my life in general.

At the end of my thesis I would like to thank all those several peoples knowingly and unknowingly helped me in the successful completion of this thesis.

*All the work presented in this PhD thesis has been funded by the project FP7-PEOPLE-RADIOMI (project reference: 316882).*



## ABSTRACT

The main focus of the current PhD thesis is to develop novel strategies for the preparation of  $^{13}\text{N}$ -labelled radiotracers, which might potentially be used in the future as probes with application in the field of *in vivo* imaging.

During the last decades, a plethora of radiotracers labelled with different positron emitters for the *in vivo* visualization of biological, physiological or pathological processes using Positron Emission Tomography (PET) have been developed and reported in the literature. Most of these tracers are labelled with Fluorine-18 ( $^{18}\text{F}$ ), Carbon-11 ( $^{11}\text{C}$ ), Gallium-68 ( $^{68}\text{Ga}$ ), Copper-64 ( $^{64}\text{Cu}$ ) or Zirconium-89 ( $^{89}\text{Zr}$ ). However, the use of Nitrogen-13 has been restricted mainly due to its short half-life (9.97 min). Despite this drawback, Nitrogen is present in the majority of biologically active molecules. Hence, the incorporation of the positron emitter  $^{13}\text{N}$  to the toolbox of PET chemists would represent a unique opportunity to label a wide variety of molecules in different positions, or to prepare radiolabelled molecules for which incorporation of the above mentioned longer-lived positron emitters is challenging or impossible.

The work performed in this PhD thesis has been divided in three main parts. First, a method for the preparation of  $^{13}\text{N}$ -labelled aromatic azides was developed. After identification of potential synthetic routes, the most convenient one (based on the reaction of aromatic diazonium salts with hydrazoic acid) was selected. Different experimental approaches were tackled in order to gain knowledge regarding the precise mechanism of the reaction, which ultimately enabled the selection of the optimal experimental design. Experimental results combined with computational studies provided unambiguous information to elucidate the reaction mechanism, which occurs *via* acyclic zwitterionic intermediates.

The second part of the PhD thesis focused on the development of synthetic strategies for the preparation of  $^{13}\text{N}$ -labelled triazoles *via* (3+2) Huisgen cycloaddition, by reaction of labelled azides (labelled precursor) with alkynes and aldehydes. The experimental conditions were optimized and the methodology was applied to the preparation of different  $^{13}\text{N}$ -labelled triazoles. A short library of compounds could be synthesized, including one specific molecule with potential application as  $\beta$ -amyloid marker. The procedure for the preparation of this compound was fully automated using one of the synthetic boxes currently available at CIC biomaGUNE.

The last part of this PhD thesis pursued the preparation of  $^{13}\text{N}$ -labelled tetrazoles by reaction of the labelled azides with nitriles. However, this reaction is very slow under non-

radioactive conditions, and requires the use of a catalyst. Because the catalysts reported in the literature were anticipated not to be convenient in radioactive conditions, novel nanostructured, copper-based heterogeneous catalysts were developed and tested in a small library of tetrazoles in cold conditions. After optimization of the experimental conditions and selection of the most promising catalyst, one selected tetrazole was labelled with Nitrogen-13.

## RESUMEN

La Tomografía por Emisión de Positrones (PET) es una técnica de imagen molecular que permite conocer, de manera mínimamente invasiva y prácticamente a tiempo real, la distribución espacio-temporal de un radiotrazador marcado con un isótopo emisor de positrones tras su administración a un organismo vivo. Entre las aplicaciones de la PET en el entorno clínico destacan el diagnóstico precoz, la evaluación de la respuesta al tratamiento y el desarrollo de nuevos fármacos. En el entorno pre-clínico, supone una herramienta fundamental para afrontar cuestiones biológicas y fisiológicas inabordables mediante otras técnicas y puede contribuir a la elucidación mecanística de ciertos procesos biológicos o patológicos.

La aplicación de la PET va asociada al uso de un radiotrazador marcado con un isótopo emisor de positrones. Dichos isótopos (por ejemplo,  $^{18}\text{F}$ ,  $^{11}\text{C}$ ,  $^{13}\text{N}$ ,  $^{15}\text{O}$ ) pueden generarse utilizando ciclotrones biomédicos comerciales y presentan períodos de semidesintegración cortos. Tradicionalmente, la mayoría de los grupos de investigación han centrado sus esfuerzos en el desarrollo de radiotrazadores marcados con Flúor-18, cuya vida media de 109.8 minutos permite su distribución desde unidades de producción centralizadas a centros satélite, y con Carbono-11, ya que su vida media no es extremadamente corta (20.4 minutos) y las formas químicas en las que puede obtenerse ( $[^{11}\text{C}]\text{CO}_2$ ,  $[^{11}\text{C}]\text{CH}_4$ ) presentan una elevada versatilidad sintética. El uso de otros radionucleidos de vida media más corta (por ejemplo Nitrógeno-13,  $T_{1/2}=9.97$  minutos) se ha visto históricamente muy restringido y no hay prácticamente trabajos publicados relacionados con el desarrollo de estrategias sintéticas con estos isótopos.

La reciente salida al mercado de pequeños ciclotrones más económicos, de menor tamaño y que permiten producir cantidades moderadas de isótopos emisores de positrones, unida a la recientemente emergente tecnología de microfluidos y su aplicación al área de la radioquímica (su eficacia ha sido probada en procesos químicos en los que intervienen isótopos PET como  $^{18}\text{F}$  y  $^{11}\text{C}$ ), podrían cambiar en los próximos años el panorama de la imagen PET desde la situación actual hacia un escenario en el que los radiotrazadores se producirían *in situ*, en pequeños lotes y bajo el criterio “dosis bajo demanda” (una producción para un estudio). En este contexto, cobrarían importancia los radionucleidos de vida media más corta, por ejemplo el Nitrógeno-13, resultando fundamental el desarrollo de nuevas estrategias sintéticas que permitan preparar radiotrazadores marcados con estos isótopos de manera eficiente, rápida y reproducible. Hasta la fecha, tan sólo se han descrito unas pocas estrategias sintéticas para la incorporación de este radioisótopo a moléculas bioactivas.

Durante la última década, el grupo de Radioquímica e Imagen Nuclear de CIC biomaGUNE, liderado por el Dr. Llop y en el cual se ha llevado a cabo la presente tesis doctoral, ha desarrollado nuevas estrategias sintéticas para la radiosíntesis de aminoácidos marcados con  $^{13}\text{N}$ , a través de reacciones enzimáticas y utilizando  $[^{13}\text{N}]\text{NH}_3$  como agente de marcaje. Se ha propuesto un nuevo método para la reducción química y biocatalizada de  $[^{13}\text{N}]\text{NO}_3^-$  a  $[^{13}\text{N}]\text{NO}_2^-$ , donde además se ha demostrado que el uso de  $[^{13}\text{N}]\text{NO}_2^-$  como agente de marcaje es útil para la radiosíntesis de  $[^{13}\text{N}]$ nitrosaminas,  $[^{13}\text{N}]$ nitrosotioles y derivados  $[^{13}\text{N}]$ azo.

En esta tesis doctoral, el trabajo experimental se ha centrado en el desarrollo de nuevas estrategias para la preparación de compuestos marcados con  $^{13}\text{N}$  utilizando  $[^{13}\text{N}]\text{NO}_2^-$  como agente de marcaje, y el trabajo se ha dividido en tres partes, que corresponden a los capítulos 3, 4 y 5 del presente documento.

La primera parte del trabajo (**capítulo 3**) consistía en desarrollar estrategias sintéticas para la preparación de arilazidas marcadas con  $^{13}\text{N}$ , que posteriormente pudieran ser utilizadas como sintones para la preparación de moléculas más complejas. Con este objetivo, se propuso una metodología sintética para la preparación de azidas marcadas con  $^{13}\text{N}$ . En primera instancia, se consideró la posibilidad de utilizar la reacción de Dutt-Wormall. Este método funciona muy bien en condiciones no radiactivas e implica la hidrólisis básica de un diazoaminosulfonato aromático, pudiéndose sintetizar fácilmente a partir de sal de diazonio aromático y alquil- o aril-sulfonamida. De este modo, se abordó la síntesis de fenilazida marcada con  $^{13}\text{N}$  mediante la reacción de Dutt-Wormall en 2 pasos (Figura 1): (i) Adición de  $[^{13}\text{N}]\text{NO}_2^-$  a una solución de anilina (0.25 mmol) en HCl frío (0.1 ml de HCl al 37% en 0.15 ml de agua),  $t=4$  min,  $T = 0^\circ\text{C}$ ; y (ii) tras extracción con diclorometano para eliminar el exceso de anilina, la fase acuosa de la mezcla de reacción se añadió gota a gota a un vial precargado con una solución fría de *p*-toluensulfonamida (0.25 mmol) en NaOH (1.60 Mmol en 1 ml de agua,  $t = 1$  min,  $T = 0^\circ\text{C}$ ).

El método presentado en la Figura 1 presentaba ciertas limitaciones, por ejemplo la necesidad de dos etapas de purificación mediante extracción líquido-líquido, que son complejas de implementar en el entorno radiactivo. En consecuencia se exploraron alternativas más convenientes. De este modo, se encontró un método para la formación de fenilazidas basado en la reacción de sales de diazonio con ácido hidrazóico generado *in situ* (por reacción de monohidrato de hidrazina con nitrito de sodio en medio ácido). Este método fue abordado siguiendo dos rutas diferentes, esquematizadas como A y B en la Figura 2.

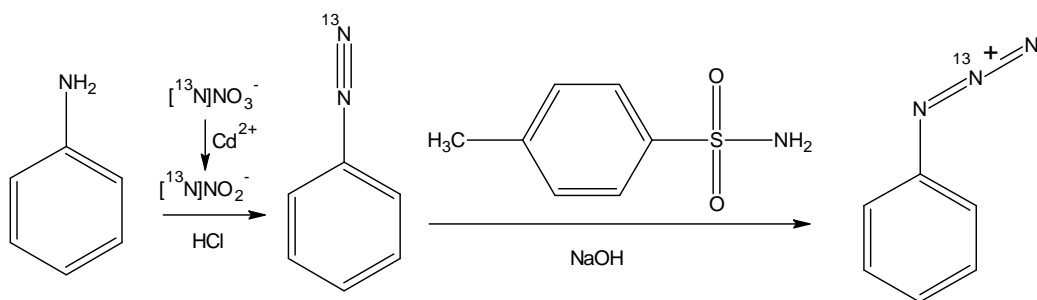


**Figura 1.** Esquema de la reacción utilizada para la preparación de fenilazida marcada con  $^{13}\text{N}$  mediante reacción de Dutt-Wormall.

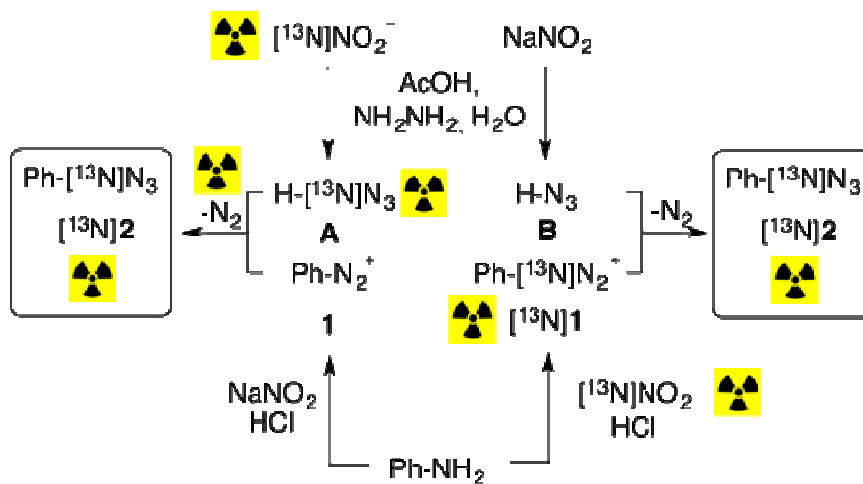


**Figura 2.** Estrategias sintéticas (A y B) utilizadas para sintetizar fenil-azida marcada con  $^{13}\text{N}$  ( $[\text{}^{13}\text{N}]\text{N}_2$  en la Figura).

Como puede observarse en la Figura 2, en esta reacción se libera gas nitrógeno  $[\text{}^{13}\text{N}]\text{N}_2$  como subproducto, lo cual puede tener un impacto negativo en el rendimiento radioquímico global de la reacción. Para lograr las condiciones óptimas, se decidió en primera instancia explorar ambas rutas sintéticas. Ambas estrategias sintéticas condujeron a la formación de fenil-azida marcada con  $^{13}\text{N}$ . Sin embargo, la cantidad de azida marcada obtenida en la ruta B era significativamente más alta que la obtenida en la ruta A. Cuando se seguía la ruta A, la mitad de la radiactividad se perdía como  $[\text{}^{13}\text{N}]\text{N}_2$ , mientras que en la ruta B la radioactividad se transfería de manera prácticamente cuantitativa a la azida.

En vista de los resultados, se decidió abordar estudios computacionales en colaboración con el profesor Fernando P. Cossío (UPV-EHU) con el fin de determinar el mecanismo de la reacción. Los estudios computacionales confirmaron que la formación de la azida

transcurre a través de un mecanismo de reacción *stepwise* pasando por intermedios de reacción zwitteriónicos y acíclicos. De dicho trabajo resultó la primera publicación de esta tesis doctoral [1].

La segunda parte del trabajo, que constituye el **capítulo 4** de la presente tesis doctoral, consistió en el desarrollo de estrategias para la preparación de triazoles marcados con  $^{13}\text{N}$  mediante cicloadición (3+2) de Huisgen entre azidas aromáticas (marcadas con Nitrógeno-13) y alquinos. Con el fin de preparar la cicloadición (3+2) de Huisgen bajo condiciones radioactivas, la reacción se llevó a cabo utilizando fenilazida marcada con  $^{13}\text{N}$  (utilizando la metodología desarrollada en el capítulo 3) y fenilacetileno usando diferentes catalizadores de cobre. Finalmente, se demostró que el  $[(\text{Icy})_2\text{Cu}]\text{PF}_6$  resultaba ser el mejor catalizador para la preparación de triazol marcado con  $^{13}\text{N}$ . Tras estos alentadores resultados, se decidió extender la metodología para la preparación de otros triazoles funcionalizados utilizando otros alquinos, para lo cual se preparó una pequeña librería de triazoles marcados con  $^{13}\text{N}$  (Figura 3).

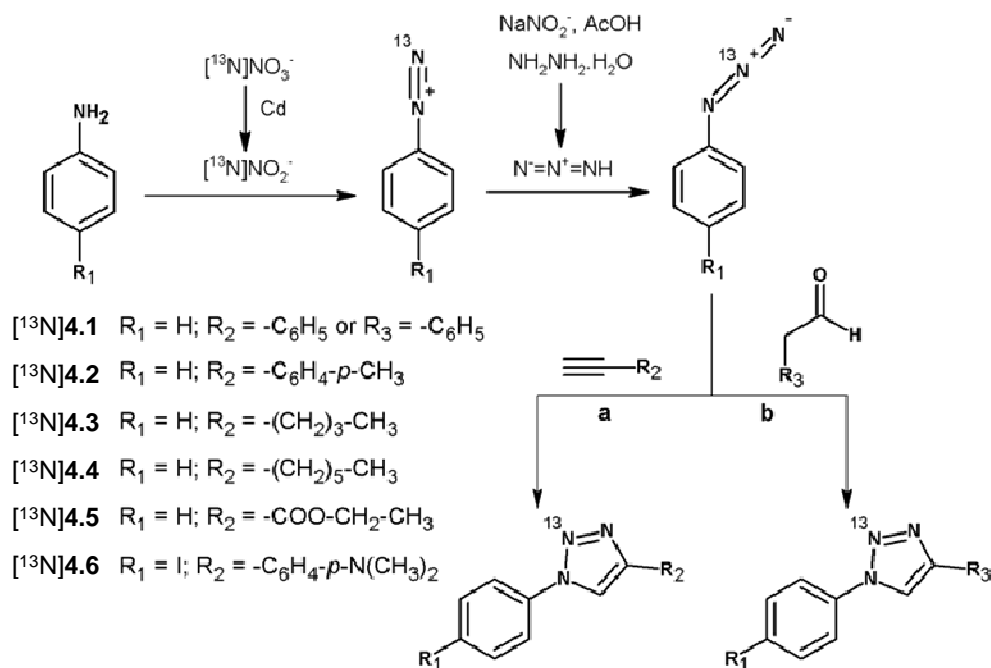


**Figura 3.** Esquema del proceso de síntesis en 4 etapas seguido para la preparación de triazoles marcados con  $^{13}\text{N}$  mediante la reacción de azidas marcadas con  $^{13}\text{N}$  con alquinos (a) y aldehídos (b).

En vista de estos resultados, se decidió ampliar el trabajo explorando la posibilidad de preparar triazoles marcados con  $^{13}\text{N}$  mediante reacción de la azida marcada con un aldehído.



Una vez optimizadas las condiciones experimentales, se procedió a la automatización del proceso de síntesis para uno de los compuestos [ $^{13}\text{N}$ ]6 en la Figura 3), que podría tener aplicación como marcador  $\beta$ -amiloide. Para ello, se utilizó un módulo automático para el cual se tuvo que adecuar la configuración, tal y como se muestra en la Figura 4. De la ejecución de este trabajo resultó la segunda publicación de esta tesis doctoral [2].

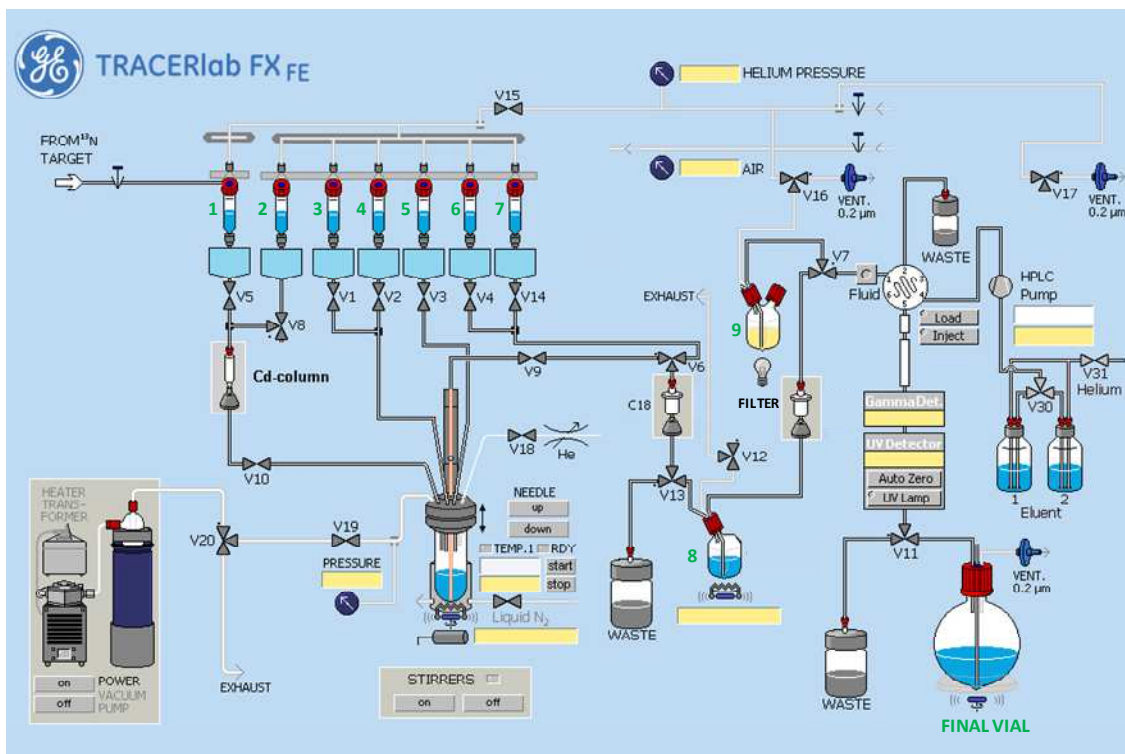


**Figura 4.** Representación esquemática del módulo de síntesis automatizado utilizado para la producción de [ $^{13}\text{N}$ ]. Los viales 1-8 se indican con números verdes. Las posiciones normalmente abiertas para las válvulas de tres vías se indican con un punto. Todas las válvulas de dos vías están cerradas.

La última parte del presente trabajo, incluido en el **capítulo 5** de esta tesis doctoral, ha consistido en el desarrollo de nuevas estrategias para la preparación rápida y eficiente de tetrazoles marcados con  $^{13}\text{N}$ . A pesar de que los tetrazoles han sido marcados con Nitrógeno-15, la síntesis de tetrazoles marcados con  $^{13}\text{N}$  no tiene precedente. Según la literatura, las reacciones ya descritas por calentamiento convencional requieren tiempos de reacción muy largos, que no son compatibles con la vida media corta del Nitrógeno-13. Por esta razón, se exploró la viabilidad de alternativas como el calentamiento por microondas. Tras observar que existía muy poca información referente a la síntesis de tetrazoles utilizando catalizadores heterogéneos mediante microondas, se decidió abordar el desarrollo de nuevos catalizadores heterogéneos basados en nanotecnología que permitieran la conversión de azidas en tetrazoles de una manera rápida y eficiente.

Para lograr este objetivo, se prepararon catalizadores heterogéneos inorgánicos, nano estructurados y basados en cobre, y se ensayaron en condiciones frías (no radiactivas). Concretamente, se desarrollaron y ensayaron tres catalizadores, denominados en el presente trabajo como 50%Cu-Al, 30%Cu-Cr-Al y 20%Cu/SiO<sub>2</sub>. En primer lugar, se procedió a una caracterización rigurosa de los catalizadores mediante difracción de rayos-X (XRD), microscopía electrónica de transmisión (TEM) y espectroscopia de desorción térmica (NH<sub>3</sub>-TPD). Una vez caracterizados, los catalizadores desarrollados (y otros comúnmente utilizados en la preparación de tetrazoles) se ensayaron en la síntesis de tetrazoles mediante cicloadición [3+2] a partir de los correspondientes nitrilos y azidas sódicas, utilizando para ello calefacción por microondas (Figura 5).

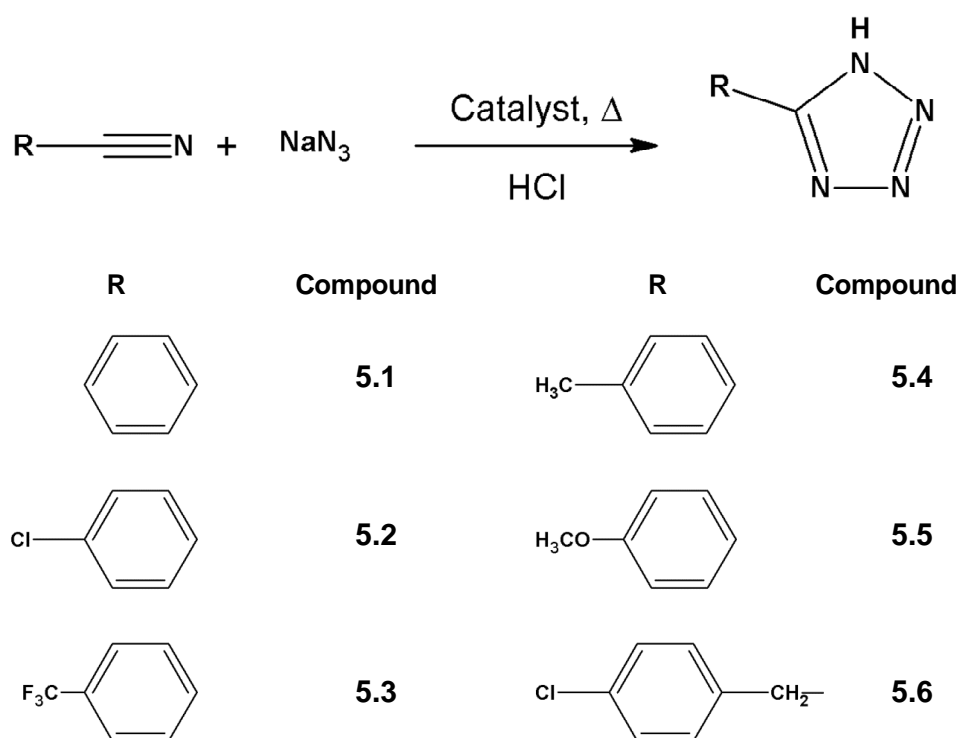


**Figura 5.** Síntesis de 1*H*-tetrazoles 5-sustituidos por reacción de azida de sodio con nitrilos.

Tras optimización de las condiciones experimentales se seleccionó el que presentaba mayor actividad catalítica (30%Cu-Cr-Al) y éste se utilizó para abordar la síntesis de un tetrazol (compuesto **5.1** en la Figura 5) en condiciones de radiactividad. Debido a ciertas limitaciones técnicas, en este caso la calefacción se llevó a cabo mediante métodos convencionales; aun así, pudo identificarse la formación del compuesto deseado marcado con nitrógeno-13. Para este trabajo, se ha preparado el manuscrito que ha sido enviado a una revista científica (New Journal of Chemistry) para su evaluación y posible publicación.

**Referencias:**

1. Stevens, E.D. and H. Hope, *A study of the electron-density distribution in sodium azide, NaN<sub>3</sub>*. Acta Crystallographica Section A, 1977. **33**(5): p. 723-729.
2. Joshi, S.M., et al., *Synthesis of <sup>13</sup>N-labelled polysubstituted triazoles: Via Huisgen cycloaddition*. RSC Advances, 2016. **6**(111): p. 109633-109638.



## Table of Contents

1. INTRODUCTION.....	1
1.1. MOLECULAR IMAGING.....	1
1.2. POSITRON EMISSION TOMOGRAPHY.....	2
1.2.1. Overview .....	2
1.2.2. PET isotopes.....	5
1.3. NITROGEN-13 .....	6
1.3.1. Production of nitrogen-13.....	7
1.3.2. Radiochemistry of nitrogen-13 using [ <sup>13</sup> N]NH <sub>3</sub> as the labelling agent.....	8
1.3.2.1. Radiosynthesis of amino acids .....	8
1.3.2.2. Radiosynthesis of amines and amides .....	11
1.3.2.3. Radiosynthesis of other compounds.....	12
1.3.3. Radiochemistry of nitrogen-13 using [ <sup>13</sup> N]NO <sub>2</sub> <sup>-</sup> as the labelling agent.....	13
1.3.3.1. Radiosynthesis of [ <sup>13</sup> N]nitroso compounds.....	13
1.3.3.2. Radiosynthesis of [ <sup>13</sup> N]azo compounds.....	14
1.4. CONSIDERATIONS ABOUT NITROGEN-13.....	15
1.5. REFERENCES.....	19
2. JUSTIFICATION AND OBJECTIVES .....	25
2.1. JUSTIFICATION.....	25
2.2. OBJECTIVES .....	27
2.3. REFERENCES.....	27
3. SYNTHESIS OF <sup>13</sup> N-LABELLED AZIDES.....	31
3.1. INTRODUCTION .....	31
3.1.1. Inorganic azides .....	31
3.1.2. Organic azides .....	31
3.2. AIM AND OBJECTIVES .....	34
3.3. MATERIALS AND METHODS.....	36
3.3.1. General Information .....	36
3.3.2. Radiochemistry: Synthesis of [ <sup>13</sup> N]labelled phenylazide .....	36
3.3.2.1. General.....	36
3.3.2.2. Production of the primary labelling agent.....	37
3.3.2.3. Preparation of <sup>13</sup> N-labelled phenylazide via Dutt-Wormall reaction .....	37
3.3.2.4. Preparation of <sup>13</sup> N-labelled phenylazide by reaction of hydrazoic acid with diazonium salt.....	38
3.3.2.5. Analysis of the radioactive gas [ <sup>13</sup> N]N <sub>2</sub> .....	39
3.4. RESULTS AND DISCUSSION .....	39
3.4.1. Synthesis of <sup>13</sup> N-labelled azides by Dutt-Wormall reaction.....	39
3.4.2. Synthesis of <sup>13</sup> N-labelled azides by reaction of diazonium salts with hydrazoic acid.....	41
3.4.3. Computational Results.....	44
3.5. SUMMARY AND CONCLUSIONS.....	48
3.6. REFERENCES.....	49
4. SYNTHESIS OF <sup>13</sup> N-LABELLED TRIAZOLES .....	57
4.1. INTRODUCTION .....	57
4.2. AIM AND OBJECTIVES .....	60
4.3. MATERIALS AND METHODS.....	61
4.3.1. General Information .....	61
4.3.2. Synthesis of reference compounds 4.1-4.6 .....	62
4.3.3. Radiochemistry: Synthesis of compounds [ <sup>13</sup> N]4.1-4.6 .....	62
4.3.3.1. General.....	62

4.3.3.2.	<i>Production of the primary labelling agent</i> .....	63
4.3.3.3.	<i>Production of <sup>13</sup>N-labelled azide</i> .....	63
4.3.3.4.	<i>Production of <sup>13</sup>N-labelled triazoles ([<sup>13</sup>N]4.1-[<sup>13</sup>N]4.6)</i> .....	63
4.3.3.5.	<i>Automatic synthesis of [<sup>13</sup>N]4.6</i> .....	64
4.4.	RESULTS AND DISCUSSION .....	67
4.4.1.	Preparation of the reference compounds.....	67
4.4.2.	Preparation of <sup>13</sup> N-labelled triazoles ([ <sup>13</sup> N]4.1-[ <sup>13</sup> N]4.6) in manual mode...69	69
4.4.3.	Implementation of an intermediate purification step based on SPE.....75	75
	Automatisation of the synthetic process for [ <sup>13</sup> N] 4.6 .....	75
4.5.	SUMMARY AND CONCLUSIONS.....	78
4.6.	REFERENCES.....	78
5.	NEW HETEROGENEOUS CATALYSTS: APPLICATION TO THE SYNTHESIS OF <sup>13</sup> N-LABELLED TETRAZOLES.....	85
5.1.	INTRODUCTION .....	85
5.2.	AIM AND OBJECTIVES .....	87
5.3.	MATERIALS AND METHODS.....	88
5.3.1.	General Information .....	88
5.3.2.	Preparation of the catalysts.....	89
5.3.3.	Characterization of the catalysts .....	89
5.3.4.	Synthetic procedures: chemistry .....	90
5.3.5.	Radiochemistry: Synthesis of [ <sup>13</sup> N]5.1 .....	91
5.3.5.1.	General .....	91
5.3.5.2.	Production of the primary labelling agent .....	91
5.3.5.3.	Synthesis of <sup>13</sup> N-labelled tetrazoles [ <sup>13</sup> N]5.1 .....	91
5.4.	RESULTS AND DISCUSSION .....	91
5.4.1.	Synthesis of tetrazoles (5.1-5.6) using Copper based heterogeneous catalysts .....	91
5.4.2.	Preparation and characterization of the catalysts .....	92
5.4.3.	Catalytic activity.....	95
5.4.4.	Radiochemistry: Synthesis of [ <sup>13</sup> N]5.1 .....	100
5.5.	SUMMARY AND CONCLUSIONS.....	101
5.6.	REFERENCES.....	102
6.	CONCLUDING REMARKS.....	109
	ABBREVIATIONS.....	111
	SELECTED <sup>1</sup> H NMR SPECTRA.....	115

# **1. Introduction**





# 1. INTRODUCTION

## 1.1. MOLECULAR IMAGING

Molecular imaging can be defined as a set of non invasive techniques that allow the visualization of cell function and the monitoring of molecular processes in living organisms. Contrary to traditional imaging techniques, molecular imaging uses biomarkers, which can interact with the surrounding. The images obtained are a result of the molecular changes taking place.

Molecular imaging has opened a wide range of possibilities for the investigation of biological, physiological and medical processes which cannot be studied using other techniques. Nuclear imaging techniques such as positron emission tomography (PET) or single photon emission computerized tomography (SPECT), together with optical/fluoresce imaging and magnetic resonance spectroscopy (MRS) are the most widely utilized molecular imaging techniques.

Molecular imaging techniques usually provide very poor anatomical information (see Figure 1.1).

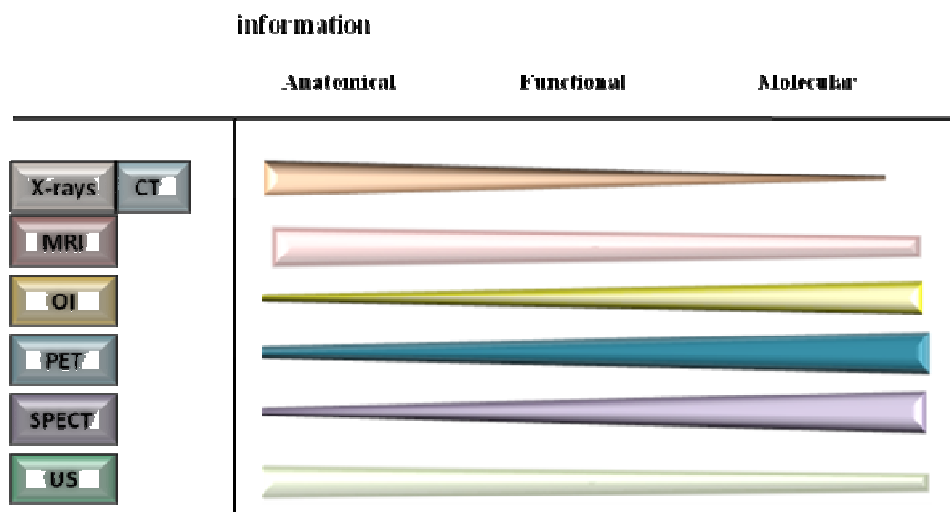


**Figure 1.1:** Representative illustration of the information provided by different *in vivo* imaging modalities. Obtained from [1]; CT: Computed tomography; MRI: Magnetic resonance imaging, OI: optical imaging; US: Ultra sound imaging.

For example, PET and SPECT images just provide information about the spatiotemporal distribution of a labelled entity after administration to a living organism (see section 1.2 for details about PET). However, no information about the anatomical localization of the

radioactive signal can be obtained (see Figure 1). Because of this, molecular imaging techniques are usually combined with anatomical techniques, able to provide accurate anatomical information. The combination of the resulting images (multimodality) offers information at anatomical and molecular levels. Anatomical modalities include magnetic resonance imaging (MRI), ultra-sound imaging (US), X-ray imaging and computed tomography (CT).

None of the imaging modalities are perfect: They can just provide certain information and have a collection of intrinsic limitations. Thus, while nuclear imaging (PET and SPECT) offer unparalleled sensitivity, they offer a poor resolution, which is usually in the range of 1 mm in the preclinical setting and a few mm in clinical systems. On the contrary, MRI can offer high resolution (up to a few micrometers) while its sensitivity is very low. As a consequence, the application of one modality or another will depend on the problem under investigation and often the combination of two or more modalities will provide the most accurate data.

The description of the different imaging modalities including their principles and applications is out of the scope of this chapter. Only an introduction to the imaging modality of application in the context of the current PhD thesis (PET) will be provided.

## 1.2. POSITRON EMISSION TOMOGRAPHY

### 1.2.1. Overview

Positron emission tomography (PET) is an *in vivo* and non-invasive molecular imaging technique based on the administration of compounds labelled with short-lived positron-emitting radionuclides to obtain three-dimensional images of functional processes in animals and/or humans. Typical isotopes used as radionuclides in PET are fluorine-18 ( $^{18}\text{F}$ ), carbon-11 ( $^{11}\text{C}$ ), nitrogen-13 ( $^{13}\text{N}$ ) and oxygen-15 ( $^{15}\text{O}$ ) (see Table 1.1). These radionuclides are incorporated into biological compounds that play a specific role in living organisms.

**Table 1.1.** Most commonly used positron emitters and their physical properties.

Radionuclide	Half-life (min)	Max. Energy (MeV)	Max. Range (mm)*
Fluorine-18	109.8	0.69	2.4
Carbon-11	20.4	0.96	4.1
Nitrogen-13	9.98	1.19	5.4
Oxygen-15	2.05	1.70	8.0

\* In water

Positron emitters undergo radioactive decay by emitting a positron, which is the antiparticle of the electron, with equivalent mass but positive electrical charge. After radioactive decay, the emitted positron interacts with other charged particles while losing its kinetic energy. When most of this energy has been lost and the positron is almost at rest, it interacts with an electron of a surrounding atom in a process called annihilation, which results in the emission of a pair of gamma rays with energies of 511 keV each and travelling 180° from each other (see Figure 1.2a). The distance between the locations where the radioactive decay and the annihilation take place is called positron range, and depends on the energy of the emitted positron and the media. Positrons are emitted simultaneously with one neutrino, and hence positrons are not emitted at one single energy, but with an energy distribution. For example, Nitrogen-13 has a maximum energy for positron emission of 1.19 MeV, which results in a maximum range in water of 5.4 mm (Table 1.1). Typical positron emitters have maximum positron ranges of a few mm in water. The positron range has an effect on the resolution of the images acquired using PET: The larger the range of the positron, the lower the spatial resolution achieved.

The generation of the above-mentioned gamma rays (resulting from the annihilation process) is the basis of PET: High-energy gamma rays can travel through biological tissues without suffering significant scatter or attenuation, and can be detected and quantified using specific instrumentation and tomographic reconstruction algorithms. Hence, when a tracer containing a positron emitter is administered to an organism, the high-energy gamma rays produced can escape from the body and be detected by an external ring of detectors as a coincident event (Figure 1.2b).

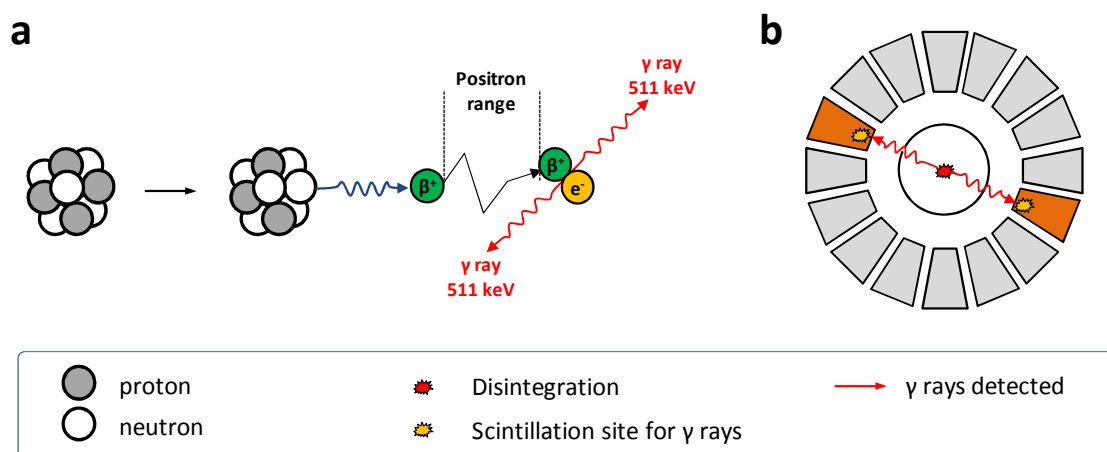


**Figure 1.2.** (a) Schematic representation of the annihilation process of one positron and one electron, with subsequent emission of two gamma rays. (b) Representation of a PET camera. The two photons emitted after the annihilation process are detected simultaneously by two detectors of the ring, placed around the subject under investigation.

The direction of the incident rays is determined as the line crossing the two detectors, and hence PET imaging relies in back-to-back detection heads (coincidence detection). The detection of hundreds of thousands of such coincident events permits the reconstruction of a 3D-image that contains information about the distribution of the radiolabelled tracer within the organism.

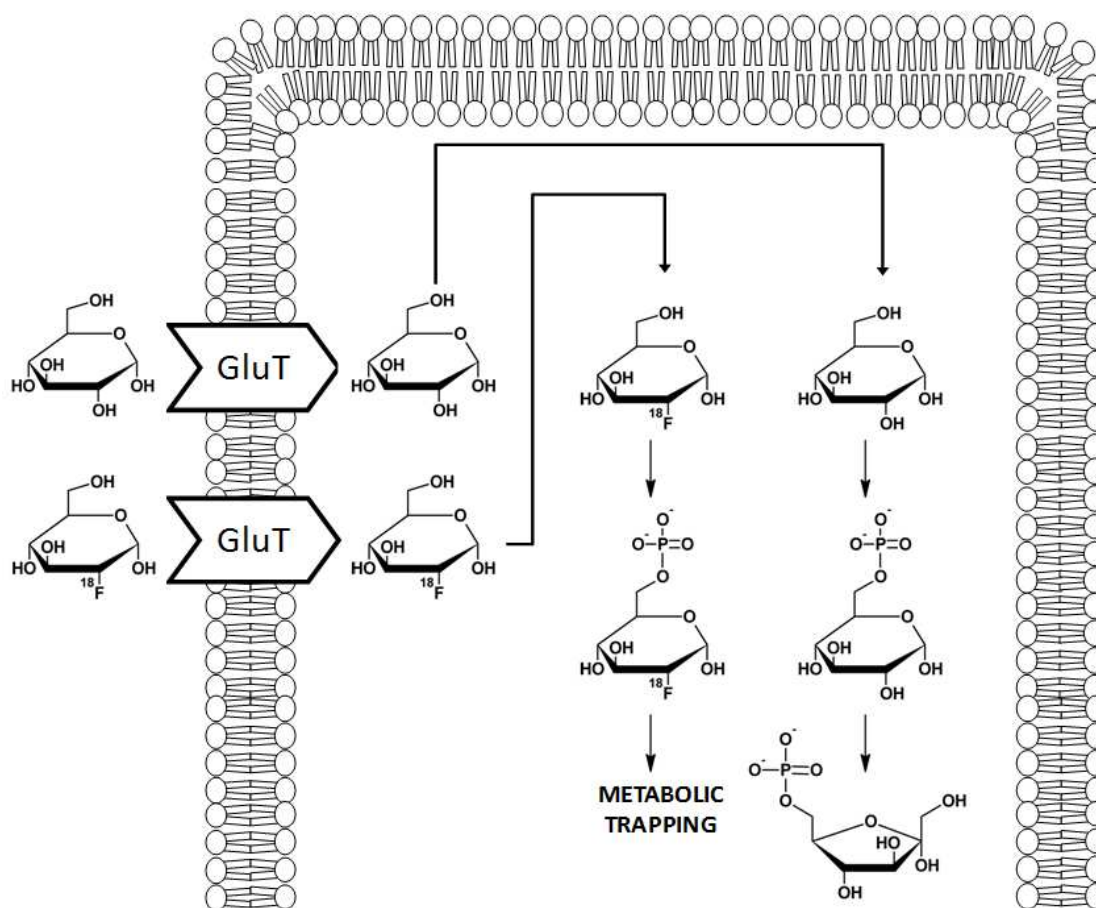


**Figure 1.3.** Intracellular metabolism of glucose and  $[^{18}\text{F}]$ FDG. Both are taken up by cells by means of glucose transporters (GluT). Once into the cell, they are phosphorylated to glucose-6-phosphate and  $[^{18}\text{F}]$ glucose-6-phosphate, respectively. Unlike glucose,  $[^{18}\text{F}]$ glucose-6-phosphate does not undergo further metabolism and is trapped in the cell.

The mainstay of PET imaging has been 2-deoxy-2- $[^{18}\text{F}]$ fluoro-D-glucose ( $[^{18}\text{F}]$ FDG or FDG), a radio-fluorinated glucose metabolism marker widely adopted in clinical oncology, which has made an unparalleled contribution in the early diagnosis and evaluation of the response to treatment of a wide variety of tumours. The principle behind the application of FDG is quite intuitive (Figure 1.3): In this radiotracer, an  $^{18}\text{F}$  atom is incorporated in the 2 position of glucose in substitution of a hydroxyl group. After administration to a living organism,  $[^{18}\text{F}]$ FDG is distributed all over the organism and then taken up by cells through

the same pathways as glucose (glucose transporters), phosphorylated and trapped in the cells, because subsequent metabolic steps cannot occur due to the presence of the fluorine atom (this is known as metabolic trapping); as a result, the [ $^{18}\text{F}$ ]FDG concentration increases in proportion to the rate of utilization of glucose, and therefore it can be used as an indirect proliferation marker. It is well known that most tumours present accelerated (and anaerobic) metabolism and hence the amount of FDG uptake can aid in the identification and classification of different tumours.

The widespread installation of biomedical cyclotrons and the rapid advances in imaging technologies have opened new avenues in the potential applications of PET far beyond medical diagnosis. PET can effectively provide early and reliable answers to key questions emerging during the drug development process, e.g. the elucidation of pharmacokinetic properties of new chemical and biological entities, the determination of the effective dose of a drug or the evaluation of the response to a particular treatment. PET has also become an essential tool among the basic and medical research communities, by enabling the non-invasive and translational investigation of a wide variety of biological, physiological and pathological phenomena.

Emerging PET applications, together with the need for better, more efficient and even personalized diagnostic tools, have resulted in a boost in the demand for new molecular probes for biological targets currently unavailable to this technique. The development of such molecular probes (radiotracers) requires a multidisciplinary approach, which should start at target identification, structure design, and development/implementation of labelling strategies, followed by exhaustive *in vitro* and *in vivo* testing, ultimately leading to radiotracer characterization. This PhD is framed mainly in the context of developing novel radiolabelling strategies.

### **1.2.2. PET isotopes**

Only certain radionuclides have appropriate physical properties to become suitable candidates for the preparation of radiotracers. In the particular case of positron emitters, there are four radioisotopes which have been historically used: carbon-11, nitrogen-13, fluorine-18 and oxygen-15. The wide historical use of these isotopes is due to a combination of different factors, including: (i) they can be produced in relatively high yields in commercially available biomedical cyclotrons; (ii) their decay mode is close to 100% positron emission; (iii) they can be easily introduced in biomolecules, and (iv) their stable isotopes are present in all organic molecules. Of course, this is not the case for fluorine-18. However, the substitution of a hydroxyl group or hydrogen atom by a fluorine atom may not dramatically alter the biological behaviour of the resulting molecule.

Among these four radionuclides, fluorine-18 has been the most widely used, especially for clinical applications. Fluorine-18 forms strong covalent bonds with carbon atoms and can be incorporated into a large variety of organic molecules. Moreover, fluorine-18 has a small positron range and its half-life (110 min) allows for the preparation of complex molecules with acceptable radiochemical yields, as well as the centralised production of radiotracers and distribution to satellite centres.

Out of the above mentioned clinical environment, other positron emitters such as carbon-11 and nitrogen-13 have a huge potential for the synthesis of radiotracers. The preparation of radiotracers with these two radionuclides is far from trivial due to their short half-life (20.4 and 9.98 min, respectively). Carbon-11 can be obtained in cyclotrons in different chemical forms:  $[^{11}\text{C}]\text{CO}_2$  (obtained by proton irradiation of  $\text{N}_2/\text{O}_2$  gas mixtures) and  $[^{11}\text{C}]\text{CH}_4$  (obtained by irradiation of  $\text{N}_2/\text{H}_2$  mixtures). On the other hand, nitrogen-13 is obtained by irradiation of water solutions and is usually produced as  $[^{13}\text{N}]\text{NH}_4^+$  after irradiation of diluted ethanol aqueous solutions; this radiochemical specie has direct application in the clinical environment as perfusion marker. Oxygen-15 is the shortest-lived positron emitting isotope of oxygen. Its half-life is close to 2 minutes, and hence it is mainly used as produced  $[^{15}\text{O}]\text{O}_2$  or for the preparation of  $[^{15}\text{O}]\text{H}_2\text{O}$ .

The main drawback of the above-mentioned radionuclides is their short half-lives, which limit the duration of the *in vivo* investigations to a maximum of ca. a few hours in the case of Fluorine-18 and less than 2 hours in the case of  $^{11}\text{C}$  and  $^{13}\text{N}$ . Recently, other longer-lived positron emitters have gained attention, including copper-64 and zirconium-89 (half-lives of 12.7 and 78.4 h, respectively), which have been widely used for the preparation of labelled peptides, macromolecules (proteins, antibodies) and nanoparticles. Gallium-68, a 68 min half-lived positron emitter, has also gained relevance because it can be easily obtained from commercially available  $^{68}\text{Ge}/^{68}\text{Ga}$  generators.

This PhD thesis is framed in the use of nitrogen-13 and the development of innovative radiolabelling strategies concerning this radionuclide. Because of this, an overview of the  $^{13}\text{N}$ -radiochemistry developed to date will be included in this introductory chapter. The radiochemistry of other commonly used positron emitters such as fluorine-18 or carbon-11 has been widely reviewed in the literature (see for example [2, 3]).

### 1.3. NITROGEN-13

With a half-life of 9.97 min, nitrogen-13 was one of the first positron emitters to be produced, and was discovered in 1934 by F. Joliot and I. Joliot-Curie [4], who irradiated boron nitride with  $\alpha$  particles and produced  $^{13}\text{N}$  via the  $^{10}\text{B}(\alpha, n)^{13}\text{N}$  nuclear reaction. The

authors reported that “our latest experiments have shown a very striking fact: when an aluminium foil is irradiated on a polonium preparation, the emission of positrons does not cease immediately, when the active preparation is removed. The foil remains radioactive and the emission of radiation decays exponentially as for an ordinary radio-element. We observed the same phenomenon with boron and magnesium. The half life period of the activity is 14 min. for boron, 2 min. 30 sec. for magnesium, 3 min. 15 sec. for aluminium”. When the irradiated boron nitride was treated with sodium hydroxide, a gas was generated. This gas, in contact with a paper soaked in hydrochloric acid, produced a radioactive white deposit which was identified as  $\text{NH}_4\text{Cl}$ . Joliot and Curie were awarded with the Nobel Prize in 1935 “for their synthesis of new radioactive elements”. In the same year, alternative routes for the production of  $^{13}\text{N}$ , based on the irradiation of  $^{13}\text{C}$ -enriched graphite with protons and by irradiation of natural graphite with deuterons, were reported by J. Cockcroft, C. W. Gilbert and E. T. S. Walton [5].

### 1.3.1. Production of nitrogen-13

After the pioneering works by Joliot and Curie, several routes for the production of  $^{13}\text{N}$  by proton, deuteron or neutron irradiation of stable materials have been developed (see table 1.2). Mainly, 3 nuclear reactions using accelerated ions can be utilized:  $^{12}\text{C}(\text{d},\text{n})^{13}\text{N}$ ,  $^{13}\text{C}(\text{p},\text{n})^{13}\text{N}$  and  $^{16}\text{O}(\text{p},\alpha)^{13}\text{N}$ . In addition, irradiation of natural nitrogen ( $^{14}\text{N}$ ) with neutrons also produces  $^{13}\text{N}$  via an  $(\text{n},2\text{n})$  reaction. The nuclear reaction  $^{16}\text{O}(\text{p},\alpha)^{13}\text{N}$  is by far the most commonly utilized nowadays. However, by modification of the incident particle and chemical and physical forms of the irradiated material, different  $^{13}\text{N}$ -labelled species can be produced.

**Table 1.2:** Methods for the production of  $^{13}\text{N}$  using nuclear reactions.

Target material	Nuclear reaction	In-target product
$\text{CO}_2$ (trace $\text{N}_2$ )	$^{12}\text{C}(\text{d},\text{n})^{13}\text{N}$	$[^{13}\text{N}]\text{N}_2$
Graphite	$^{12}\text{C}(\text{d},\text{n})^{13}\text{N}$	$[^{13}\text{N}]\text{CN}$
Charcoal	$^{12}\text{C}(\text{d},\text{n})^{13}\text{N}$	$[^{13}\text{N}]\text{N}_2$ + trapped $[^{13}\text{N}]\text{CN}$
$^{13}\text{C}$ -enriched charcoal	$^{13}\text{C}(\text{p},\text{n})^{13}\text{N}$	Trapped $[^{13}\text{N}]\text{CN}$
$\text{H}_2\text{O}$ / ethanol	$^{16}\text{O}(\text{p},\alpha)^{13}\text{N}$	$[^{13}\text{N}]\text{NH}_3$
$\text{H}_2\text{O}$	$^{16}\text{O}(\text{p},\alpha)^{13}\text{N}$	$[^{13}\text{N}]\text{NH}_3$ + $[^{13}\text{N}]\text{NO}_3^-$ + $[^{13}\text{N}]\text{NO}_2^-$
$\text{NaNO}_3$ (aq)	$^{14}\text{N}(\text{n},2\text{n})^{13}\text{N}$	$[^{13}\text{N}]\text{NH}_3$
$\text{Al}_4\text{C}_3$	$^{12}\text{C}(\text{d},\text{n})^{13}\text{N}$	Matrix trapped $^{13}\text{N}$
$\text{CH}_4$ (flowing)	$^{12}\text{C}(\text{d},\text{n})^{13}\text{N}$	$[^{13}\text{N}]\text{NH}_3$ + $[^{13}\text{N}]\text{HCN}$ + $[^{13}\text{N}]\text{CH}_3\text{NH}_2$

It was early discovered that irradiation of pure water with high energy protons results in the formation of  $[^{13}\text{N}]\text{NO}_3^-$ , and the formation of this species increases with increased target dose due to radiolytic oxidations [6]. Such irradiation is generally carried out in liquid targets (see Figure 1.4 for general scheme of a typical target configuration).

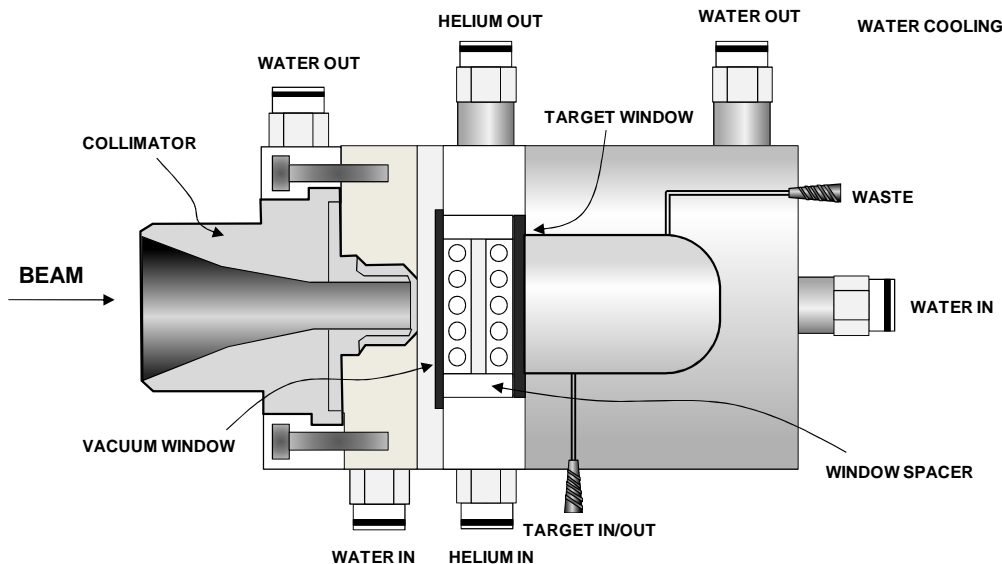


**Figure 1.4.** Typical target design for the production of  $[^{13}\text{N}]\text{NH}_3$  by irradiation of 5mM ethanol aqueous solution with protons, based on the target Nirta® Liquid provided by IBA Molecular.

However, the presence of minor amounts of  $[^{13}\text{N}]\text{NO}_2$  and  $[^{13}\text{N}]\text{NH}_4^+$  could be also detected. A few years later, Wieland and co-workers realized that the addition of scavengers to the irradiated water modified the percentage of the different  $^{13}\text{N}$ -labelled species ( $[^{13}\text{N}]\text{NO}_3^-$ ,  $[^{13}\text{N}]\text{NH}_4^+$ ,  $[^{13}\text{N}]\text{NO}_2^-$ , and  $[^{13}\text{N}]_2$ ) [7]. For example, addition of 5mM ethanol to the target resulted in >96% of the radioactivity as  $[^{13}\text{N}]\text{NH}_3$ , irrespective of the beam intensity (15-30  $\mu\text{A}$ ), and similar results were obtained after addition of acetic acid. The mechanisms behind this experimental finding are not well understood, although it is thought to be due to prevention of radiolytic oxidation due to the presence of the scavenger. Irradiation of solid water (ice) [8], and pressurization of the target with hydrogen [9-11] and methane [12] also prevent radiolytic oxidation and result in preferential formation of  $[^{13}\text{N}]\text{NH}_3$ .

### 1.3.2. Radiochemistry of nitrogen-13 using $[^{13}\text{N}]\text{NH}_3$ as the labelling agent

#### 1.3.2.1. Radiosynthesis of amino acids

Nitrogen-13 has been widely exploited in the preparation of  $^{13}\text{N}$ -labelled amino acids, mainly during the 70's and 80's, most of them with the ultimate goal to investigate protein synthesis rates, particularly in tumours. Chemical methods for the preparation of  $^{13}\text{N}$ -labelled amino acids are usually time-consuming and inefficient, lead to the formation of



intermediate compounds and yield racemic mixtures. Consequently, only a few examples have been reported in the literature. Just to mention one, in 1979 the synthesis of L-[ $^{13}\text{N}$ ]asparagine by reaction of L- $\alpha$ -N-Boc-aspartate with [ $^{13}\text{N}$ ]NH $_3$  and further hydrolysis was reported by Elmalech and co-workers [13] (Figure 1.5).

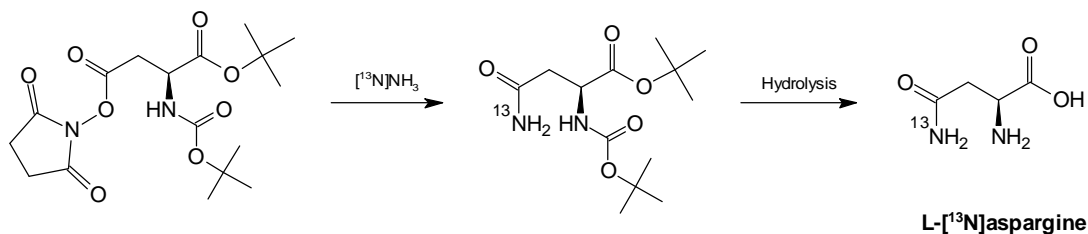


**Figure 1.5.** Synthesis of L-[ $^{13}\text{N}$ ]asparagine by a synthetic chemistry method.

Comparatively, biosynthetic methods using enzymes are rapid and yield the enantiomerically pure compounds. Therefore, these are usually anticipated to be more convenient. Several attempts have been carried out to synthesize labelled amino acids using enzymes. The general approach consists of incubating [ $^{13}\text{N}$ ]NH $_3$  with the appropriate precursor and the enzyme (with cofactors) in buffered aqueous solution. Under these conditions, L-[ $^{13}\text{N}$ ] glutamate was rapidly synthesized by incubation of [ $^{13}\text{N}$ ]NH $_3$  with  $\alpha$ -ketoglutarate in the presence of L-glutamate dehydrogenase as the enzyme, which catalyses the reductive amination of alpha-keto acids to amino acids, and NADPH (nicotinamide adenine dinucleotide phosphate) as cofactor in phosphate buffer (Figure 1.6a) [14]. Removal of unreacted [ $^{13}\text{N}$ ]NH $_3$  was carried out by boiling the crude reaction mixture and filtered to yield 8mCi (296 MBq) of L-[ $^{13}\text{N}$ ] glutamate (radiochemical yield = 15%).

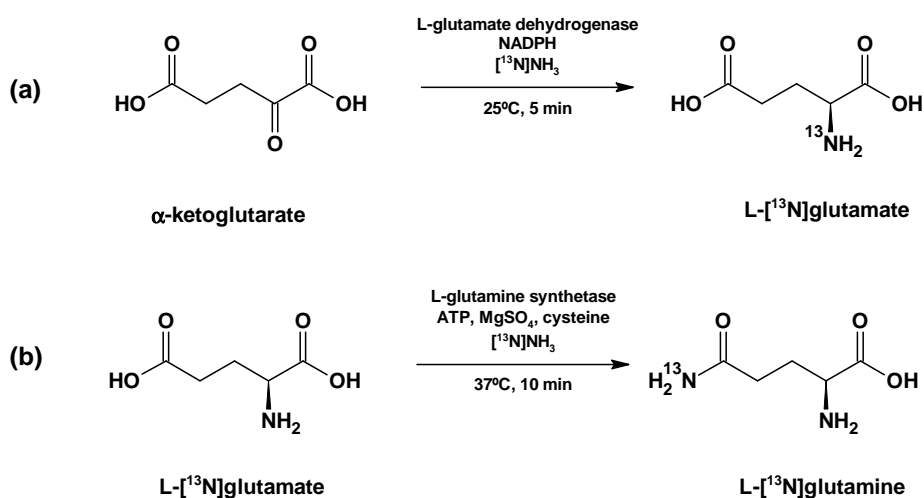


**Figure 1.6.** Synthesis of L-[ $^{13}\text{N}$ ]glutamate (a) and L-[ $^{13}\text{N}$ ]glutamine (b) *via* biosynthetic routes.

By using a parallel strategy, L-[<sup>13</sup>N]glutamine was synthesized by incubation at of [<sup>13</sup>N]NH<sub>3</sub> with glutamic acid and glutamine synthetase as the enzyme in the presence of cysteine and adenosine triphosphate and magnesium sulphate as cofactors (Figure 1.6b) [15].

In 1973, Straatman and Welch demonstrated the feasibility of utilizing glutamate dehydrogenase to introduce <sup>13</sup>N into amino acids other than glutamate by synthesizing L-[<sup>13</sup>N]valine, L-[<sup>13</sup>N]alanine and L-[<sup>13</sup>N]leucine from the corresponding α-keto acids and [<sup>13</sup>N]ammonia with decay-corrected yields ranging from 6.8% to 26% [16].

The above mentioned method for the preparation of labelled amino acids is extremely convenient. However, contamination of the final tracer with enzymes may pose problems for putative human applications. A purification method based on column chromatography was attempted for the synthesis of L-[<sup>13</sup>N]glutamic acid and L-[<sup>13</sup>N]alanine [17]. However, because of the short half-life of <sup>13</sup>N, application of pressure was required to achieve rapid purification; this resulted in suboptimal results and the presence of enzyme in the final product could be detected. To overcome this drawback, an alternative synthetic strategy based on the use of 'immobilized enzymes' (enzymes that are synthetically attached to a water-insoluble support by either physical or chemical means) was developed. The preparation of L-[<sup>13</sup>N]glutamic acid and L-[<sup>13</sup>N]alanine were carried out by using this strategy (Figure 1.7) [17]. Using similar strategies, the preparation of L-[<sup>13</sup>N]glutamic acid could be achieved by using immobilization of the enzyme (glutamic acid dehydrogenase) on an activated CNBr-Sepharose support [18], and the same support was successfully applied to the synthesis of the branched-chain L-amino acids L-[<sup>13</sup>N]valine and L-[<sup>13</sup>N]leucine [19], as well as other amino acids such as L-[<sup>13</sup>N]alanine, L-α-[<sup>13</sup>N]aminobutirate or L-[<sup>13</sup>N]methionine [20].

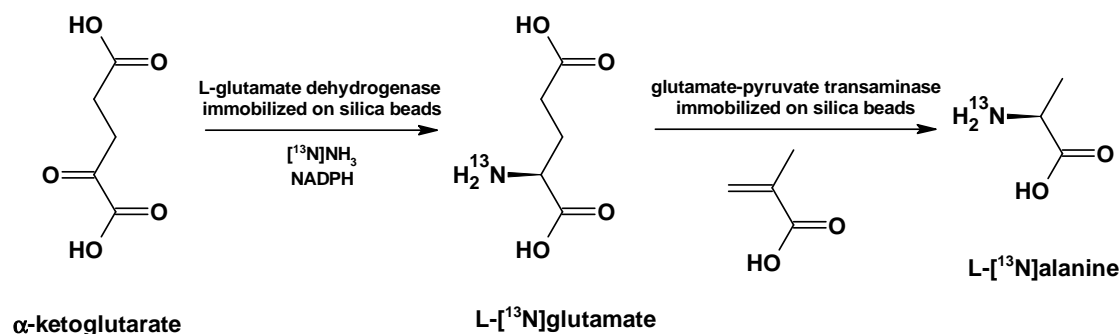


**Figure 1.7.** Synthesis of L-[<sup>13</sup>N]glutamate and L-[<sup>13</sup>N]alanine using immobilized enzymes.

Very recently, the one-pot, enzymatic and non-carrier-added synthesis of the <sup>13</sup>N-labelled amino acids L-[<sup>13</sup>N]alanine, [<sup>13</sup>N]glycine, and L-[<sup>13</sup>N]serine by using L-alanine

dehydrogenase from *Bacillus subtilis*, an enzyme that catalyses the reductive amination of  $\alpha$ -keto acids by using nicotinamide adenine dinucleotide (NADH) as the redox cofactor and ammonia as the amine source, has been reported by our research group [21]. Interestingly, the integration of both L-alanine dehydrogenase and formate dehydrogenase from *Candida boidinii* in the same reaction vessel to facilitate the *in situ* regeneration of NADH during the radiochemical synthesis of the amino acids allowed a 50-fold decrease in the concentration of the cofactor without compromising reaction yields.

### 1.3.2.2. Radiosynthesis of amines and amides

Amines and amides can be synthesised by using different synthetic methods. The synthesis of  $^{13}\text{N}$ -labelled amines has been achieved *via* Hoffman rearrangement [22] (Figure 1.8a), reduction of amides [23] (Figure 1.8b), reduction of imines [24] (Figure 1.9), and by using amination of organoboranes [25]. The latter could be optimized by using polymeric borane reagents (Figure 1.10). Ammonolysis of halo-substrates has been also employed in the preparation of [ $^{13}\text{N}$ ]adenosine.

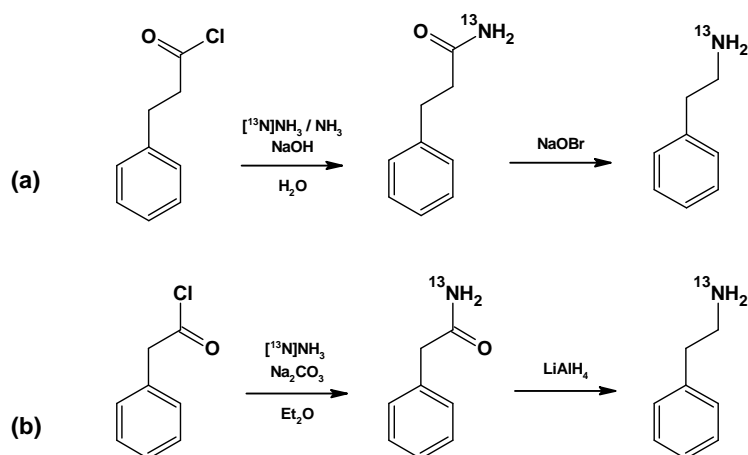


**Figure 1.8.** Synthesis of  $^{13}\text{N}$ -labeled  $\beta$ -phenethylamine via Hofmann rearrangement (a) and reduction of the amide (b).

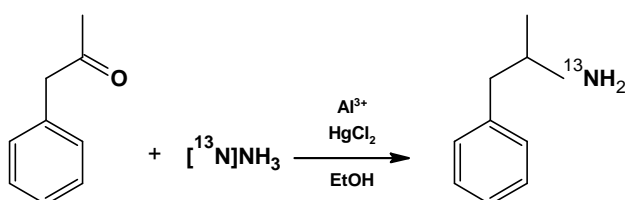


**Figure 1.9.** Synthesis of [ $^{13}\text{N}$ ]amphetamine *via* formation of the imine.

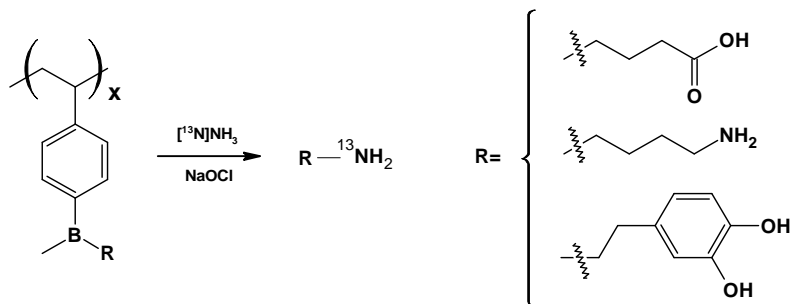


**Figure 1.10.** Synthesis of [ $^{13}\text{N}$ ]amines using polymeric borane reagents.

$^{13}\text{N}$ -labelled amides have been prepared as intermediates for the preparation of amines *via* Hoffman rearrangement (see Figure 1.8a).

### 1.3.2.3. Radiosynthesis of other compounds

[ $^{13}\text{N}$ ]ammonia has been used for the preparation of different labelled compounds that do not fall into one of the above mentioned categories. There are only a few examples described in the literature and because of this, they have been grouped into this section.

One of the most remarkable examples is the preparation of the well know compound *cis*-platin, which was prepared in a multi-step process [26]. First,  $\text{K}_2\text{PtCl}_4$  was reacted with potassium iodide to yield  $\text{K}_2\text{PtI}_4$ , which was further treated with carrier-added [ $^{13}\text{N}$ ]NH $_3$  to form *cis*-Pt([ $^{13}\text{N}$ ]NH $_3$ ) $_2\text{I}_2$ . After addition of  $\text{AgNO}_3$  and filtering, *cis*-Pt([ $^{13}\text{N}$ ]NH $_3$ ) $_2\text{Cl}_2$  could be obtained in 27.1% decay-corrected radiochemical yield. The method was then improved by directly sparging [ $^{13}\text{N}$ ]NH $_3$  into  $\text{K}_2\text{PtI}_4$  [27].

Other families of compounds have been prepared from the labelling agent [ $^{13}\text{N}$ ]NH $_3$ . For example, the opioid tetrapeptide H-Tyr-D-Met(O)-Phe-Gly-[ $^{13}\text{N}$ ]NH $_2$  (SD-62) could be synthesized by amination reaction of its activated p-nitrophenol ester with anhydrous [ $^{13}\text{N}$ ]NH $_3$  [28].

In 1977, Krizek and co-workers developed a method for prepreparation of [ $^{13}\text{N}$ ]urea by boiling [ $^{13}\text{N}$ ]NH $_3$  in the presence of ammonium cyanate [29]. After purification of the reaction mixture with ion exchange resin [ $^{13}\text{N}$ ]urea could be obtained in decay-corrected radiochemical yield of 56% in 10 min. By using a parallel approach, the one-pot synthesis of [ $^{13}\text{N}$ ]urea and [ $^{13}\text{N}$ ]carbamate analogues by using anhydrous [ $^{13}\text{N}$ ]NH $_3$  under non-carrier added conditions was reported by Kumata [30]. In this approach, a primary amine, a secondary amine or an alcohol were treated with triphosgene to yield the intermediate isocyanate, carbamoyl chloride or chloroformate, respectively; these were further reacted with [ $^{13}\text{N}$ ]NH $_3$  to yield the corresponding [ $^{13}\text{N}$ ]urea and [ $^{13}\text{N}$ ]carbamate analogues (Figure 1.11). [ $^{13}\text{N}$ ]NH $_3$  was also recently used by the same group to approach the preparation of

[ $^{13}\text{N}$ ]thalidomide (Figure 1.12) [31], which could be achieved by reaction of *N*-phthaloylglutamic anhydride with [ $^{13}\text{N}$ ]NH $_3$ , followed by cyclization using carbonyldiimidazole. The preparation of [ $^{13}\text{N}$ ]dantrolene was also reported by the same research group [32].

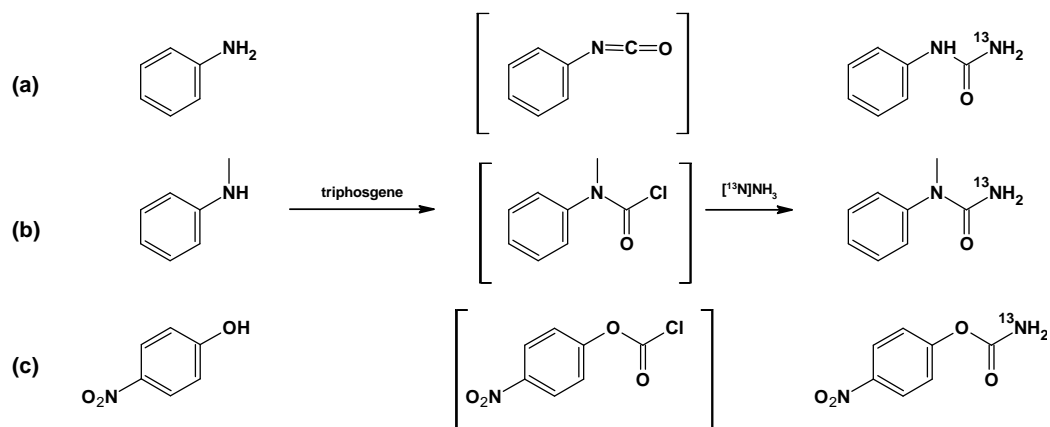


**Figure 1.11.** One-pot synthesis of [ $^{13}\text{N}$ ]urea (a) and [ $^{13}\text{N}$ ]carbamate (b, c) analogues using non carrier added [ $^{13}\text{N}$ ]NH $_3$ .

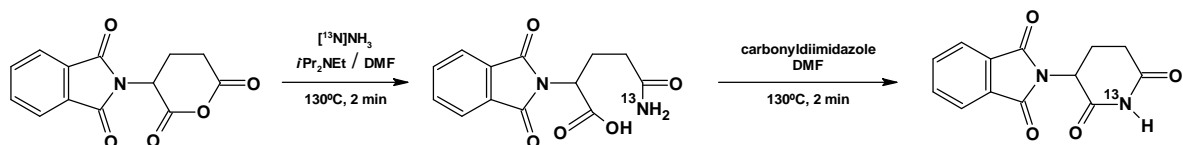


**Figure 1.12.** Synthesis of [ $^{13}\text{N}$ ]thalidomide using non carrier added [ $^{13}\text{N}$ ]NH $_3$ .

### 1.3.3. Radiochemistry of nitrogen-13 using [ $^{13}\text{N}$ ]NO $_2^-$ as the labelling agent

This PhD has focused on the development of innovative strategies for the preparation of  $^{13}\text{N}$ -labelled compounds starting from the labelling agent [ $^{13}\text{N}$ ]NO $_2^-$ , which was obtained after reduction of cyclotron produced [ $^{13}\text{N}$ ]NO $_3^-$ . Such labelling agent has been previously used by other research groups and by us for the preparation of different labelled molecules. The most relevant examples are included below.

#### 1.3.3.1. Radiosynthesis of [ $^{13}\text{N}$ ]nitroso compounds

One of the first examples found in the literature include the preparation of [ $^{13}\text{N}$ ]nitrosamines and [ $^{13}\text{N}$ ]nitrosothiols, which were first reported by Vavrek and Mulholland [33]. The reduction of cyclotron produced [ $^{13}\text{N}$ ]NO $_3^-$  was achieved using an activated cadmium column and the nitrosation reaction was conducted on thiols and secondary amines in an anion exchange resin after selective trapping of the reduced species [ $^{13}\text{N}$ ]NO $_2^-$ . Based on this method, our group developed some years ago a fast and

simple strategy for production of  $^{13}\text{N}$ -labelled nitroso-glutathione ( $[^{13}\text{N}]\text{GSNO}$ ) *via* the radio-nitrosation of GSH [34] (Figure 1.13). The formation of the desired product could be achieved with overall radiochemical yield above 20%. The same methodology was later on further expanded and applied to the preparation of other  $^{13}\text{N}$ -labeled nitrosothiols using conventional chemistry [35] and microfluidics chemistry [36]. In the latter case, as expected, higher yields could be obtained under equivalent experimental conditions. The nitrosation reaction was also applied by our research group to the preparation of  $^{13}\text{N}$ -labeled nitrosamines [37]. In this particular case, low yields were obtained probably due to the low nucleophilic character of secondary amines when compared to thiols. Hence, a pre-activation step by treatment with  $\text{Ph}_3\text{P}/\text{Br}_2$  was required (Figure 1.14), and four different  $^{13}\text{N}$ -nitrosamines could be obtained with acceptable radiochemical yields.

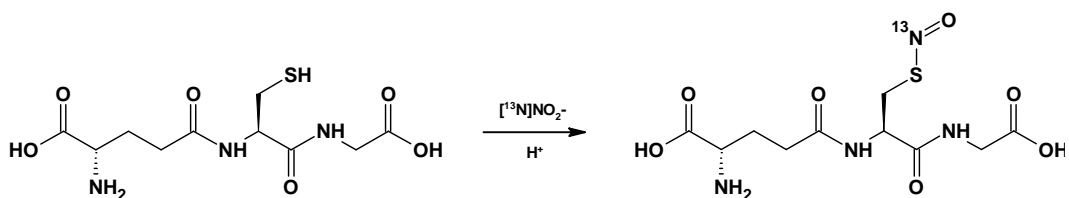


**Figure 1.13.** Synthesis of  $[^{13}\text{N}]\text{GSNO}$ .



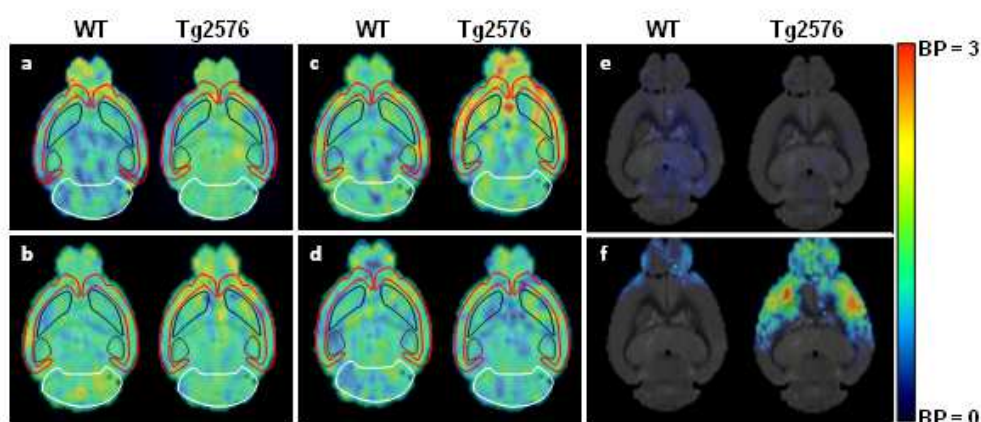
**Figure 1.14.** Activation of amines for subsequent production of  $^{13}\text{N}$ -labelled nitrosamines.

### 1.3.3.2. Radiosynthesis of $[^{13}\text{N}]\text{azo}$ compounds

The use of the labelling agent  $[^{13}\text{N}]\text{NO}_2^-$  has been recently used by our research group for the preparation of  $^{13}\text{N}$ -labeled azo compounds [38], using a two-step synthetic route. First,  $[^{13}\text{N}]\text{NO}_2^-$  was reacted with aromatic primary amines to generate the corresponding  $^{13}\text{N}$ -labeled diazonium salts, which were subsequently reacted with aromatic amines or phenols. In a posterior work, a library of compounds was synthesized and the resulting labelled azo compounds were assayed as  $\beta$ -Amyloid markers in a mouse model of Alzheimer disease [39] (see Table 1.3). Selective accumulation of the  $^{13}\text{N}$ -labelled azo derivatives 2, 3 and 5 (Table 1.3) could be detected in Tg2576 mice brain regions with high plaque load. Among these three radiotracers, compounds 2 and 3 showed good *in vivo* performance in PET assays (see Figure 1.15 for example of images).

**Table 1.3:** Library of  $^{13}\text{N}$ -labelled azo compounds evaluated as  $\beta$ -amyloid markers in ref [39].

Compound	Precursor A	Precursor B	Structure
1			
2			
3			
4			
5			

**Figure 1.15.** (a-d) PET images obtained with  $[^{13}\text{N}]$ azo derivatives 1 (a), 2 (b), 3 (c) and 5 (d) using Tg2576 and wild type (WT) animals; (e-f) parametric images of binding potential (BP) obtained after administration of compounds 1 (e) and 3 (f) in transgenic (Tg2576) and wild type (WT) animals.

#### 1.4. CONSIDERATIONS ABOUT NITROGEN-13

Nitrogen-13 has been historically “forgotten” as a useful radionuclide for the preparation of complex structures. Indeed, there are several limitations in its use both in the pre-clinical and clinical settings. Because of this, only a few groups in the world are working on

the development of new strategies for the preparation of  $^{13}\text{N}$ -labelled compounds. The major limitation of this radionuclide is its short half-life, which poses three main difficulties: (i) its use is restricted to those clinical and research organizations with access to a cyclotron. Nitrogen-13 has to be produced and used *on site*, and distribution from centralized production centres to surrounding facilities is unfeasible; (ii) because of this short half-life, extremely rapid and efficient methods have to be applied to the preparation of  $^{13}\text{N}$ -labelled radiotracers, to prevent significant decay-associated radioactivity loss; and (iii) even when the preparation of the radiotracer is feasible, the amount of radioactivity has to be sufficient for subsequent imaging studies; additionally, the biological half-life of the radiotracer should match the physical half-life of the isotope. In other words, nitrogen-13 can be only used to investigate fast *in vivo* processes. Besides the short half-life, nitrogen-13 has a high positron emission energy, which ultimately results in a high positron range (especially compared to e.g. fluorine-18). As a result, lower resolution images are obtained, and this can be critical in the case of imaging studies involving small rodents such as mice and rats.

It is worth mentioning that nitrogen-13 has also positive aspects. First, the stable isotopes of nitrogen ( $^{14}\text{N}$  and  $^{15}\text{N}$ ) are present in the majority of biological active molecules. This means that any biological molecule, *a priori*, can be labelled with nitrogen-13 in order to have a radiotracer with a chemical structure which is identical to that of the molecule to be investigated. Hence, incorporation of nitrogen-13 to the toolbox of PET chemists may provide unique opportunities to achieve labelling of molecules of interest in different positions, which may help in understanding certain aspects of *in vivo* behaviour, for example metabolism. Additionally, due to the short half-life of the radionuclide, repeated studies may be performed on the same individual within a short period of time and the radiation dose posed on the subject under investigation is minor when compared to longer-lived radionuclides.

The above mentioned inconveniences (i) and (ii) might be overcome in the next future. First, there is a growing interest in the development of a new generation of smaller (and hopefully cheaper and with lower investment requirements) cyclotrons. If this happens, more research centres might have access to their own a particle accelerator, facilitating the progressive implementation of a “dose on demand” PET scenario. Hence, short-lived isotopes may gain relevance. Such small cyclotrons will have particle energy limitations, which may hamper the production of nitrogen-13 using liquid targets and the  $^{16}\text{O}(\text{p},\alpha)^{13}\text{N}$  nuclear reaction. This nuclear reaction requires proton energies above 10 MeV to obtain significant amounts of radioactivity (see Figure 1.16 for activation function). However,



lower proton energies can be used to successfully produce nitrogen-13 when the  $^{13}\text{C}(p, n)^{13}\text{N}$  nuclear reaction is used (see Figure 1.17). In this case, irradiation of powder is required, and hence the development of new cyclotrons has to be paralleled by the development of easy to operate solid targets.

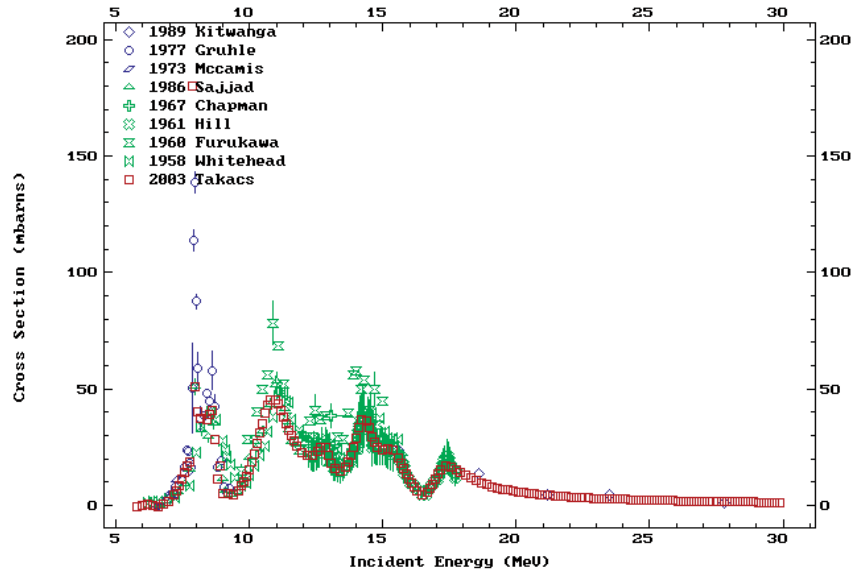


**Figure 1.16.** Excitation function for the  $^{16}\text{O}(p, \alpha)^{13}\text{N}$  nuclear reaction. Obtained from [40].

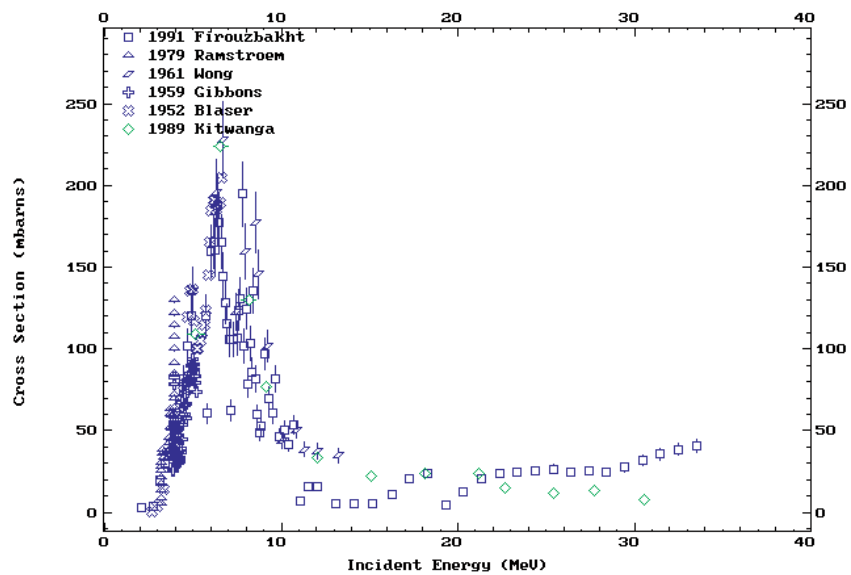


**Figure 1.17.** Excitation function for the  $^{13}\text{C}(p, n)^{13}\text{N}$  nuclear reaction. Obtained from [40].

The use of nitrogen-13 can also benefit from recent developments in the field of microfluidics. Under microfluidics conditions, more efficient incorporation of the radioisotope can be achieved in short times. This technology has been applied to the preparation of  $^{18}\text{F}$ - [41-43],  $^{11}\text{C}$ -[44, 45], and  $^{13}\text{N}$ -labelled compounds [36] with promising

results. Although the real application of microfluidics to the preparation of labelled compounds under Good Manufacturing Practices (GMP) and in sufficient quantity to approach *in vivo* experiments in humans needs still further development, realistic expectancies have been created and future improvement is quite likely.

The above mentioned problem (iii) is probably the most challenging. Due to the short half-life of the radionuclide, exploration of long-lasting biological phenomena with  $^{13}\text{N}$ -labelled molecules is not possible. However, literature data demonstrates that 60 minutes image acquisition is sufficient in many occasions to get very interesting information. For example, our research group demonstrated that  $^{13}\text{N}$ -labelled nanoparticles can provide relevant information about initial biodistribution [46]. In this work, a clear relationship between particle size and accumulation in major organs could be observed in very short image acquisition times (Figure 1.18).

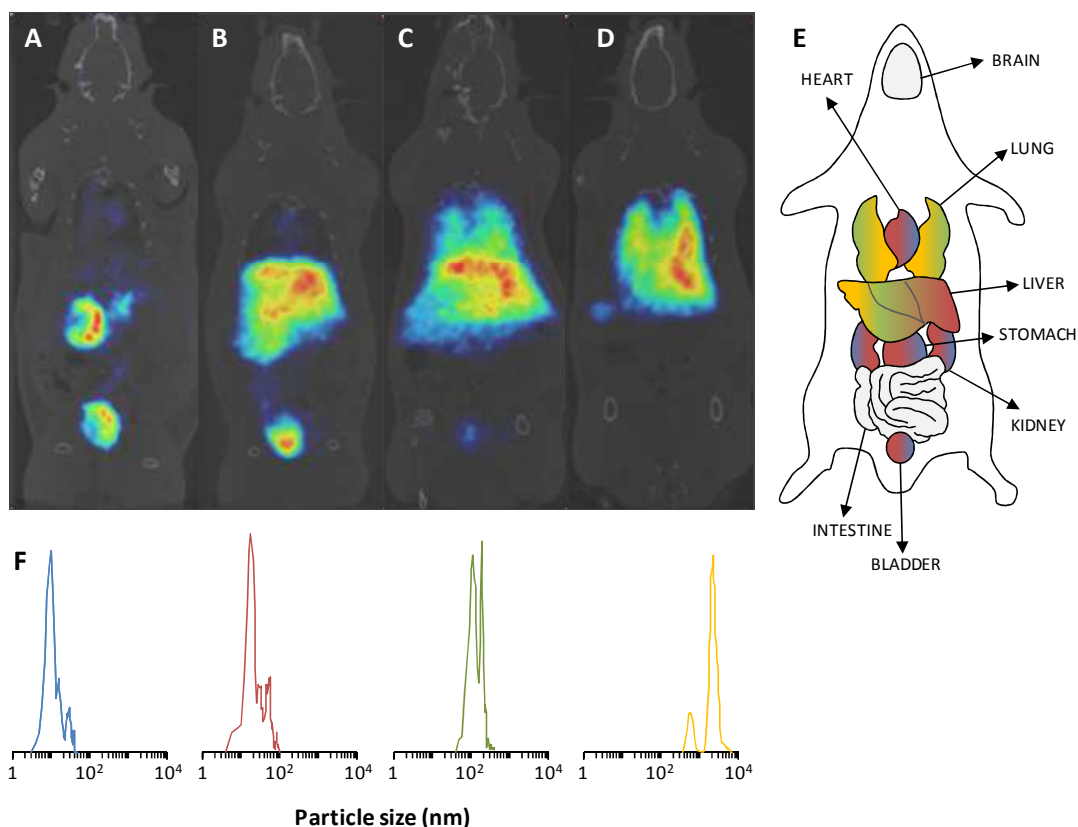


**Figure 1.18.** A-D: PET images of different sized  $^{13}\text{N}$ -labeled  $\text{Al}_2\text{O}_3$  NPs signal at  $t=60$  min. Computerised tomography (CT) images were adjusted along the Y axis for an appropriate fitting with the tracer distribution image; E: organ accumulation as a function of particle size, according to colour codes depicted in F; F: particle size distribution; grey colour in E indicates low accumulation irrespective of particle size.

Taking into account all these issues, it is expected that the use of  $^{13}\text{N}$ -labelled compounds will increase in the future and synthetic approaches which have been unexplored to date

will be investigated. Efficient strategies that were widely used in the past (e.g., enzymatic synthesis) might be revived considering the new technologies and possibilities of automation, as well as the novel tools for characterization of macromolecules. Dual labelling to gain additional information related to the short term metabolism of newly developed compounds might also become an interesting tool in research centres and to pharmaceutical industry. Hence, the results obtained within the frame of this PhD thesis might become very useful for the scientific community in the near future.

## 1.5. REFERENCES

1. Pérez-Campaña, C., *Direct activation of metal oxide nanoparticles: application to biodistribution studies using positron emission tomography*, in *Organic Chemistry I*, 2014, UPV/EHU. p. 130.
2. Miller, P.W., et al., *Synthesis of  $^{11}\text{C}$ ,  $^{18}\text{F}$ ,  $^{15}\text{O}$ , and  $^{13}\text{N}$  radiolabels for positron emission tomography*. *Angewandte Chemie - International Edition*, 2008. **47**(47): p. 8998-9033.
3. Itsenko, O., et al., *On  $^{11}\text{C}$  chemistry reviews - surveying and filling the gaps*. *Current Organic Chemistry*, 2013. **17**(19): p. 2067-2096.
4. Joliot, F. and I. Curie, *Artificial production of a new kind of radio-element*. *Nature*, 1934. **133**(3354): p. 201-202.
5. Cockcroft, J.D., C.W. Gilbert, and E.T.S. Walton, *Production of induced radioactivity by high velocity protons*. *Nature*, 1934. **133**(3357): p. 328.
6. Parks, N.J. and K.A. Krohn, *The synthesis of  $^{13}\text{N}$ -labeled ammonia, dinitrogen, nitrite, and nitrate using a single cyclotron target system*. *The International Journal Of Applied Radiation And Isotopes*, 1978. **29**(12): p. 754-757.
7. Wieland, B., et al., *In-target production of  $^{13}\text{N}$ ammonia via proton irradiation of dilute aqueous ethanol and acetic acid mixtures*. *International Journal of Radiation Applications and Instrumentation*, 1991. **42**(11): p. 1095-1098.
8. Firouzbakht, M.L., et al., *Mechanism of nitrogen-13-labeled ammonia formation in a cryogenic water target*. *Nuclear medicine and biology*, 1999. **26**(4): p. 437-441.
9. Mulholland, G.K., M.R. Kilbourn, and J.J. Moskwa, *Direct simultaneous production of  $^{15}\text{O}$ water and  $^{13}\text{N}$ ammonia or  $^{18}\text{F}$ fluoride ion by 26 MeV proton irradiation of a double chamber water target*. *International Journal of Radiation Applications and Instrumentation*, 1990. **41**(12): p. 1193-1199.
10. Korsakov, M.V., R.N. Krasikova, and O.S. Fedorova, *Production of high yield  $^{13}\text{N}$ ammonia by proton irradiation from pressurized aqueous solutions*. *Journal of Radioanalytical and Nuclear Chemistry*, 1996. **204**(2): p. 231-239.

11. Berridge, M.S. and B.J. Landmeier, *In-target production of [<sup>13</sup>N]ammonia: Target design, products, and operating parameters*. Applied Radiation and Isotopes, 1993. **44**(12): p. 1433-1441.
12. Krasikova, R.N., et al., *Improved [<sup>13</sup>N]ammonia yield from the proton irradiation of water using methane gas*. Applied Radiation and Isotopes, 1999. **51**(4): p. 395-401.
13. Elmaleh, D.R., D.J. Hnatowich, and S. Kulprathipanja, *A novel synthesis of <sup>13</sup>N-L-asparagine*. Journal of Labelled Compounds and Radiopharmaceuticals, 1979. **16**(1): p. 92-93.
14. Lembares, N., et al., *Rapid Enzymatic Synthesis of 10-Min <sup>13</sup>N-glutamate and Its Pancreatic Localization*. Journal of Nuclear Medicine, 1972. **13**(10): p. 1.
15. Cohen, M.B., et al., *Enzymatic Synthesis of <sup>13</sup>N L-Glutamine*. journal of Nuclear Medicine, 1972. **13**(6): p. 1.
16. Straatmann, M.G. and M.J. Welch, *Enzymatic synthesis of nitrogen 13 labeled amino acids*. Radiation Research, 1973. **56**(1): p. 48-56.
17. Cohen, M.B., et al., *Immobilized enzymes in the production of radiopharmaceutically pure amino acids labeled with <sup>13</sup>N*. Journal of Nuclear Medicine, 1974. **15**(12): p. 1192-1195.
18. Gelbard, A.S., et al., *Imaging of the human heart after administration of L-(N-13)glutamate*. Journal of Nuclear Medicine, 1980. **21**(10): p. 988-991.
19. Barrio, J.R., et al., *Synthesis and myocardial kinetics of N-13 and C-11 labeled branched-chain l-amino acids*. Journal of Nuclear Medicine, 1983. **24**(10): p. 937-944.
20. Cooper, A.J.L. and A.S. Gelbard, *The use of immobilized glutamate dehydrogenase to synthesize <sup>13</sup>N-labeled l-amino acids*. Analytical Biochemistry, 1981. **111**(1): p. 42-48.
21. da Silva, E.S., et al., *Efficient Enzymatic Preparation of <sup>13</sup>N-Labelled Amino Acids: Towards Multipurpose Synthetic Systems*. Chemistry - A European Journal, 2016. **22**(38): p. 13619-13626.
22. Tominaga, T., et al., *Preparation of <sup>13</sup>N-β-phenethylamine*. The International Journal Of Applied Radiation And Isotopes, 1985. **36**(7): p. 555-560.
23. Tominaga, T., et al., *Synthesis of <sup>13</sup>N-labelled amines by reduction of <sup>13</sup>N-labelled amides*. International Journal of Radiation Applications and Instrumentation, 1986. **37**(12): p. 1209-1212.
24. Finn, R.D., D.R. Christman, and A.P. Wolf, *A rapid synthesis of nitrogen-13 labelled amphetamine*. Journal of Labelled Compounds and Radiopharmaceuticals, 1981. **18**(6): p. 909-913.

25. Kothari, P.J., et al., *Synthesis of nitrogen-13 labeled alkylamines via amination of organoboranes*. International Journal of Radiation Applications and Instrumentation, 1986. **37**(6): p. 469-470.
26. de Spiegeleer, B., et al., *Microscale synthesis of nitrogen-13-labeled cisplatin*. Journal of Nuclear Medicine, 1986. **27**(3): p. 399-403.
27. Ginos, J.Z., et al., *[<sup>13</sup>N]Cisplatin PET to assess pharmacokinetics of intra-arterial versus intravenous chemotherapy for malignant brain tumors*. Journal of Nuclear Medicine, 1987. **28**(12): p. 1844-1852.
28. Saji, H., et al., *Synthesis and biological evaluation of a <sup>13</sup>N-labeled opioid peptide*. International Journal of Radiation Applications and Instrumentation, 1992. **19**(4): p. 455-460.
29. Krizek, H., P.V. Harper, and B. Mock, *Adapting the old to new needs: <sup>13</sup>N labeled urea*. Journal of Labelled Compounds and Radiopharmaceuticals, 1977. **13**(2): p. 207.
30. Kumata, K., et al., *One-pot radiosynthesis of [<sup>13</sup>N]urea and [<sup>13</sup>N] carbamate using no-carrier-added [<sup>13</sup>N]NH<sub>3</sub>*. Journal of Labelled Compounds and Radiopharmaceuticals, 2009. **52**(5): p. 166-172.
31. Kumata, K., et al., *Radiosynthesis of <sup>13</sup>N-labeled thalidomide using no-carrier-added [<sup>13</sup>N]NH<sub>3</sub>*. Journal of Labelled Compounds and Radiopharmaceuticals, 2010. **53**(2): p. 53-57.
32. Kumata, K., et al., *Radiosynthesis of [<sup>13</sup>N]dantrolene, a positron emission tomography probe for breast cancer resistant protein, using no-carrier-added [<sup>13</sup>N]ammonia*. Bioorganic and Medicinal Chemistry, 2012. **20**(1): p. 305-310.
33. Vavrek, M.T. and G.K. Mulholland, *Simple general synthesis of NCA nitrosothiols and nitrosamines*. Journal of Labelled Compounds and Radiopharmaceuticals, 1995. **37**(0): p. 2.
34. Llop, J., et al., *Synthesis of S-[<sup>13</sup>N]nitrosoglutathione (<sup>13</sup>N-GSNO) as a new potential PET imaging agent*. Applied Radiation and Isotopes, 2009. **67**(1): p. 95-99.
35. Gómez-Vallejo, V., et al., *Fully automated synthesis of <sup>13</sup>N-labeled nitrosothiols*. Tetrahedron Letters, 2010. **51**(22): p. 2990-2993.
36. Gaja, V., et al., *Synthesis of <sup>13</sup>N-labelled radiotracers by using microfluidic technology*. Journal of Labelled Compounds and Radiopharmaceuticals, 2012. **55**(9): p. 332-338.
37. Gómez-Vallejo, V., et al., *Efficient system for the preparation of [<sup>13</sup>N]labeled nitrosamines*. Bioorganic and Medicinal Chemistry Letters, 2009. **19**(7): p. 1913-1915.

38. Gómez-Vallejo, V., J.I. Borrell, and J. Llop, *A convenient synthesis of  $^{13}\text{N}$ -labelled azo compounds: A new route for the preparation of amyloid imaging PET probes*. *European Journal of Medicinal Chemistry*, 2010. **45**(11): p. 5318-5323.
39. Gaja, V., et al., *Synthesis and evaluation of  $^{13}\text{N}$ -labelled azo compounds for  $\beta$ -amyloid imaging in mice*. *Molecular Imaging and Biology*, 2014. **16**(4): p. 538-549.
40. *Cyclotron produced radionuclides: Physical characteristics and production methods*, in *Technical reports series n<sup>o</sup> 4682009*, International Atomic Energy Agency: Vienna. p. 196-203.
41. Zheng, M.Q., et al., *Synthesis of  $^{18}\text{F}$ FMISO in a flow-through microfluidic reactor: Development and clinical application*. *Nuclear medicine and biology*, 2015. **42**(6): p. 578-584.
42. Javed, M.R., et al., *High yield and high specific activity synthesis of  $^{18}\text{F}$ fallypride in a batch microfluidic reactor for micro-PET imaging*. *Chemical Communications*, 2014. **50**(10): p. 1192-1194.
43. Chen, S., et al., *Radiolabelling diverse positron emission tomography (PET) tracers using a single digital microfluidic reactor chip*. *Lab on a Chip - Miniaturisation for Chemistry and Biology*, 2014. **14**(5): p. 902-910.
44. Dahl, K., et al.,  *$^{11}\text{C}$ -carbonylation reactions using gas-liquid segmented microfluidics*. *RSC Advances*, 2015. **5**(108): p. 88886-88889.
45. Ungersboeck, J., et al., *Optimization of  $^{11}\text{C}$ DASB-synthesis: Vessel-based and flow-through microreactor methods*. *Applied Radiation and Isotopes*, 2012. **70**(11): p. 2615-2620.
46. Pérez-Campaña, C., et al., *Biodistribution of different sized nanoparticles assessed by positron emission tomography: A general strategy for direct activation of metal oxide particles*. *ACS Nano*, 2013. **7**(4): p. 3498-3505.

## **2. Justification and Objectives**





## 2. JUSTIFICATION AND OBJECTIVES

### 2.1. JUSTIFICATION

Emerging PET applications, together with the need for better, more efficient and even personalized diagnostic tools, have resulted in a boost in the demand for new molecular probes for biological targets currently inaccessible to this technique. The development of such molecular probes (radiotracers) requires a multidisciplinary vision and approach, which should start at target identification, structure design and development / implementation of radiolabelling strategies, followed by exhaustive *in vitro* and *in vivo* testing, ultimately leading to radiotracer validation.

The radiochemistry associated with the synthesis of radiotracers is far from trivial, especially for short half-lived radionuclides. Because of the limited availability of training programs in this field, PET centres and (radio)pharmaceutical companies compete for a limited pool of talent. This gap was identified by Prof. V. Gouverneur (University of Oxford), coordinator of the Marie-Curie FP7-PEOPLE-ITN action **RADIOMI** (2012-2016). In this initiative, six academic (University of Oxford in UK, King's College London in UK, University of Turku in Finland, VU University Medical Center in Amsterdam, Medical & Health Science Center in Debrecen, University Claude Bernard in Lyon and CIC biomaGUNE in San Sebastian) and two industrial partners (Advanced Accelerator Applications and GE Healthcare), all of them leading experts in the areas of chemistry and radiochemistry, pooled their expertises to implement a coordinated, first-class training program to produce new talent in PET radiochemistry, focused on the development of innovative radiolabelling strategies for the preparation of small molecules labelled with short-lived positron emitters, namely fluorine-18, carbon-11 and nitrogen-13, while spanning over a wide range of molecular formats. Besides establishing a cutting-edge, scientifically sound research program, this successful initiative aimed to provide transnational and cross-sectorial training to 15 ESRs and 3 ERs, covering different aspects of radiolabelling using positron emitters.

CIC biomaGUNE, a research institution located in San Sebastian and where the experimental part of the current PhD thesis was conducted, participated in such initiative. Due to the previous work and tracked experience of Dr. Llop's group in the field of <sup>13</sup>N-radiochemistry, the specific role of CIC biomaGUNE team within the project was to develop innovative labelling strategies using nitrogen-13. With that aim, two PhD students were selected. One of them, Eunice S. Da Silva, was focussed on developing innovative

enzymatic strategies for the preparation of radiolabelled amino acids. The project for the second PhD student, myself, Sameer M. Joshi, author of the work presented here, should focus on the development of novel strategies for the preparation of  $^{13}\text{N}$ -labelled compounds using the labelling agent  $[^{13}\text{N}]\text{NO}_2^-$ . Besides conducting the experimental work and getting involved in a cutting-edge research program at the local level, participation in the **RADIOMI** Initiative provided the opportunity to perform one stay at University of Oxford under the supervision of Prof. V. Gouverneur and a short stay at King's College London under the supervision of Prof. A. D. Gee, and to attend periodic meetings and different workshops, schools and international conferences, which have contributed to my overall education.

In this context, the first main goal of the current PhD was to develop strategies for the preparation of  $^{13}\text{N}$ -labelled azides, which can be used as suitable building blocks for the subsequent preparation of more complex molecules. For this, a methodology for the preparation of  $^{13}\text{N}$ -labelled azides was first implemented. Execution of the experimental part led to surprising results and because of this, certain mechanistic aspects of the synthesis of azides were investigated using  $^{13}\text{N}$ -radiolabelling together with computational studies, which were performed in collaboration with the group of Prof. Fernando Cossío (UPV-EHU). It is worth mentioning that the use of  $^{13}\text{N}$ -radiochemistry to investigate mechanistic aspects of reactions is unprecedented. The results obtained were published in *Chemical Communications* (see ref. [1]) and are the basis of chapter 3 of this PhD.

The knowledge gained during this first work was then applied to the development of suitable strategies for the preparation of  $^{13}\text{N}$ -labelled triazoles using (3+2) Huisgen cycloaddition between labelled aromatic azides and alkynes. A small library of compounds could be prepared, including one molecule with potential application as  $\beta$ -amyloid marker. The synthetic process for the preparation of this compound was fully automated. Moreover, the methodology was expanded to the formation of triazoles *via* reaction of labelled azides with aldehydes. This work, which is the basis of chapter 4 of the current PhD thesis, was published in *RSC Advances* (see ref. [2]).

The third experimental part of the PhD thesis consisted of developing innovative radiolabelling strategies for the preparation of  $^{13}\text{N}$ -labelled tetrazoles *via* (3+2) Huisgen cycloadditions. These reactions proceed slowly, and hence the first part of this work consisted of developing inorganic, nanostructured, copper-based heterogeneous catalysts in collaboration with Dr. Chandrashekhhar V. Rode (Chemical Engineering & Process Development Division, National Chemical Laboratory, Pune, India). These catalyst were

first tested in cold (non radioactive) conditions. After optimization of the experimental conditions and selection of the best catalyst, the experimental set up was then applied to the synthesis of labelled tetrazoles. Most of the experimental work was performed in CIC biomaGUNE, San Sebastain, Spain. However, the copper based heterogeneous catalysts reported in this chapter were synthesized in NCL, India. The manuscript has been prepared and has been submitted to a scientific journal (New Journal of Chemistry) for consideration for publication.

## 2.2. OBJECTIVES

As mentioned above, the general objective of this PhD thesis was the development of labelling strategies for the preparation of novel  $^{13}\text{N}$ -labelled radiotracers. To achieve this ambitious goal, the following specific objectives were defined:

- 1- To develop fast and efficient strategies for the synthesis, purification and characterization of  $^{13}\text{N}$ -labelled aromatic azides.
- 2- To investigate mechanistic aspects about the formation of aromatic azides using  $^{13}\text{N}$ -labelling and computational methods.
- 3- To apply the results obtained in objectives (1) and (2) to develop efficient strategies for the preparation of  $^{13}\text{N}$ -labelled triazoles using (3+2) cycloaddition with alkynes and aldehydes.
- 4- To implement a fully automated process for the production (synthesis, purification and formulation) of selected  $^{13}\text{N}$ -labelled triazoles.
- 5- To develop novel nanostructured copper based heterogeneous catalysts for the efficient production of tetrazoles.
- 6- To apply the most promising catalysts from objective (5) to the preparation of  $^{13}\text{N}$ -labelled tetrazoles.

## 2.3. REFERENCES

1. Joshi, S.M., et al., *Synthesis of radiolabelled aryl azides from diazonium salts: Experimental and computational results permit the identification of the preferred mechanism*. Chemical Communications, 2015. **51**(43): p. 8954-8957.
2. Joshi, S.M., et al., *Synthesis of  $^{13}\text{N}$ -labelled polysubstituted triazoles: Via Huisgen cycloaddition*. RSC Advances, 2016. **6**(111): p. 109633-109638.



### **3. Synthesis of $^{13}\text{N}$ -labelled azides**



### 3. SYNTHESIS OF $^{13}\text{N}$ -LABELLED AZIDES

#### 3.1. INTRODUCTION

Azide is an anion which contains three nitrogen atoms with the basic formula  $\text{N}_3^-$  (Figure 3.1a). The azide functional group can be represented by two resonance structures (Figure 3.1b). From a wide perspective, azides can be classified into two main groups: organic and inorganic azides. Azides are energy-rich molecules with many applications; however, it is worth mentioning that both organic and inorganic azides can be heat- and shock-sensitive and can explosively decompose with a small input of external energy; hence, extreme precaution is required while handling azides.

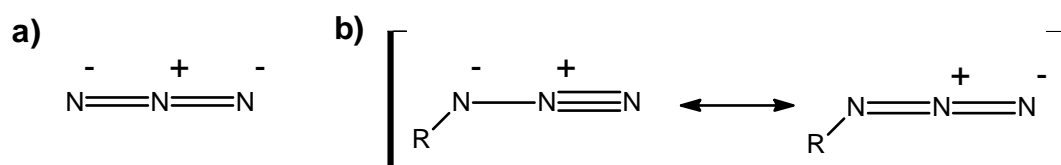


**Figure 3.1.** a) Basic formula of azide anion; b) resonance structures of azides.

##### 3.1.1. Inorganic azides

Inorganic azides can be prepared from sodium azide, which is an inorganic compound with formula  $\text{NaN}_3$ . Sodium azide, which under normal conditions is an ionic solid which exists in two crystalline forms (rhombohedral and hexagonal, [1]) is industrially prepared from metallic sodium and ammonia to form the sodium amine, which in a second step is reacted with nitrous oxide to produce sodium azide, ammonia and sodium hydroxide. An alternative production process better suited for laboratory application was developed by Curtius and Thiele [2-4]. In this process, a nitrite ester is converted into sodium azide using hydrazine.

##### 3.1.2. Organic azides

Organic azides are considered as powerful precursors for reactive species such as nitrenes and nitrenium ions as well as nitrogen-rich compounds such as aziridines, azirines, triazoles, triazolines and triazenes. Moreover, organic azides can be easily transformed into amines, isocyanates and other functional molecules, and recently they have received an increasing interest as valuable reagents within the concept of "Click Chemistry".

Organic azides can be prepared using different routes. The most important ones are briefly introduced in Table 3.1.

**Table 3.1.** Production of organic azides

Route	Scheme
Reaction of haloarenes with sodium azide by nucleophilic aromatic substitution reaction [5, 6].	
Reaction of diazonium salts with hydrazine [7, 8].	
Formation of arylazide by reaction of arene diazonium perbromides with ammonia [9, 10].	
Dutt-Wormall reaction, in which a diazonium salt initially reacts with a sulfonamide to form diazoaminosulfinate; subsequent hydrolysis results in the formation of the azide and sulfonic acid [11].	
Aromatic and aliphatic azides, acyl azides, and sulfonyl azides can be prepared by reaction of hydrazines with nitrosyl ions or their precursors $\text{N}_2\text{O}_4$ [12, 13].	
Cleavage of triazenes into azides [14].	
Addition of halogen azides to olefins. This reaction is a general synthetic process for the formation of alkenyl azides [15-17].	

In 1864, the preparation of the first organic azide (phenyl azide) was reported by Peter Grieb. Later on, these azides have become flexible intermediates and have gained remarkable interest [18-20]. A few years later Curtius developed a methodology in which



alkyl, aryl or acyl chlorides react with sodium azide in an aqueous solution to form acyl azides [21, 22] which give isocyanates *via* Curtius rearrangement. Additionally, acyl azide can also be prepared by the reaction of acylhydrazines with nitrous acid [13] as well as by the reaction of carboxylic acid with diphenylphosphorylazide (DPPA) [23].

**Table 3.2** Applications of organic azides

Reactions	Scheme
[3+2] cycloaddition of organoazides with alkynes to give triazoles [24].	
[3+2] cycloaddition of azides with nitriles to give tetrazoles [25].	
Formation of an amidic phosphine oxide by Staudinger ligation [26].	
Azidoalkyl-substituted epoxides undergo Schmidt reaction [27].	
Asymmetric synthesis of 2,3-diamino-3-phenylpropanoic acid derivatives by using Mitsunobu reaction [28].	
Preparation of pyrazoloisoquinoline by Aza-Wittig cyclization of a formyl group with the azide group of a 4-azido-1-(benzyloxy)-5-(2-formylphenyl)pyrazole [29].	

Azide  $RN_3$  as a functional group can be used in a wide variety of applications in organic chemistry [30] (see Table 3.2). In the 1950s and 1960s, the organic azides received considerable attention [14, 31] with new applications in the chemistry of the wide variety of azides such as acyl, aryl, and alkyl azides. Organic azides can be used in the preparation

of heterocyclic compounds. Also they can be used in synthesis of peptides [32, 33] as well as in pharmaceuticals [34]. Among organic azides, aryl azides have relatively high stability and therefore, can be used in industrial and biological field [35-37].

Organic azides can be used more effectively in Huisgen 1,3-dipolar azide-alkyne cycloadditions [38] and also can be used for the preparation of anilines, nitrenes and *N*-alkyl-substituted anilines [39], and have been employed in the preparation of biologically active compounds and in the synthesis of natural products [40, 41]. The number of articles reporting on the use of organic azides has continuously increased in the last years. Currently, there are more than 1000 publications per year.

One of the most important applications of organic azides is in the preparation of triazoles and tetrazoles by reaction with alkynes [24] and nitriles [25], respectively. They are also employed in a wide variety of well known reactions such as Staudinger ligation [26], Hemetsberger-Knittel [42], Schmidt [27], Mitsunobu [28] and Wittig (aza- Wittig) reactions [29].

### 3.2. AIM AND OBJECTIVES

As mentioned above, organic azides and particularly phenyl azides have many applications in organic synthesis. However their use in the preparation of radiolabelled compounds to be evaluated *in vitro* or *in vivo* by means of nuclear imaging requires the development of strategies for the incorporation of positron or gamma emitters. In the research group where this PhD was conducted, there is a high interest in the development of novel strategies for the synthesis of <sup>13</sup>N-labelled compounds. In this context, access to labelled aromatic azides would provide access to a versatile tool which might be used in the preparation of a wide variety of labelled molecules.

To date, azides have been labelled with the stable isotope Nitrogen-15 and the label was used in the investigation of mechanistic aspects using nuclear magnetic resonance [43]. When we first explored in the literature potential routes for the preparation of <sup>13</sup>N-labelled aromatic azides, we first considered the possibility to apply the well known Dutt-Wormall reaction, which works very well under non-radioactive conditions and is based on the basic hydrolysis of aromatic diazoaminosulfinate, which can be easily synthesized from aromatic diazonium salt and arylsulfonamide or alkylsulfonamide. This reaction offered sub-optimal results under radioactive conditions, because two purification steps *via* liquid-liquid extraction were required; hence other alternatives were pursued. Finally, a convenient route based on the reaction of diazonium salts with *in situ* generated hydrazoic acid (by reaction of hydrazine monohydrate with sodium nitrite in acidic media)

was found in the literature. Considering that (i)  $[^{13}\text{N}]\text{NO}_2^-$  can be easily achieved by irradiation of pure water with high energy protons followed by reduction of the resulting species (mainly  $[^{13}\text{N}]\text{NO}_3^-$ ), and (ii)  $[^{13}\text{N}]\text{NO}_2^-$  is the precursor for the preparation of both diazonium salts and hydrazoic acid, we were in the lucky situation that two different approaches could be used for the preparation of labelled aryl azides, schematized in Figure 3.2.

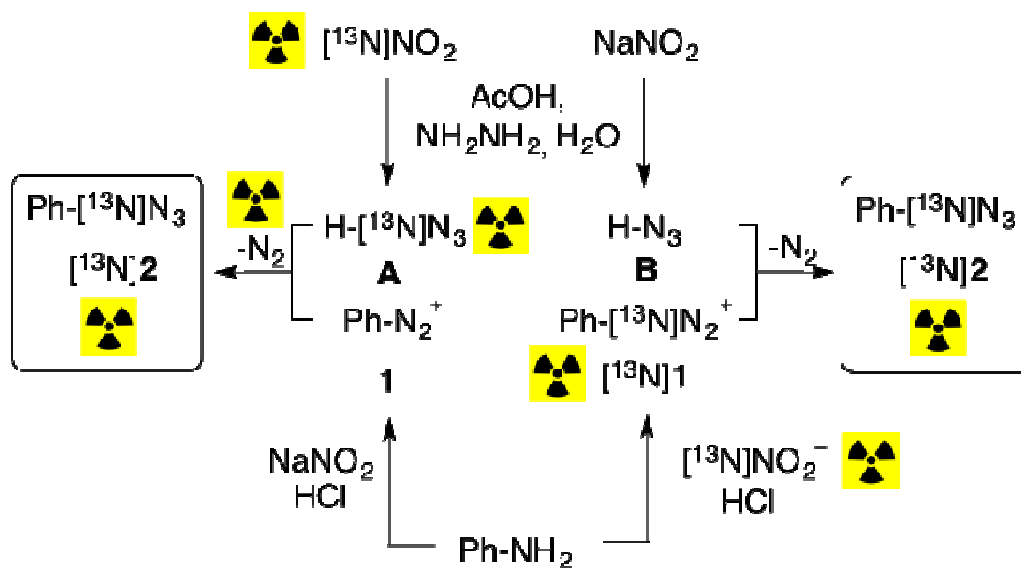


**Figure 3.2.** The two alternative strategies A and B followed to synthesize  $^{13}\text{N}$ -labelled phenyl azide ( $[\text{Ph}-^{13}\text{N}]\text{N}_2$ ) from  $^{13}\text{N}$ -labelled diazonium salt ( $[\text{Ph}-^{13}\text{N}]\text{N}_2$ ) in this thesis.

The first approach (A in the Figure) consists of reacting  $[\text{Ph}-^{13}\text{N}]\text{NO}_2^-$  with hydrazine monohydrate in acetic acid to yield the corresponding  $^{13}\text{N}$ -labelled hydrazoic acid, which is further reacted with the non-labelled diazonium salt to yield the desired labelled phenyl azide. The second approach (B in the Figure) consists of reacting  $[\text{Ph}-^{13}\text{N}]\text{NO}_2^-$  with an aromatic amine in acidic media to yield the corresponding  $^{13}\text{N}$ -labelled diazonium salt, which is further reacted with non-labelled hydrazoic acid to yield the desired labelled phenyl azide. In this reaction, nitrogen gas is released as a by-product, and release of  $[\text{Ph}-^{13}\text{N}]\text{N}_2$  could be a drawback in terms of overall radiochemical yield. In order to achieve the best method, we decided to explore both routes. As a result, the mechanistic study presented in this chapter could be conducted.

In this context, the following specific objectives were defined:

1. To develop a synthetic strategy for the preparation of  $^{13}\text{N}$ -labelled phenyl azides *via* Dutt-Wormall reaction.

2. To develop an optimized synthetic strategy for the preparation of  $^{13}\text{N}$ -labelled phenyl azides *via* reaction of diazonium salts with *in situ* generated hydrazoic acid.
3. To determine the mechanism of the reaction mentioned in objective 2, with the ultimate goal to establish the best radio-synthetic approach.
4. To proof the mechanism suggested by experimental results using computational methods.

**IMPORTANT REMARK:** All the experimental work included in this chapter was performed in CIC biomaGUNE, San Sebastian, Spain. In order to obtain the evidences about the most plausible reaction mechanism and get a better understanding of the experimental data, computational calculations were carried out. The Computational work reported in this chapter has been conducted by the group led by Prof. Dr. Fernando P. Cossío and by Dr. Abel De Cozar (Ikerbasque Research Fellow) at the University of the Basque Country (UPV/EHU). Because of this, details on computational methods are not provided in the experimental section and only the main results to confirm the mechanism of the reaction are presented in the section “results and discussion”.

### 3.3. MATERIALS AND METHODS

#### 3.3.1. General Information

Aniline (reagent plus grade 99%), sodium nitrite (ACS reagent, 97%), acetic acid (Reagentplus®, >99%), hydrazine hydrate solution (iodometric, 78-82%), and azidobenzene solution (0.5 M in tert-butyl methyl ether, >95%), methanesulfonamide (97%), *p*-toluenesulfonamide (Reagentplus®, >99%), sodium hydroxide, (ACS reagent, >97%), were purchased from Sigma-Aldrich and used without further purification. Hydrochloric acid (37%, extrapure, Ph. Eur.) and dichloromethane (synthesis grade) were purchased from Scharlau. Ultrapure water (Type I water, ISO 3696) was obtained from a Milli-Q® system (Merck Millipore).

#### 3.3.2. Radiochemistry: Synthesis of [ $^{13}\text{N}$ ]labelled phenylazide

##### 3.3.2.1. General

All procedures were carried out under EU standards in terms of radioprotection and following internal procedures. Initial experiments to set up experimental conditions were performed manually in a lead-shielded hot cell (Manuela, Comecer) especially designed to conduct manual operations.

### 3.3.2.2. Production of the primary labelling agent ( $[^{13}\text{N}]\text{NO}_2^-$ )

Nitrogen-13 was produced in an IBA Cyclone 18/9 cyclotron by irradiation of ultrapure water (1.8 mL) via the  $^{16}\text{O}(\text{p},\alpha)^{13}\text{N}$  nuclear reaction. The irradiated solution, containing mainly  $[^{13}\text{N}]\text{NO}_3^-$  and tiny amounts of  $[^{13}\text{N}]\text{NO}_2^-$  and  $[^{13}\text{N}]\text{NH}_4^+$ , was passed through a glass column filled with pre-treated cadmium (pellets, 15 g) to reduce  $[^{13}\text{N}]\text{NO}_3^-$  into  $[^{13}\text{N}]\text{NO}_2^-$ . Pre-treatment was carried out by sequential elution with 1 M hydrochloric acid solution (25 mL), purified water (35 mL), copper (II) sulphate pentahydrate solution (20 g/L, 25 mL), ammonium chloride solution (5 g/L, 25 mL) and purified water (25 mL). After the reduction step, the cadmium column was further rinsed with purified water (1 mL), the eluates were combined and used in subsequent steps.

During initial experiments, a sample of this solution (20  $\mu\text{L}$ ) was routinely analyzed by HPLC to monitor the reduction of  $[^{13}\text{N}]\text{NO}_3^-$  into  $[^{13}\text{N}]\text{NO}_2^-$ . The analysis was carried out using an Agilent 1200 series HPLC equipped with a quaternary pump, a multiple wavelength detector and a radiometric detector (Gabi, Raytest). An HP Asahipak ODP-50 (5  $\mu\text{m}$ , 125x4 mm, Teknokroma, Spain) was used as stationary phase, and a solution containing additive for ionic chromatography (15 mL) in a mixture water/acetonitrile (86/14, V = 1L) basified to pH = 8.6 with 1M sodium hydroxide solution was used as the mobile phase at a flow rate of 1 mL/min. Simultaneous UV ( $\lambda = 254 \text{ nm}$ ) and isotopic detection (Gabi, Raytest) were used. Retention times for  $[^{13}\text{N}]\text{NH}_4^+$ ,  $[^{13}\text{N}]\text{NO}_2^-$  and  $[^{13}\text{N}]\text{NO}_3^-$  were 1.1, 5.2 and 10.4 min, respectively.

### 3.3.2.3. Preparation of $^{13}\text{N}$ -labelled phenylazide via Dutt-Wormall reaction

Preparation of  $^{13}\text{N}$ -labeled phenyl azides via Dutt-Wormall reaction [11] was carried out by adapting an already reported methodology [44], based on the reaction of a diazonium salt with an aromatic sulfonamide. The whole synthetic procedure for the preparation of  $[^{13}\text{N}]\text{NO}_2^-$  was carried out using the procedure followed in section 3.3.2.2 (see above). The solution containing  $[^{13}\text{N}]\text{NO}_2^-$  was added drop-wise slowly to a second solution containing aniline (0.25 mmol) in ice-cold HCl (0.1mL of 37% HCl in 0.15mL water). The reaction for the formation of the diazonium salt was allowed to occur (4 minutes,  $T = 0^\circ\text{C}$ ). After extraction with dichloromethane to remove the excess of aniline, the aqueous layer of the reaction mixture was added drop wise to a vial pre-charged with an ice-cold solution of *p*-toluene sulphonamide (0.25 mmol) in NaOH (1.60 mmol in 1 mL water) and the reaction for the formation of  $^{13}\text{N}$ -labelled azide was allowed to occur for (1 minute,  $T = 0^\circ\text{C}$ ). Finally, the  $^{13}\text{N}$ -labelled azide was extracted with dichloromethane. The solvent was evaporated and after quenching the reaction by dilution with aqueous ammonium formate (pH=3.9), radiochemical conversion was determined by radio-HPLC, using an Agilent 1200

Series HPLC system with a multiple wavelength UV detector ( $\lambda = 254 \text{ nm}$ ) and a radiometric detector (Gabi, Raytest). A RP-C18 column (Mediterranean Sea18, 4.6x250 mm, 5  $\mu\text{m}$  particle size) was used as the stationary phase and ammonium formate (pH = 3.9) (A)/methanol (B) was used as the mobile phase. The following gradient was applied: t=0 min, 90%A/10%B; t=2 min, 90%A/10%B; t=4 min, 35%A/65%B; t=6 min, 20%A/80%B; t=12 min, 20%A/80%B; t=15 min, 90%A/10%B. The presence of the desired labelled specie was confirmed by co-elution with reference standard (retention time = 9.6 min).

#### 3.3.2.4. Preparation of $^{13}\text{N}$ -labelled phenylazide by reaction of hydrazoic acid with diazonium salt

The preparation of  $^{13}\text{N}$ -labeled phenylazide using this reaction was conducted under two different scenarios, noted as A and B in Figure 3.2.

For route B, the solution containing  $[^{13}\text{N}]\text{NO}_2^-$  was added drop-wise to a second solution containing aniline (23mg, 0.25 mmole) in HCl (0.1mL of 37% HCl in 0.15mL water). The reaction for the formation of the  $^{13}\text{N}$ -labelled diazonium salt was allowed to occur (1 minute, RT). In a separate vial, a mixture of sodium nitrite solution (17mg in 0.1mL water, 0.25 mmole), acetic acid (120  $\mu\text{L}$ , 1.98 mmole) and hydrazine monohydrate solution (70  $\mu\text{L}$ , 1.41 mmole) was prepared and added drop-wise to the previous solution and the reaction for the formation of  $^{13}\text{N}$ -labeled azide was allowed to occur for 1 min at RT. The activity ( $A_1$ ) was measured in a dose calibrator (PETDOSE HC, Comcer), the vial was flushed with nitrogen gas (1 minute) and the activity was measured again ( $A_2$ ). The amount of  $[^{13}\text{N}]\text{N}_2$  was calculated as  $A_2 - A_1$ . The reaction crude was analyzed by HPLC using an Agilent 1200 Series HPLC system with a multiple wavelength UV detector ( $\lambda = 254 \text{ nm}$ ) and a radiometric detector (Gabi, Raytest). A RP-C18 column (Mediterranean Sea18, 4.6x250 mm, 5  $\mu\text{m}$  particle size) was used as stationary phase and ammonium formate (pH = 3.9) (A)/methanol (B) was used as the mobile phase. The following gradient was used: t=0 min, 90%A/10%B; t=2 min, 90%A/10%B; t=4 min, 35%A/65%B; t=6 min, 20%A/80%B; t=12 min, 20%A/80%B; t=15 min, 90%A/10%B. The presence of the desired labelled specie was confirmed by co-elution with reference standard (retention time = 9.6 min). The amount of  $[^{13}\text{N}]$ phenylazide was determined as the product ( $A_2 \times A_0$ ), where  $A_0$  is the area under the peak for phenyl azide (radiometric detector, expressed as percentage with respect to all integrated peaks in the chromatogram). All radioactivity values were decay corrected to the same time point.

For route A, the solution of  $[^{13}\text{N}]\text{NO}_2^-$  prepared as mentioned above was added drop-wise to a solution containing hydrazine monohydrate solution (70  $\mu\text{L}$ , 1.41 mmole) and acetic

acid (120  $\mu\text{L}$ , 1.98 mmole), and the reaction was allowed to occur (1 minute, RT). In a separate vial, a solution of aniline (23mg, 0.25 mmole) in HCl (0.1mL of 37% HCl in 0.15mL water) was reacted with sodium nitrite (17mg in 0.1mL water, 0.25 mmole) for 1 minute at RT to form the non-radioactive diazonium salt. The first solution was added drop wise to the second solution (total duration 1 minute) and the reaction was allowed to occur (1 min, RT). Sample processing, identification of the labelled species and determination of the amount of  $[^{13}\text{N}]\text{N}_2$  and  $[^{13}\text{N}]\text{phenyl azide}$  was performed as in Route B (see above).

### 3.3.2.5. Analysis of the radioactive gas $[^{13}\text{N}]\text{N}_2$

The synthesis of  $^{13}\text{N}$ -labelled phenylazide was performed following the methodologies described above. However, before flushing the reaction vials with nitrogen gas, a sample of the gas from the sealed reaction vial was withdrawn with a gas-tight syringe and analyzed by radio-GC-MS. Analyses were performed on an Agilent 7820A network GC with an automatic loop injection system (loop volume = 250  $\mu\text{L}$ ) combined with an Agilent 5975c inert XL MSD with Triple axis detector. A J&W Poraplot column (length 27.5m, internal diameter 0.32 mm) was used as stationary phase. The inlet conditions were 150  $^\circ\text{C}$ , 25 psi and a flow rate of 3.5 mL/min using a 1:10 split injector with helium (99.9999%) as the carrier gas. The oven temperature was set of 36 $^\circ\text{C}$ . Total run time was 6 min (retention time = 1.45 min). Simultaneous detection using a radiometric detector (Gabi, raytest) and MS were used using a post-colum split. MS was operated in scan mode in the range 10-150 Da.

## 3.4. RESULTS AND DISCUSSION

### 3.4.1. Synthesis of $^{13}\text{N}$ -labelled azides by Dutt-Wormall reaction

The synthetic process for the preparation of  $^{13}\text{N}$ -labeled aryl azides *via* Dutt-Wormall reaction is shown in Figure 3.3.

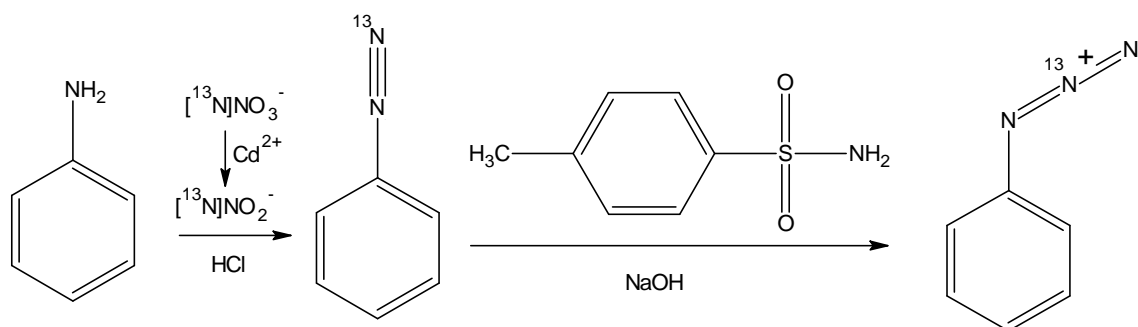


**Figure 3.3.** Scheme of the reaction used for the preparation of  $^{13}\text{N}$ -labelled phenylazide *via* Dutt-Wormall reaction.

In our first attempts, the reaction was carried out by reacting the  $^{13}\text{N}$ -labelled diazonium salt with methanesulfonamide under basic conditions. Different reaction times and reaction temperatures were assayed, but the formation of the desired labelled aryl azide could not be detected by radio-HPLC.

In view of these results, we decided to use *p*-toluene sulfonamide under basic conditions, which has proven efficient in Dutt-Wormall reactions under non-radioactive conditions [11]. In a first set of experiments, the purification step based on extraction with dichloromethane was omitted; in other words, the solution containing the  $^{13}\text{N}$ -labelled diazonium salt was directly added to *p*-toluene sulfonamide in 1M NaOH. However, the formation of the desired  $^{13}\text{N}$ -labelled phenyl azide could not be detected.

In order to check if the problem was the low concentration of labelled diazonium salt, carrier added tests (performed by addition of sodium nitrite to the  $[^{13}\text{N}]\text{NO}_2^-$  solution used for the preparation of the labelled diazonium salt) were also carried out. Again, no positive results could be obtained. However, after incorporation of the intermediate purification step based on liquid-liquid extraction, the  $^{13}\text{N}$ -labelled phenylazide could be obtained in chromatographic yields close of  $41\pm 6\%$ , suggesting that the large excess of starting, unreacted aniline may have a negative effect on the formation of the labelled azide. Interestingly, incorporation of sodium nitrite in 0.5:1 and 1:1 ratios with respect to aniline (carrier added conditions), improved the chromatographic yields up to  $48\pm 7\%$  and  $53\pm 8\%$ , respectively (see table 3.3). Although the specific activity of the final labelled compound was not measured at this stage, the addition of the carrier always results in a dramatic decrease in the specific activity values. After final extraction with dichloromethane, pure azide could be obtained in the organic phase (Figure 3.4). As it can be seen in Figure 3.5, the aqueous phase contained mainly unreacted  $[^{13}\text{N}]\text{NO}_3^-$  which was not reduced during the treatment in the cadmium column. The presence of an unidentified species at retention time = 4.6 minutes could be also detected.

**Table 3.3.** Radiochemical conversion values for the preparation  $^{13}\text{N}$ -labelled azides *via* Dutt-Wormall reaction with different carrier concentrations.

Entry	Carrier amount <sup>a</sup>	Chromatographic yield (%)
1	1:1	$53\pm 8$
2	1:0.5	$48\pm 7$
3	0	$41\pm 6$

<sup>a</sup> Molar ratios with respect to aniline; results are expressed as mean $\pm$ standard deviation, n=3.



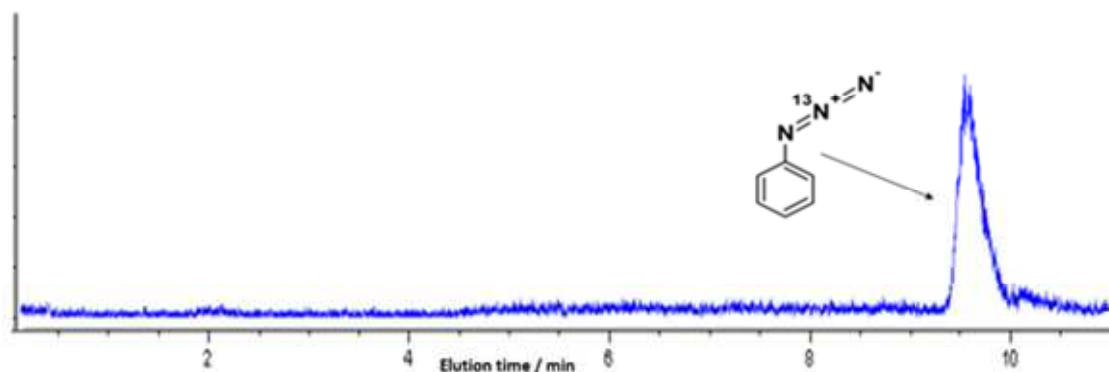


**Figure 3.4.** Chromatographic profile (radioactive detector) after extraction with dichloromethane (organic phase). The presence of the pure labelled azide can be observed.

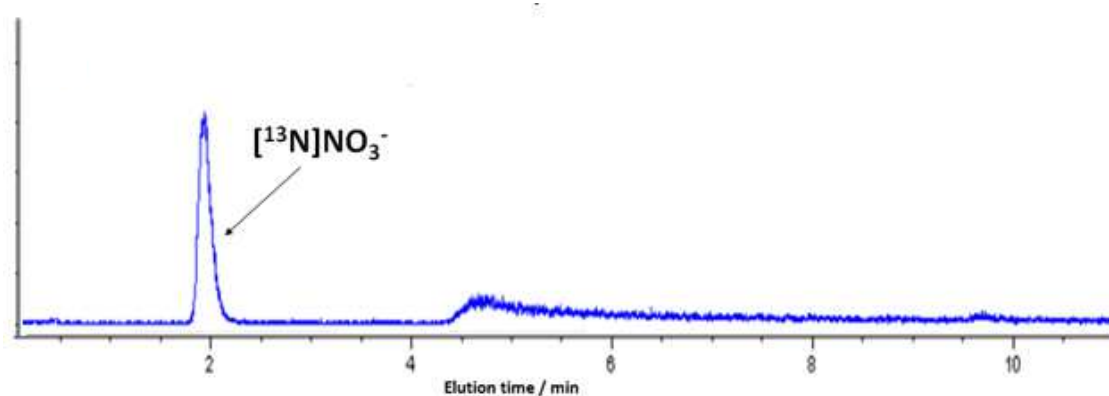


**Figure 3.5.** Chromatographic profile (radioactive detector) after extraction with dichloromethane (aqueous phase). The presence of  $[^{13}\text{N}]\text{NO}_3^-$  and one unidentified peak at retention time = 4.6 min can be observed.

### 3.4.2. Synthesis of $^{13}\text{N}$ -labelled azides by reaction of diazonium salts with hydrazoic acid

In view of the sub-optimal results obtained *via* Dutt-Wormall reaction, the synthesis of the labelled azides was envisaged by reaction of diazonium salts with *in situ* generated hydrazoic acid. In principle, at least three possible mechanisms can be envisaged for this reaction. The first one consists of a  $\text{S}_{\text{N}}^2\text{Ar}$  process similar to that observed for solvolysis reactions of diazonium salts [45-48], as indicated in Figure 3.6.

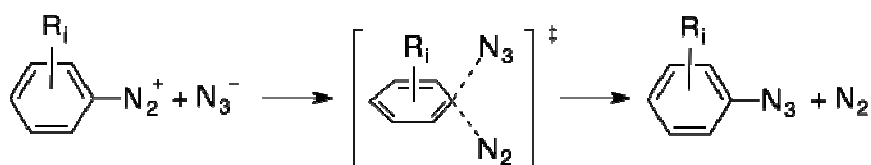


**Figure 3.6.** Potential mechanism of the reaction *via*  $\text{S}_{\text{N}}^2\text{Ar}$ .

A second plausible mechanism involves a thermal (3+2) cycloaddition to form a 1H-pentazole cycloadduct [49] that, in turn, can yield the product *via* a second retro-(3+2) reaction (Figure 3.7).

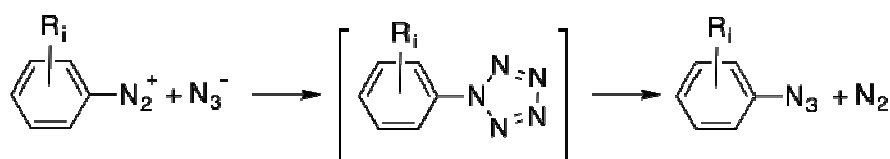


**Figure 3.7.** Potential mechanism of the reaction *via* thermal (3+2)cycloaddition.

Finally, an addition-elimination process *via* an acyclic intermediate can be also considered, according to Figure 3.8.

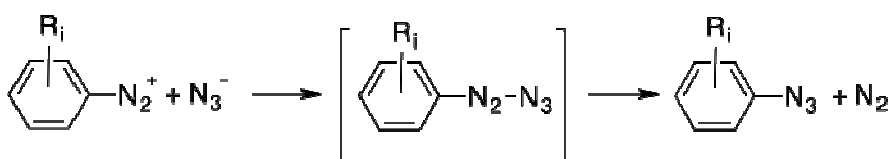


**Figure 3.8.** Potential mechanism of the reaction *via* addition-elimination process

Previous studies [43] suggest that this latter mechanism is quite plausible. The process involves the attack of the azide on the diazonium ion with formation of aryl pentazenes and/or pentazoles, which subsequently lose dinitrogen. Whether the reaction occurs through a concerted [3+2] mechanism or takes place step-wise, and the nature of the intermediate products are questions that remain unresolved. Studies performed with  $^1\text{H}$  and  $^{15}\text{N}$ -NMR spectroscopy suggest the formation of three isomeric aryl pentazenes [43]. One of them would lead to the formation of the aryl azide directly, while the other two would require the formation of intermediate ring structures to finally yield the aryl azide.

It is worth mentioning that when transitioning to radioactive conditions the reaction mechanism may have an impact on radiochemical yield. If the reaction proceeds *via* the mechanism shown in Figure 3.6, the radiolabelling information contained in the azide anion should be completely transferred to the corresponding aryl azide; however, if the radiolabelled diazonium salt is reacted with non-radioactive azide ion, labelled aryl azide would never be obtained. Similar reasoning can be applied to mechanisms shown in Figures 3.7 and 3.8; hence the position of the label is paramount to prevent formation of  $^{13}\text{N}[\text{N}_2]$  with the consequent decrease in labelling efficiency. With the aim of optimizing radiochemical yields, we envisaged a unique opportunity to further explore the mechanism of this reaction.

Both synthetic strategies (noted as A and B in Figure 3.2) led to the formation of  $^{13}\text{N}$ -labeled phenyl azide (see Figure 3.9). However, the amount of radioactive gas generated during the reaction, determined as the difference between  $A_1$  and  $A_2$ , and referred to the total amount of  $^{13}\text{N}$ -labelled azide (the latter calculated as the product  $A_2 \times A_{UC}$ , where  $A_{UC}$  is the area under the peak for phenyl azide as measured in the radiometric detector and expressed as percentage with respect to all integrated peaks in the chromatogram) was  $100.3 \pm 1.7\%$  and  $4.0 \pm 1.1\%$  for strategies A and B, respectively. Analysis of the flushed gas by radio-GC-MS showed the presence of a single radioactive peak, which was identified as  $[^{13}\text{N}]\text{N}_2$  while the amount of labelled azide obtained in route B was twice the amount obtained in A. These results confirm that approximately half of the radioactivity is lost as  $[^{13}\text{N}]\text{N}_2$  when route A is followed, while the information of the radiolabel is almost quantitatively transferred to the azide under route B (Figure 3.2).

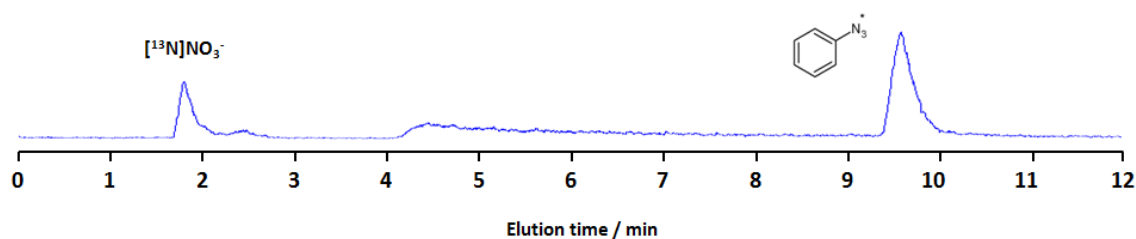


**Figure 3.9:** HPLC Chromatographic profile of the reaction mixture. The labelled azide appears at  $t=9.6$  min.

The experimental data completely discard the reaction mechanism based on  $\text{S}_{\text{N}}2\text{Ar}$  (Figure 3.6) and cleavage of the C-heteroatom bond, which would lead to complete radioactivity loss (as  $[^{13}\text{N}]\text{N}_2$ ) when route B is followed. On the other hand, they strongly suggest that the formation of the intermediate ring (Figure 3.7) is not taking place; in such a case,  $[^{13}\text{N}]\text{N}_2$  would be detected in significant amount (c.a. 100% with respect to the final amount of labelled aryl azide) when route B was used.

It is worth mentioning that the maximum amount of labelled azide was obtained when Route B was followed (Figure 3.2), with the radiolabel almost quantitatively transferred to the azide. Therefore, this route was considered as the most appropriate to achieve optimal results.

## 3.4.3. Computational Results

In view of the experimental results described above, we performed DFT [50] calculations on the parent  $\text{PhN}_2^+(\mathbf{1}) + \text{N}_3^- \rightarrow \text{PhN}_3(\mathbf{2}) + \text{N}_2$  reaction in order to obtain evidences about the most plausible reaction mechanism and get a better understanding of the experimental data. A M06-2X [51, 52] (PCM) [53, 54] /def2-TZVPP [55] study of the reactants in aqueous solution revealed the presence of a local minimum associated with a weak complex formed denoted as **RC** in Figure 3.10.

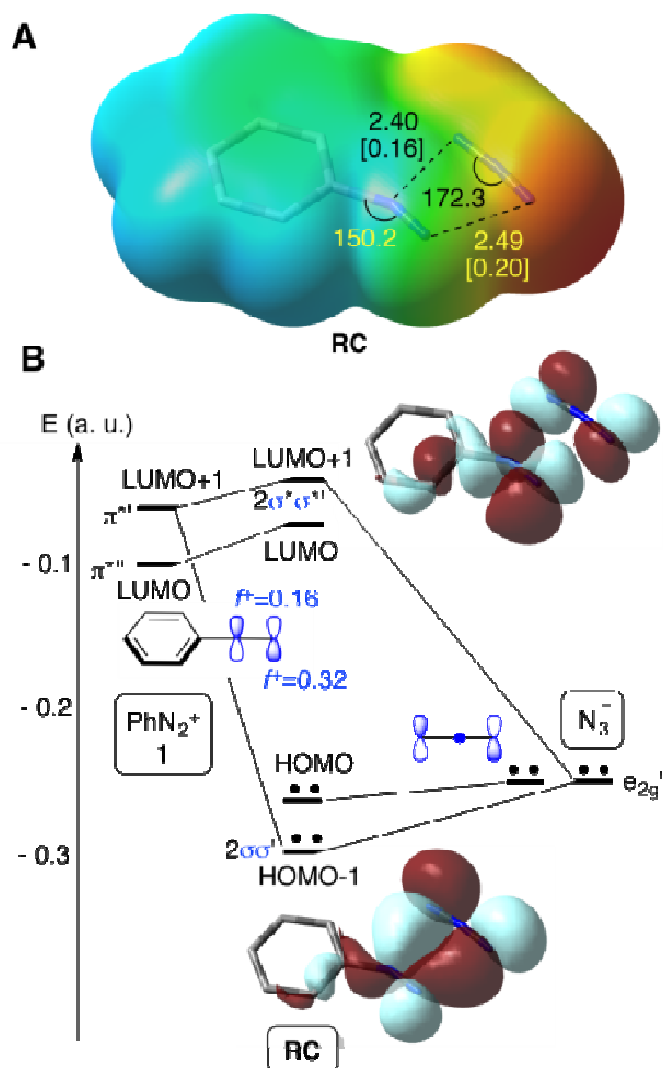


**Figure 3.10.** (A) Electrostatic potential and chief geometric features of complex RC associated with the interaction between azide anion and diazonium cation **1**. Bond distances and angles are given in Å and deg., respectively. Numbers in square brackets are the corresponding bond indices. (B) Selected Kohn-Sham molecular orbitals of RC. Descriptors  $f^+$  on the nitrogen atoms correspond to the local Fukui indices.

This stationary point on the potential energy surface (PES) consists of a charge transfer complex, in which both reactants are in close contact. The new N-N bond distances are ca. 2.4-2.5 Å (Figure 3.10 A), the respective Wiberg bond indices [56] being of ca. 0.2. This

weak bonding pattern stems from a two-electron interaction between one of the  $e_{2g}''$  molecular orbitals (MO's) of the azide anion and the in-plane  $\pi^*$  LUMO+1 of **1** (Figure 3.10B). The occupied MO's  $\pi^*$  of **1** and  $e_{1g}$  of  $\text{N}_3^-$  lead to a destabilizing four-electron interaction (not shown), thus resulting in a very weak bonding pattern between both reactants at **RC**. Actually, this stationary point is not stabilized with respect to the separate reactants at 298 K (Figure 3.11).

From these reactants we characterized saddle point **TS<sub>SN2</sub>** (Figure 3.11) with computed activation energy of ca. 27 kcal/mol. The geometric features of this transition structure are quite similar to those obtained for solvolysis reactions of aromatic diazonium salts [49]. In our case, however, there is an additional interaction between the diazonium and azide moieties (Figure 3.10 A). This remarkable barrier and our experimental results permit to discard the  $\text{S}_{\text{N}}^2\text{Ar}$  mechanism for this particular reaction.

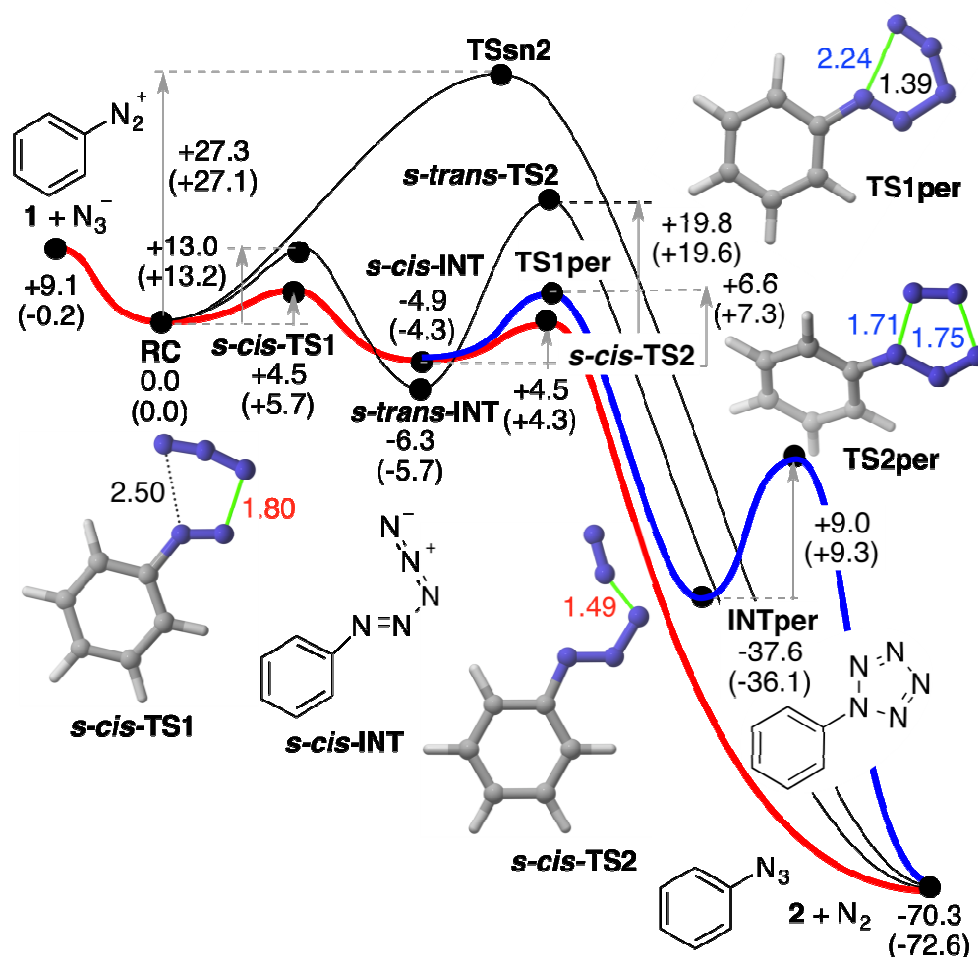


**Figure 3.11.** M06-2X/def2-TZVPP reaction profiles associated with the reaction between diazonium cation **1** and azide anion to yield phenyl azide **2** and dinitrogen. Numbers close to reactants, intermediates and products indicate the relative energies in kcal/mol. Numbers close to the arrows indicate the respective activation energies, in kcal/mol. Numbers in parentheses indicate the respective Gibbs energies, computed at 298 K, in kcal/mol. The lowest energy reaction paths are highlighted in red and blue.

The frontier MO's of the reactants at **RC** are also indicated in Figure 3.10 B and correspond to in-plane  $\sigma$ -MO's  $e_{2g}''$  and  $\pi^*$ . These computational data are compatible with a high electrophilicity associated with the terminal nitrogen of the diazonium moiety of **1**, with a local electrophilic Fukui index [57-59]  $f^+$  of 0.32 a.u. (Figure 3.10 B). The interaction between the terminal nitrogen atoms of both reactants according to the mechanism reported in Figure 3.8 lead to saddle points *s-cis*- and *s-trans*-**TS1** (Figure 3.11). The former transition structure was calculated to be ca. 7 kcal/mol less energetic than the latter. The chief geometric features of *s-cis*-**TS1** closely resemble those expected for an asynchronous transition structure associated with a (3+2) cycloaddition [60, 61]. However; all our attempts to connect directly *s-cis*-**TS1** with 2-phenyl-2*H*-pentazole **INTper** were unfruitful. Instead, this saddle point led to zwitterionic intermediate *s-cis*-**INT1**, from which we located transition structure **TS1per**. This latter saddle point led to 2-phenyl-2*H*-pentazole **INTper** (Figure 3.11), associated with this hypothetical (3+2) cycloaddition. From this local minimum we found saddle point **TS2per** leading to phenyl azide **2**. Although this latter transition structure associated with a retro-(3+2) cycloaddition is compatible with the reaction scheme gathered in Figure 3.7, it is important to note that **INTper** does not stem from **RC** but from *s-cis*-**INT1**, which constitutes the key intermediate of the less energetic reaction profiles. In addition, our calculations indicate that formation of **INTper** occurs with an activation barrier that is ca. 2 kcal/mol higher than that associated with formation of phenyl azide **2**.

Intrinsic Reaction coordinate [62] (IRC) scans from both *s-cis*- and *s-trans*-**TS1** led to the corresponding zwitterionic intermediates *s-cis*- and *s-trans*-**INT** (see Figures 3.12 and 3.13). The relative stabilities of these polar intermediates were found to be the opposite ones with respect to the corresponding transition structures. Therefore, the preferred route to yield azidobenzene **2** and dinitrogen occurs *via s-cis*-**TS2** in which the cleavage of the  $\text{PhN}_3(-)\text{-N}_2(+)$  delocalized bond is produced (Figure 3.11). This low barrier is associated with the formation of dinitrogen and azidobenzene **2**, two neutral stabilized species.

In order to confirm the preference for the mechanism outlined in Figure 3.8 we carried out Car-Parrinello [63] Molecular Dynamics (CPMD) [by using CPMD code (<http://www.cpmc.org>)] within the DFT framework, using the BLYP gradient-corrected functional [64, 65] and ultrasoft Vanderbilt pseudopotentials [66]. These simulations were carried out at different temperatures with a 1 fs time step for integration of equations of motion. Our CPMD results for the entire  $\text{PhN}_2^+(\mathbf{1})+\text{N}_3^- \rightarrow \text{PhN}_3(\mathbf{2})+\text{N}_2$  reaction confirmed that the reactants form *s-cis*-**INT** zwitterion in less than 100 fs at 100 K (Figure 3.14). This

intermediate is stable at this temperature within a time span of at least 1.2 ns. When the system was heated at ca. 300 K, the system reached *s-cis*-TS2 in ca. 300 fs to yield the reaction products [67], thus confirming the stepwise nature of the reaction *via* open intermediates of type INT. These results are in agreement with our experimental results and provide a rationale for the loss of radioactivity observed when radiolabelled azide anion was used following method A (Figure 3.2).

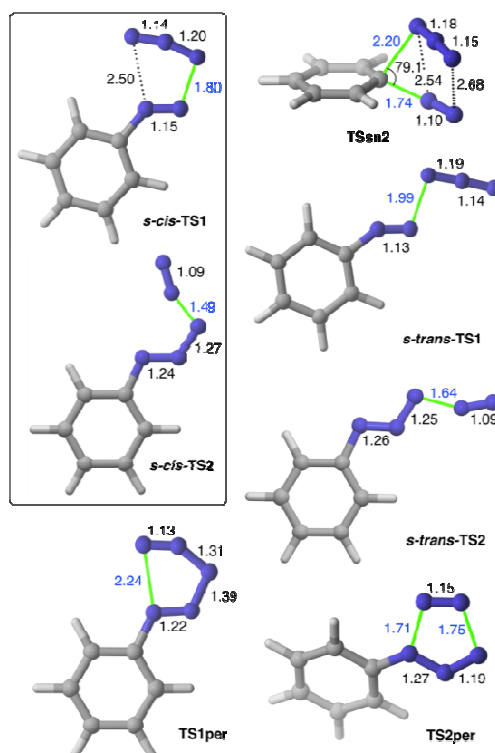


**Figure 3.12.** Chief geometric features (M06-2X/def2-TZVPP level of theory) of transition structures gathered in Figure 3.11. Bond distances and angles are given in Å and deg., respectively.

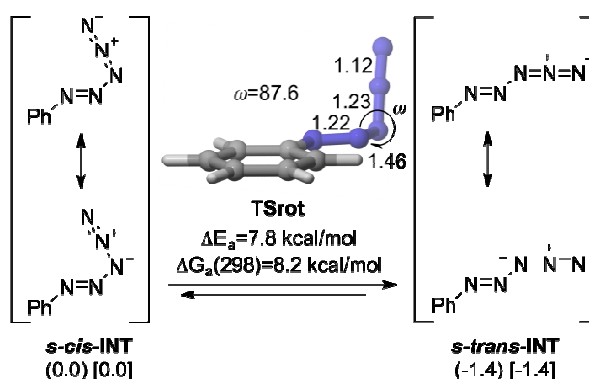


**Figure 3.13.** M06-2X/def2-TXVPP relative energies (in kcal/mol, numbers in parentheses) and relative Gibbs energies (at 298 K, in kcal/mol, numbers in square brackets) of zwitterionic intermediates *s-cis*- and *s-trans*-INT. The main geometric features and activation energies of transition structure **TSrot** that connects both conformers are also indicated. Bond distances and angles are given in Å and deg., respectively. Dihedral angle  $\omega$  describes the torsion about the  $\text{N}_2\text{-N}_3$  bond.

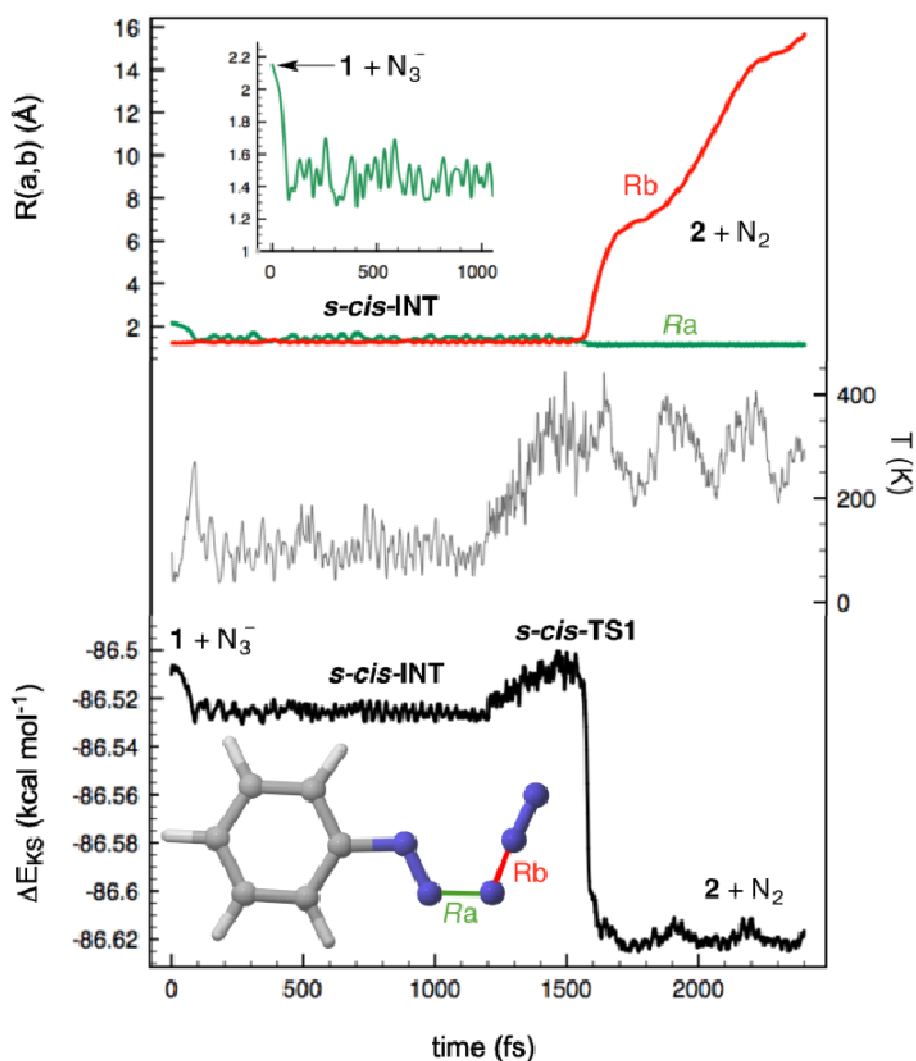


**Figure 3.14.** Car-Parrinello Molecular Dynamics (CPMD) plots of the reaction between diazonium cation **1** and azide anion to yield phenyl azide **2** and dinitrogen.

Kinetic simulations carried out using reaction paths highlighted in red and blue in Figure 3.11 indicate that ca. 99% of **2** stems from *s-cis-TS2*, whereas ca. 1 % of the reaction product is formed *via INTper*. These results are in good agreement with the release of  $[^{13}\text{N}]\text{N}_2$  obtained in our experimental studies following synthetic strategy shown in Figure 3.2, method A.

### 3.5. SUMMARY AND CONCLUSIONS

In conclusion, we have demonstrated using experimental and computational data that the formation of aryl azides from the corresponding diazonium salts occurs *via* a stepwise mechanism *via* acyclic zwitterionic intermediates. The use of the short-lived positron



emitter nitrogen-13 for the elucidation of reaction mechanisms is unprecedented. Additionally, we have demonstrated that the production of <sup>13</sup>N-labelled azides can be approached by using the methodology reported here. This provides unprecedented opportunities to tackle the preparation of more complex molecules, with the labelled heteroatom placed in the heterocycle, as demonstrated in the two following chapters.

### 3.6. REFERENCES

1. Stevens, E. and H. Hope, *A study of the electron-density distribution in sodium azide, NaN<sub>3</sub>*. Acta Crystallographica Section A: Crystal Physics, Diffraction, Theoretical and General Crystallography, 1977. **33**(5): p. 723-729.
2. Timén, Å.S., E. Risberg, and P. Somfai, *Improved procedure for cyclization of vinyl azides into 3-substituted-2H-azirines*. Tetrahedron Letters, 2003. **44**(28): p. 5339-5341.
3. Gilchrist, T.L. and R. Mendonça, *Addition of pyrimidine and purine bases to benzyl 2H-azirine-3-carboxylate*. Synlett, 2000. **2000**(12): p. 1843-1845.
4. Alves, M.J. and T.L. Gilchrist, *Generation and Diels-Alder reactions of t-butyl 2H-azirine-3-carboxylate*. Tetrahedron Letters, 1998. **39**(41): p. 7579-7582.
5. Lowe-Ma, C.K., R.A. Nissan, and W.S. Wilson, *Tetrazolo [1, 5-a] pyridines and Furazano [4, 5-b] pyridine 1-Oxides*. The Journal of organic chemistry, 1990. **55**(12): p. 3755-3761.
6. Stadlbauer, W., et al., *Thermal cyclization of 4-azido-3-nitropyridines to furoxanes*. Journal of Heterocyclic Chemistry, 2000. **37**(5): p. 1253-1256.
7. Noelting, E. and O. Michel, *Direkte Ueberführung von Aminen in Diazoimide mittels Stickstoffwasserstoffsäure*. Berichte der deutschen chemischen Gesellschaft, 1893. **26**(1): p. 86-87.
8. Noelting, E. and O. Michel, *Ueber die Einwirkung von Diazoverbindungen auf Hydrazine*. Berichte der deutschen chemischen Gesellschaft, 1893. **26**(1): p. 88-92.
9. Noelting, E., E. Grandmougin, and O. Michel, *Ueber die Bildung von Stickstoffwasserstoffsäure (Azoimid) aus aromatischen Azoimiden*. Berichte der deutschen chemischen Gesellschaft, 1892. **25**(2): p. 3328-3342.
10. Zincke, T. and P. Schwarz, *II. Ueber o-Dinitrosoverbindungen der Benzolreihe*. Justus Liebigs Annalen der Chemie, 1899. **307**(1-2): p. 28-49.
11. Dutt, P.K., H.R. Whitehead, and A. Wormall, *CCXLI.-The action of diazo-salts on aromatic sulphonamides. Part I*. Journal of the Chemical Society, Transactions, 1921. **119**(0): p. 2088-2094.

12. Kim, Y.H., K. Kim, and S.B. Shim, *Facile synthesis of azides: Conversion of hydrazines using dinitrogen tetroxide*. Tetrahedron Letters, 1986. **27**(39): p. 4749-4752.
13. Pozsgay, V. and H.J. Jennings, *Azide synthesis with stable nitrosyl salts*. Tetrahedron Letters, 1987. **28**(43): p. 5091-5092.
14. Boyer, J. and F. Canter, *Alkyl and Aryl Azides*. Chemical reviews, 1954. **54**(1): p. 1-57.
15. Hassner, A. and L.A. Levy, *Additions of Iodine Azide to Olefins. Stereospecific Introduction of Azide Functions1*. Journal of the American Chemical Society, 1965. **87**(18): p. 4203-4204.
16. Fowler, F.W., A. Hassner, and L.A. Levy, *Stereospecific introduction of azide functions into organic molecules*. Journal of the American Chemical Society, 1967. **89**(9): p. 2077-2082.
17. Hassner, A. and F.W. Fowler, *General synthesis of vinyl azides from olefins. Stereochemistry of elimination from. beta.-iodo azides*. The Journal of organic chemistry, 1968. **33**(7): p. 2686-2691.
18. Scriven, E.F. and K. Turnbull, *Azides: their preparation and synthetic uses*. Chemical reviews, 1988. **88**(2): p. 297-368.
19. L'abbe, G., *Decomposition and addition reactions of organic azides*. Chemical reviews, 1969. **69**(3): p. 345-363.
20. Griess, P., *On a New Class of Compounds in Which Nitrogen Is Substituted for Hydrogen*. Proceedings of the Royal Society of London, 1863. **13**: p. 375-384.
21. Curtius, T., *Ueber stickstoffwasserstoffsäure (azoimid) N<sub>3</sub>H*. Berichte der deutschen chemischen Gesellschaft, 1890. **23**(2): p. 3023-3033.
22. Curtius, T., *20. Hydrazide und Azide organischer Säuren I. Abhandlung*. Journal für Praktische Chemie, 1894. **50**(1): p. 275-294.
23. Shioiri, T., K. Ninomiya, and S. Yamada, *Diphenylphosphoryl azide. New convenient reagent for a modified Curtius reaction and for peptide synthesis*. Journal of the American Chemical Society, 1972. **94**(17): p. 6203-6205.
24. Jiang, Y., C. Kuang, and Q. Yang, *The use of calcium carbide in the synthesis of 1-monosubstituted aryl 1, 2, 3-triazole via click chemistry*. Synlett, 2009. **2009**(19): p. 3163-3166.
25. Cantillo, D., B. Gutmann, and C.O. Kappe, *Mechanistic Insights on Azide- Nitrile Cycloadditions: On the Dialkyltin Oxide- Trimethylsilyl Azide Route and a New Vilsmeier- Haack-Type Organocatalyst*. Journal of the American Chemical Society, 2011. **133**(12): p. 4465-4475.

26. Saxon, E. and C.R. Bertozzi, *Cell surface engineering by a modified Staudinger reaction*. Science, 2000. **287**(5460): p. 2007-2010.
27. Lang, S., et al., *Amination of arenes through electron-deficient reaction cascades of aryl epoxyazides*. Organic letters, 2003. **5**(20): p. 3655-3658.
28. Lee, S.-H., et al., *Efficient asymmetric synthesis of 2, 3-diamino-3-phenylpropanoic acid derivatives*. Tetrahedron, 2001. **57**(11): p. 2139-2145.
29. Pawlas, J., et al., *Synthesis of 1-Hydroxy-Substituted Pyrazolo [3, 4-c]-and Pyrazolo [4, 3-c] quinolines and-isoquinolines from 4-and 5-Aryl-Substituted 1-Benzylloxypyrazoles*. The Journal of organic chemistry, 2000. **65**(26): p. 9001-9006.
30. Bräse, S., et al., *Organic azides: an exploding diversity of a unique class of compounds*. Angewandte Chemie International Edition, 2005. **44**(33): p. 5188-5240.
31. Smith, P.A., *The Curtius Reaction*. Organic Reactions, 1946.
32. KLAUSNER, Y.S. and M. BODANSZKY, *The azide method in peptide synthesis: its scope and limitations*. Synthesis, 1974. **1974**(08): p. 549-559.
33. Han, S.-Y. and Y.-A. Kim, *Recent development of peptide coupling reagents in organic synthesis*. Tetrahedron, 2004. **60**(11): p. 2447-2467.
34. Lin, T.-S. and W.H. Prusoff, *Synthesis and biological activity of several amino analogs of thymidine*. Journal of medicinal chemistry, 1978. **21**(1): p. 109-112.
35. Cai, S.X., et al., *Chlorinated phenyl azides as photolabeling reagents. Synthesis of an ortho, ortho'-dichlorinated arylazido PCP receptor ligand*. Bioconjugate chemistry, 1993. **4**(6): p. 545-548.
36. Cai, S.X., et al., *Development of highly efficient deep-UV and electron beam mediated cross-linkers: Synthesis and photolysis of bis (perfluorophenyl) azides*. Chemistry of materials, 1994. **6**(10): p. 1822-1829.
37. Meijer, E., S. Nijhuis, and F. Van Vroonhoven, *Poly-1, 2-azepines by the photopolymerization of phenyl azides. Precursors for conducting polymer films*. Journal of the American Chemical Society, 1988. **110**(21): p. 7209-7210.
38. Tron, G.C., et al., *Click chemistry reactions in medicinal chemistry: Applications of the 1, 3-dipolar cycloaddition between azides and alkynes*. Medicinal research reviews, 2008. **28**(2): p. 278-308.
39. Kumar, H.S., et al., *A novel and efficient approach to mono-N-alkyl anilines via addition of grignard reagents to aryl azides*. Tetrahedron Letters, 1999. **40**(47): p. 8305-8306.
40. Baran, P.S., A.L. Zografos, and D.P. O'Malley, *Short total synthesis of (±)-sceptrin*. Journal of the American Chemical Society, 2004. **126**(12): p. 3726-3727.

41. Tanaka, H., A.M. Sawayama, and T.J. Wandless, *Enantioselective total synthesis of ustiloxin D*. Journal of the American Chemical Society, 2003. **125**(23): p. 6864-6865.
42. HEMETSBERGER, H. and D. KNITTEL, *SYNTH. UND THERMOLYSE VON ALPHA-AZIDOACRYLESTERN, ENAZIDE 4. MITT.* Chemischer Informationsdienst, 1972. **3**(17).
43. Butler, R. and L. Burke, *Pentazole chemistry: the mechanism of the reaction of aryldiazonium chlorides with azide ion at -80°C: concerted versus stepwise formation of arylpentazoles, detection of a pentazene intermediate, a combined <sup>1</sup>H and <sup>15</sup>N NMR experimental and ab initio theoretical study*. Journal of the Chemical Society, Perkin Transactions 2, 1998(10): p. 2243-2248.
44. Siddiki, A.A., B.S. Takale, and V.N. Telvekar, *One pot synthesis of aromatic azide using sodium nitrite and hydrazine hydrate*. Tetrahedron Letters, 2013. **54**(10): p. 1294-1297.
45. García Martínez, A., et al., *The Mechanism of Hydrolysis of Aryldiazonium Ions Revisited: Marcus Theory vs. Canonical Variational Transition State Theory*. European Journal of Organic Chemistry, 2013. **2013**(27): p. 6098-6107.
46. Ussing, B.R. and D.A. Singleton, *Isotope effects, dynamics, and the mechanism of solvolysis of aryldiazonium cations in water*. Journal of the American Chemical Society, 2005. **127**(9): p. 2888-2899.
47. Cuccovia, I.M., et al., *Revisiting the reactions of nucleophiles with arenediazonium ions: dediazonation of arenediazonium salts in aqueous and micellar solutions containing alkyl sulfates and alkanesulfonates and an ab initio analysis of the reaction pathway*. Journal of the Chemical Society, Perkin Transactions 2, 2000(9): p. 1896-1907.
48. Wu, Z. and R. Glaser, *Ab initio study of the SN<sup>1</sup>Ar and SN<sup>2</sup>Ar reactions of benzenediazonium ion with water. On the conception of "unimolecular dediazonation" in solvolysis reactions*. Journal of the American Chemical Society, 2004. **126**(34): p. 10632-10639.
49. Kuprat, M., A. Schulz, and A. Villinger, *Arsa-Diazonium Salts With an Arsenic-Nitrogen Triple Bond*. Angewandte Chemie International Edition, 2013. **52**(28): p. 7126-7130.
50. Frisch, M., et al., *Gaussian 09, revision D. 01*, 2009, Gaussian, Inc., Wallingford CT.
51. Zhao, Y. and D.G. Truhlar, *Density functionals with broad applicability in chemistry*. Accounts of chemical research, 2008. **41**(2): p. 157-167.

52. Zhao, Y. and D.G. Truhlar, *The M06 suite of density functionals for main group thermochemistry, thermochemical kinetics, noncovalent interactions, excited states, and transition elements: two new functionals and systematic testing of four M06-class functionals and 12 other functionals*. Theoretical Chemistry Accounts, 2008. **120**(1-3): p. 215-241.
53. Miertuš, S., E. Scrocco, and J. Tomasi, *Electrostatic interaction of a solute with a continuum. A direct utilization of AB initio molecular potentials for the prevision of solvent effects*. Chemical Physics, 1981. **55**(1): p. 117-129.
54. Tomasi, J., B. Mennucci, and R. Cammi, *Quantum mechanical continuum solvation models*. Chemical reviews, 2005. **105**(8): p. 2999-3094.
55. Weigend, F. and R. Ahlrichs, *Balanced basis sets of split valence, triple zeta valence and quadruple zeta valence quality for H to Rn: design and assessment of accuracy*. Physical Chemistry Chemical Physics, 2005. **7**(18): p. 3297-3305.
56. Wiberg, K.B., *Application of the pople-santry-segal CNDO method to the cyclopropylcarbanyl and cyclobutyl cation and to bicyclobutane*. Tetrahedron, 1968. **24**(3): p. 1083-1096.
57. Fukui, K., *The path of chemical reactions-the IRC approach*. Accounts of chemical research, 1981. **14**(12): p. 363-368.
58. Ayers, P.W., W. Yang, and L.J. Bartolotti, *Fukui function*, in *Chemical reactivity theory: a density functional view* 2009, CRC Press.
59. Chattaraj, P.K., *Chemical reactivity theory: a density functional view* 2009: CRC press.
60. de Cózar, A. and F.P. Cossío, *Stereocontrolled (3+ 2) cycloadditions between azomethine ylides and dipolarophiles: a fruitful interplay between theory and experiment*. Physical Chemistry Chemical Physics, 2011. **13**(23): p. 10858-10868.
61. Fernández, I., F.P. Cossío, and F.M. Bickelhaupt, *Aromaticity and activation strain analysis of [3+ 2] cycloaddition reactions between group 14 heteroallenes and triple bonds*. The Journal of organic chemistry, 2011. **76**(7): p. 2310-2314.
62. Gonzalez, C. and H.B. Schlegel, *Reaction path following in mass-weighted internal coordinates*. Journal of Physical Chemistry, 1990. **94**(14): p. 5523-5527.
63. Car, R. and M. Parrinello, *Unified approach for molecular dynamics and density-functional theory*. Physical review letters, 1985. **55**(22): p. 2471.
64. Becke, A.D., *Density-functional exchange-energy approximation with correct asymptotic behavior*. Physical review A, 1988. **38**(6): p. 3098.
65. Lee, C., W. Yang, and R.G. Parr, *Development of the Colle-Salvetti correlation-energy formula into a functional of the electron density*. Physical review B, 1988. **37**(2): p. 785.

66. Vanderbilt, D., *Soft self-consistent pseudopotentials in a generalized eigenvalue formalism*. Physical review B, 1990. **41**(11): p. 7892.
67. Joshi, S.M., et al., *Synthesis of radiolabelled aryl azides from diazonium salts: experimental and computational results permit the identification of the preferred mechanism*. Chemical Communications, 2015. **51**(43): p. 8954-8957.

## **4. Synthesis of $^{13}\text{N}$ -labelled triazoles**





## 4. SYNTHESIS OF $^{13}\text{N}$ -LABELLED TRIAZOLES

### 4.1. INTRODUCTION

Triazoles are heterocyclic compounds with molecular formula  $\text{C}_2\text{H}_3\text{N}_3$ , having a five-membered ring with two carbon atoms and three nitrogen atoms. There are two sets of isomers that differ in the relative positions of the three nitrogen atoms: 1,2,3- and 1,2,4-triazoles. In 1,2,3- triazoles, the three adjacent nitrogen atoms occupy adjacent positions, and can exist in two different tautomeric forms, depending on the nitrogen atom with a hydrogen bonded to it (Figure 4.1).

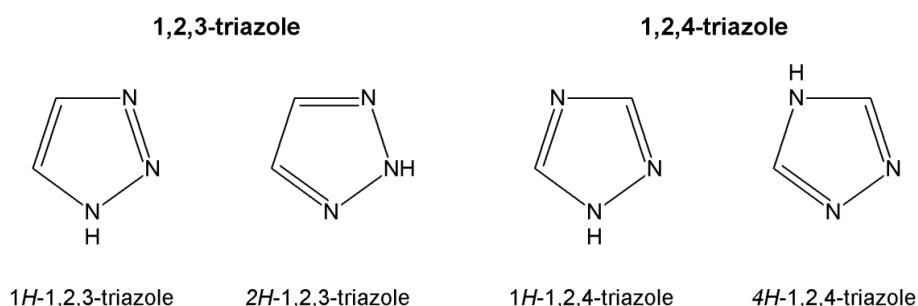


**Figure 4.1.** Chemical structure of 1,2,3- and 1,2,4-triazole in the two different tautomeric forms.

The 1,2,3-triazole core is stable against acidic and basic hydrolysis as well as against oxidative and reductive conditions [1], it has a high dipole moment [2] and participates actively in hydrogen bond formation as well as in dipole–dipole interactions [3]. These features make the variously substituted triazole moiety structurally similar to the amide (peptide) bond, but with more marked hydrogen-bonding donor and acceptor properties. Beyond mimicking the amide moiety, 1,2,3-triazoles can act as bioisosteres of trans-olefinic moieties [4] and have been used to replace the trans-olefinic moiety of resveratrol (anti-cancer, anti-inflammatory drug) [4] and diethylstilbestrol (non-steroidal estrogen), the latter leading to the synthesis of analogue molecules with estrogenic activity [5].

The above mentioned unique features turn 1,2,3-triazoles into convenient building blocks for the preparation of active drugs. One of the best-known examples of triazole-containing drugs is tazobactam (Figure 4.2, left) a commercially available  $\beta$ -lactamase inhibitor. Still in the antibiotics field, triazoles have been also used to improve pharmacokinetic properties of desired drugs. For example, cephalosporins with good oral availability were obtained by linking the triazole moiety to the cephalosporin (Figure 4.2, right).

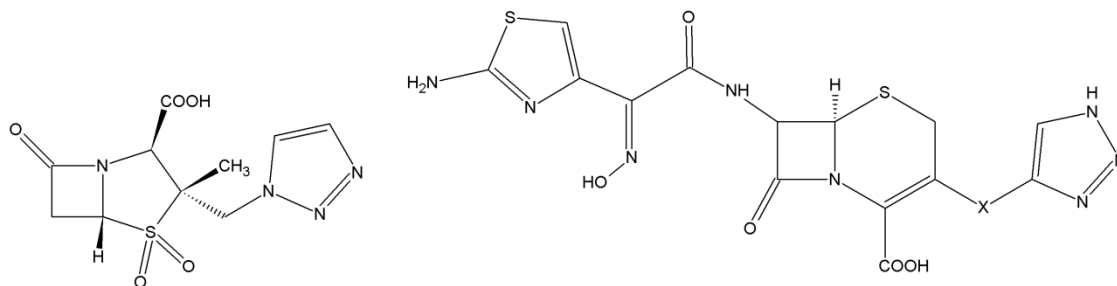


**Figure 4.2.** Example of  $\beta$ -lactamase inhibitors incorporating the 1,2,3-triazole moiety; left: tazobactam; right: example of a cephalosporin incorporating the triazole ring.

Beyond the antibiotics area, 1,2,3-triazoles have been assayed as anticancer agents, antimycotic agents, anthelmintic agents, potassium channel activators, protein kinase inhibitors, histone deacetylase (HDAC) inhibitors, ligands for specific receptors and antiviral agents, among others. Interestingly, polysubstituted triazoles have also shown promising properties to bind  $\beta$ -Amyloid aggregates (Figure 4.3). An excellent review covering the multiple biological applications of triazoles has been recently published [6]. In view of the multiple applications of triazole rings in the preparation of drugs, it is clear that the development of a method for the preparation of triazoles radiolabelled with positron emitters might become a powerful tool for the fast, *in vivo* and non-invasive evaluation of triazole-containing, newly developed drug candidates.

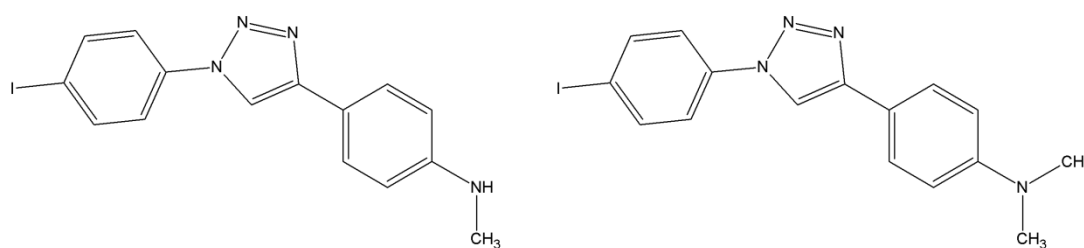


**Figure 4.3.** Example of substituted 1,2,3-triazoles with the capacity to bind  $\beta$ -Amyloid aggregates. Left: 4-[1-(4-iodophenyl)-1H-1,2,3-triazol-4-yl]-N-methylaniline; right: 4-[1-(4-iodophenyl)-1H-1,2,3-triazol-4-yl]-N,N-dimethylaniline.

Because positron emitters usually have a short half-life, the utilization of fast and efficient synthetic strategies is paramount in order to obtain acceptable radiochemical yields and a sufficient amount of radioactivity suitable for the eventual use in pre-clinical or clinical imaging studies.

To date, several different strategies for the preparation of 1,2,3-triazoles have been developed. One of the most popular and widely used synthetic methodologies is the cycloaddition of azides and terminal alkynes (Figure 4.4) or aldehydes (Figure 4.5).

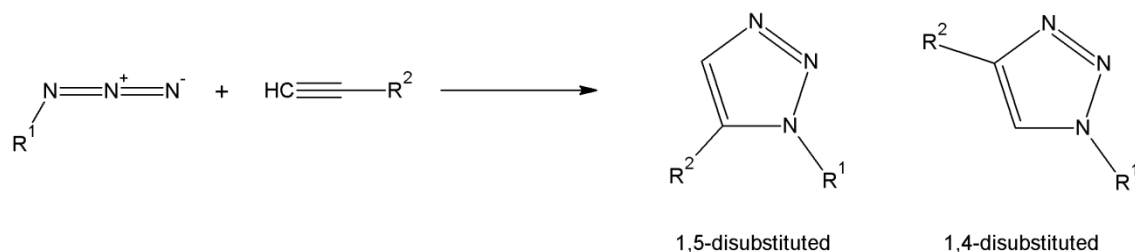


**Figure 4.4.** Preparation of triazoles by the (3+2) cycloaddition of azides with alkynes.

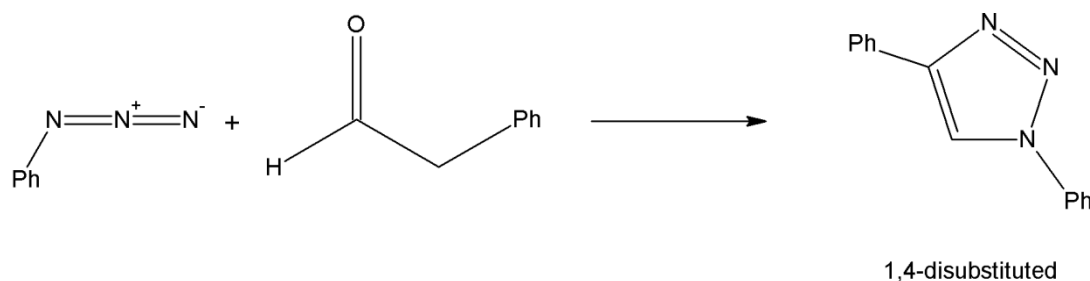


**Figure 4.5.** Preparation of triazoles by the organocatalytic (3+2) cycloaddition of azides with aldehydes.

The above mentioned reactions for the formation of triazoles fall within the general category of 1,3-dipolar cycloadditions, which involve a 1,3-dipole and a dipolarophile to form a five-membered ring. The first 1,3-dipolar cycloadditions were described at the end of the 19<sup>th</sup> century and beginning of the 20<sup>th</sup> century, following the discovery of 1,3-dipoles. In the 1960s, Rolf Huisgen developed the mechanistic investigation and described synthetic applications of the reaction [7]. Because of this, the reaction is nowadays referred to as the Huisgen cycloaddition, term that is most commonly used for those reactions resulting in the formation of 1,2,3-triazoles involving the condensation of azides and alkynes.

The Huisgen reaction is widely applied because it represents an excellent alternative for the preparation of 5-membered heterocycles. However, this reaction suffers from several drawbacks, which include the formation of a mixture of 1,4- and 1,5-regioisomers [1], which might be difficult to isolate; additionally, the reaction requires long reaction times and heating for completion under non catalytic conditions. In 2002, two research groups

reported independently the copper(I) catalyzed alkyne-azide cycloaddition (CuAAC) which proceeds as much as 10<sup>7</sup> times more rapidly than the non-catalyzed reaction [8-10]. More importantly, the reaction could be conducted at room temperature or under moderate heating, yielding only the formation of the 1,4-regioisomer.

Despite the advantages of CuAAC, the formation of two regioisomers has been observed in some occasions, with relative ratios close to 1:1. Because of this, many research groups have actively worked on the development of orthogonal cycloaddition reactions yielding exclusively 1,5-disubstituted regioisomer. In 2005, pentamethylcyclopentadienyl ruthenium(II) complexes (Cp\**Ru*), such as Cp\**Ru*Cl(PPh<sub>3</sub>)<sub>2</sub>, were reported to act as efficient catalysts for the cycloaddition reaction involving alkynes and azides. Unlike all of the previously reported catalysts, Cp\**Ru* complexes yielded only 1,5-substituted 1,2,3-triazoles [11]. Additionally, condensations using internal alkynes could be carried out with high efficiency. These reactions could not be achieved when copper catalysts were used. More recent works have shown that Cp\**Ru*Cl(PPh<sub>3</sub>)<sub>2</sub> or Cp\**Ru*Cl(COD) enable the condensation of primary and secondary azides with a broad range of terminal alkynes containing a range of functionalities, selectively producing 1,5-disubstituted 1,2,3-triazoles [12]. In 2013, the development of a mild, zinc-mediated method for the regioselective formation of 1,5-substituted 1,2,3-triazoles was reported [13].

## 4.2. AIM AND OBJECTIVES

The copper(I) alkyne-azide cycloaddition reaction has been widely used for the preparation of positron-emitter labelled molecules [14], including proteins [15, 16], peptides [17-21] and small molecules [22]. However, it has never been applied to the preparation of <sup>13</sup>N-labelled radiotracers.

In our aim to develop novel strategies for the preparation of <sup>13</sup>N-labelled radiotracers, and taking advantage of the methodology for the preparation of labelled azides developed in chapter 3 of this PhD thesis, we envisaged the possibility to use the Huisgen cycloaddition to approach the unprecedented preparation of <sup>13</sup>N-labelled heterocycles incorporating the <sup>13</sup>N atom in the heterocycle. To achieve this goal, the following specific objectives were established:

1. To develop a synthetic strategy for the preparation of <sup>13</sup>N-labelled polysubstituted triazoles **4.1-4.6** (Figure 4.6) by the reaction of <sup>13</sup>N-labelled aromatic azides with alkynes *via* (3+2) Huisgen cycloaddition.

- To develop a synthetic strategy for the preparation of  $^{13}\text{N}$ -labelled polysubstituted triazole **4.1** (Figure 4.6) by the reaction of  $^{13}\text{N}$ -labelled aromatic azides with aldehydes *via* (3+2) Huisgen cycloaddition.
- To implement an automated procedure for the preparation of  $^{13}\text{N}$ -labelled triazoles in a robust, safe and efficient fashion.

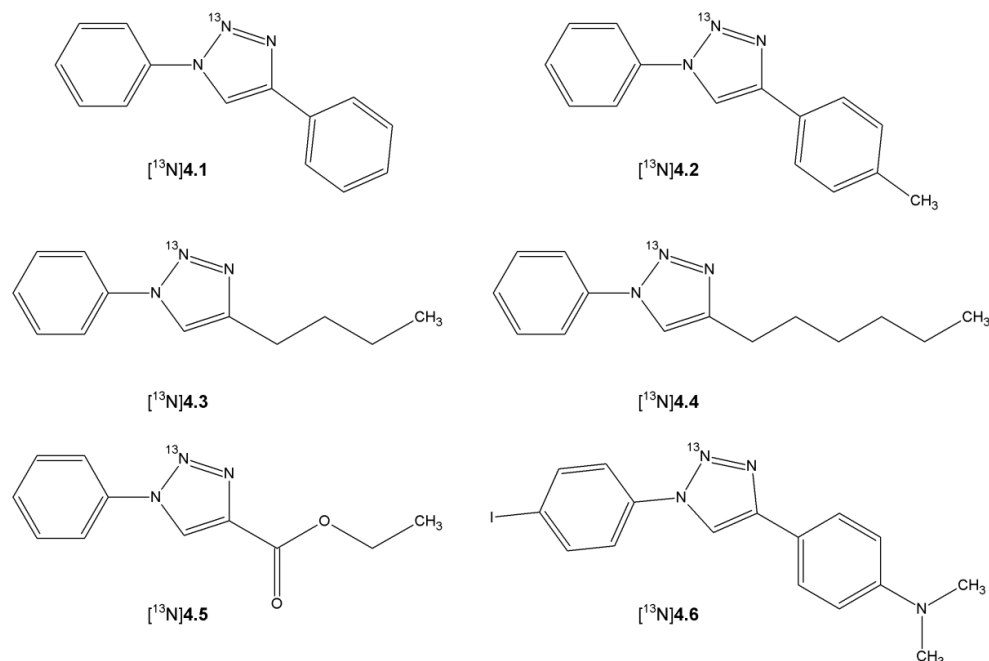


**Figure 4.6.**  $^{13}\text{N}$ -labelled triazoles prepared in this thesis.

### 4.3. MATERIALS AND METHODS

#### 4.3.1. General Information

Aniline (reagent plus grade 99%), 4-iodoaniline (98%), sodium nitrite (ACS reagent, 97%), acetic acid (Reagentplus®, >99%), hydrazine hydrate solution (iodometric, 78-82%), cyclohexylamine (Reagentplus®, >99%), paraformaldehyde (reagent plus grade crystalline), glyoxal solution (40 wt. % in H<sub>2</sub>O), sodium carbonate (ACS reagent, anhydrous), magnesium sulphate (ACS reagent, anhydrous, >99.5%), sodium sulphate (ACS reagent, anhydrous, >99%), tetrakis(acetonitrile)copper(I) hexafluorophosphate (97%), sodium tert-butoxide (97%), Celite® S (filter aid, dried, untreated), copper (II) sulphate pentahydrate (ACS reagent, >98%), copper (I) oxide (>99.99%), copper (I) iodide, purum, (>99.5%), N,N-Diisopropylethylamine (Reagentplus®, >99%), sodium ascorbate (Pharmaceutical secondary standard), 1,8-diazabicycloundec-7-ene (DBU, 98%), methanesulfonamide (97%), *p*-toluenesulfonamide (Reagentplus®, >99%), Sodium hydroxide, (ACS reagent, >97%), azidobenzene solution (0.5 M in tert-butyl methyl ether,

>95%), 1-azido-4-iodobenzene solution (0.5 M in tert-butyl methyl ether, >95%), 4-ethynyl-*N,N*-dimethylaniline (97%), phenyl acetylene (98%), ethyl propiolate (99%), 1-hexyne (97%), 1-octyne (97%), 4-ethynyltoluene (97%), phenylacetaldehyde (>90%), hydrochloric acid (37%, extrapure, Ph. Eur.), 1-hexanal (98%), 1-octanal (99%), tetrahydrofuran (absolute over molecular sieve, >99.5%), and dimethyl sulfoxide (anhydrous, >99.9%) were purchased from Sigma-Aldrich and used without further purification. Hexane (synthesis grade), ethyl acetate (synthesis grade), dichloromethane (synthesis grade), acetonitrile (HPLC grade) and diethyl ether (extra pure) were purchased from Scharlab (Sentmenat, Barcelona, Spain). Ultrapure water (Type I water, ISO 3696) was obtained from a Milli-Q® purification system (Merck Millipore).

#### 4.3.2. Synthesis of reference compounds 4.1-4.6

The synthesis of the reference compounds **4.1-4.6** was approached *via* (3+2) azide-alkyne cycloaddition following a previously published method [23]. In brief, the corresponding alkyne (2.54 mmol), CuSO<sub>4</sub>·5H<sub>2</sub>O (catalyst, 0.169 mmol) and an aqueous solution of sodium ascorbate (0.845 mmol in 1 mL) were added to a stirred solution of the corresponding azide (1.69 mmol). The vial was capped and submitted to microwave heating (80°C, 125W max, 10 min) using a Biotage® Initiator 2.0, 400 W and the reaction was monitored by TLC. Ultrapure water (25 mL) was added, the precipitate was filtered and washed with water (2 x 10 mL). Extraction with petroleum ether (40-60, 2 x 10 mL) was followed by evaporation using a rota-evaporator and the pure triazoles **4.1-4.6** were obtained.

The characterization of the pure compounds was carried out using Nuclear Magnetic Resonance (<sup>1</sup>H- and <sup>13</sup>C-NMR) and Mass Spectrometry (MS), and characterization data was compared to literature [23-25].

#### 4.3.3. Radiochemistry: Synthesis of compounds [<sup>13</sup>N]4.1-[<sup>13</sup>N]4.6

##### 4.3.3.1. General

All procedures were carried out under EU standards in terms of radioprotection and following internal procedures. Personnel protection measures and dose-exposure monitorization were applied over the entire duration of the experimental work. Initial experiments to set up experimental conditions were performed manually in a lead-shielded hot cell (Manuela, Comecer) especially designed to conduct manual operations. After optimization of the experimental conditions, the whole synthetic procedure for the preparation of the selected labelled compound was carried out using an automatic synthesis module (see below for experimental details).

#### 4.3.3.2. Production of the primary labelling agent

The whole synthetic procedure for the preparation of  $^{13}\text{N}$ NO<sub>2</sub><sup>-</sup> was carried out using same procedure followed in the chapter 3 (see above).

#### 4.3.3.3. Production of $^{13}\text{N}$ -labelled azide

The whole synthetic procedure for the preparation of  $^{13}\text{N}$ -labelled phenylazide and  $^{13}\text{N}$ -labelled 1-azido-4-iodobenzene were carried out using same procedure followed in route B, chapter 3. In brief, Nitrogen-13 was produced in an IBA Cyclone 18/9 cyclotron by irradiation of ultrapure water. The irradiated solution was passed through a glass column filled with pre-treated cadmium to reduce  $^{13}\text{N}$ NO<sub>3</sub><sup>-</sup> into  $^{13}\text{N}$ NO<sub>2</sub><sup>-</sup>. After the reduction step, the cadmium column was further rinsed with purified water (1 mL), the eluates were combined and used in subsequent steps. The solution containing  $^{13}\text{N}$ NO<sub>2</sub><sup>-</sup> was added to a second solution containing the corresponding aniline (0.25 mmol) in HCl (0.1mL of 37% HCl in 0.15mL water). In the case of  $^{13}\text{N}$ 4.6, MeOH (0.5 mL) was added to favour solubilisation of 4-iodoaniline. The reaction for the formation of the diazonium salt was allowed to occur for 1 minute at room temperature (RT). In a separate vial, a mixture of sodium nitrite solution (0.25 mmol in 0.1mL water), acetic acid (2.0 mmol) and hydrazine monohydrate solution (1.5 mmol) was prepared and added to the previous solution, and the reaction for the formation of  $^{13}\text{N}$ -labelled azide was allowed to occur for 1 min. Finally, the  $^{13}\text{N}$ -labelled azide was extracted with dichloromethane (1 mL) and the organic fraction was evaporated to dryness under a stream of nitrogen.

#### 4.3.3.4. Production of $^{13}\text{N}$ -labelled triazoles ( $^{13}\text{N}$ 4.1- $^{13}\text{N}$ 4.6)

##### Via (3+2) cycloaddition of azide and alkyne

Previously prepared [(Icy)<sub>2</sub>Cu]PF<sub>6</sub> catalyst (2 mg in 0.2 mL of acetonitrile) and the corresponding alkyne (0.14 mmol) were added to the  $^{13}\text{N}$ -labelled azide and the reaction was allowed to occur for 10 minutes at different temperatures (25°C or 50°C). After quenching the reaction by dilution with aqueous ammonium formate (pH=3.9), radiochemical conversion was determined by radio-HPLC, using an Agilent 1200 Series HPLC system with a multiple wavelength UV detector ( $\lambda = 254 \text{ nm}$ ) and a radiometric detector (Gabi, Raytest). A RP-C18 column (Mediterranean Sea18, 4.6x250 mm, 5  $\mu\text{m}$  particle size) was used as the stationary phase and ammonium formate (pH = 3.9) (A)/methanol (B) was used as the mobile phase (compounds  $^{13}\text{N}$ 4.1,  $^{13}\text{N}$ 4.3,  $^{13}\text{N}$ 4.4, and  $^{13}\text{N}$ 4.5). The following gradient was applied: t=0 min, 90%A/10%B; t=2 min, 90%A/10%B; t=4 min, 35%A/65%B; t=6 min, 20%A/80%B; t=12 min, 20%A/80%B; t=15 min, 90%A/10%B. For compounds  $^{13}\text{N}$ 4.2 and  $^{13}\text{N}$ 4.6, ammonium formate (pH =

3.9)/acetonitrile (40/60, V/V) and 0.1% TFA in water/acetonitrile (40/60 V/V) were used in isocratic mode, respectively. The presence of the desired labelled species was confirmed by co-elution with reference standards. Retention times for [ $^{13}\text{N}$ ]4.1-4.6 were 8.7, 12.5, 8.7, 10.0, 7.8 and 3.4 min, respectively.

#### Via (3+2) cycloaddition of azide and aldehyde

The  $^{13}\text{N}$ -labelled phenylazide was prepared following the above mentioned procedure. The catalyst (DBU, 0.021 mmol in 0.2 mL of DMSO) and phenylacetaldehyde (0.136 mmol) were then added and the reaction was allowed to occur for 10 minutes at different temperatures (25°C or 60°C). The reaction was quenched by addition of aqueous ammonium formate (pH=3.9), and radiochemical conversion was determined by radio-HPLC using the same methodology as above.

#### Incorporation of SPE-based intermediate purification step

The procedure for the preparation of  $^{13}\text{N}$ -labelled azide was the same as described above, but the reaction mixture containing the  $^{13}\text{N}$ -labelled azide was purified by solid phase extraction. This procedure was applied to compounds 4.1 and 4.6. With that aim, 7 mL of 0.5M sodium acetate solution ([ $^{13}\text{N}$ ]4.1) or ultrapure water ([ $^{13}\text{N}$ ]4.6) was added to the reaction mixture and the resulting solution was passed through a C-18 Cartridge (Sep-Pak C18 Plus, Waters). The cartridge was rinsed with ultrapure water (2mL) and subsequently flushed with helium gas for 1 minute. Finally the C-18 Cartridge was eluted with acetonitrile (1mL), the liquid was collected in a vial containing the corresponding alkyne and the catalyst and the resulting mixture was allowed to react for 10 min at 50°C. The reaction mixture was finally diluted with mobile phase and analyzed by HPLC using the conditions mentioned above.

#### 4.3.3.5. Automatic synthesis of [ $^{13}\text{N}$ ]4.6

Automatisation of the entire synthetic procedure was applied to the preparation of compound [ $^{13}\text{N}$ ]4.6, using a Tracerlab<sup>TM</sup> FX<sub>FE</sub> synthesis module (GE Healthcare) with modifications on its original configuration (See Figure 4.7). Vials 1-9, represented with green numbers in the Figure, were pre-loaded with the following reagents:

1. Vial 1: Empty
2. Vial 2: 1.0 mL of purified water
3. Vial 3: Mixture of 4-iodoaniline (0.25 mmol) + HCl 37% (0.1 mL) + purified water (0.15 mL) + MeOH (0.5 mL)
4. Vial 4: Sodium nitrite aqueous solution (0.25 mmol/1mL), acetic acid (2.0 mmol) and hydrazine monohydrate aqueous solution (1.5 mmol).



5. Vial 5: Purified water (7 mL)
6. Vial 6: Purified water (2 mL)
7. Vial 7: Acetonitrile (1 mL)
8. Vial 8: 4-ethynyl-N,N-dimethylaniline (0.14 mmol),  $[(\text{Icy})_2\text{Cu}]\text{PF}_6$  (10 mg).
9. Vial 9: Empty
10. Final Vial: Empty

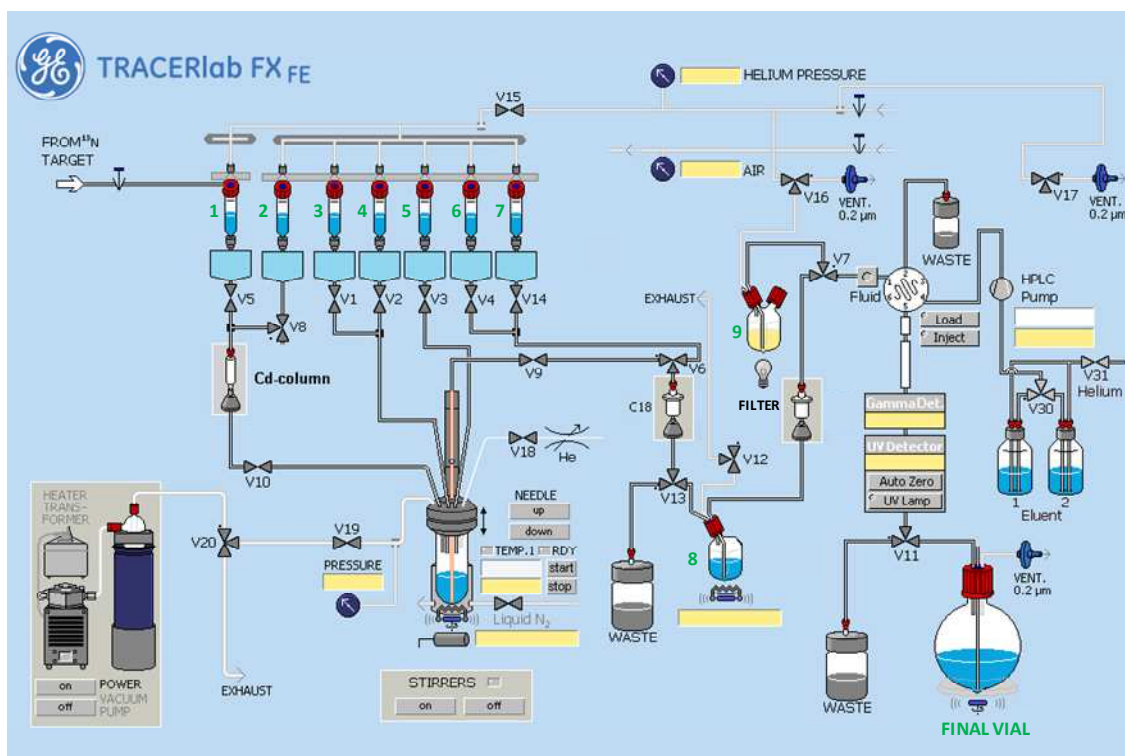


**Figure 4.7.** Schematic representation of the automated synthesis module used for the production of  $[^{13}\text{N}]\mathbf{4.6}$ . Vials 1-9 are indicated with green numbers. Normally open positions for 3-way valves are indicated with a dot. All 2-way valves are normally closed.

A C-18 (Sep-Pak® C18 Plus, Waters) and a filtering membrane were installed in the indicated locations (see Figure 4.7). Normally open positions for 3-way valves are indicated with a dot. All 2-way valves are normally closed. If not indicated otherwise, valves are returned to starting position after each individual step. Reaction time, reaction temperature and the amount of catalyst were varied in order to find optimal experimental conditions.

The procedure followed, step by step, is summarized in Table 4.1. In brief, Nitrogen-13 was produced in an IBA Cyclone 18/9 cyclotron *via* the  $^{16}\text{O}(\text{p},\alpha)^{13}\text{N}$  nuclear reaction. The target was filled with ultrapure water (1.8 mL) and irradiated with 18 MeV protons. The

irradiated solution containing  $^{13}\text{N}]\text{NO}_3^-$ ,  $^{13}\text{N}]\text{NO}_2^-$  and  $^{13}\text{N}]\text{NH}_4^+$  was transferred to the synthesis box and collected in vial 1, which had a venting needle (**step 1**, Table 4.1).

**Table 4.1.** Step-by-step procedure followed for the preparation of  $^{13}\text{N}]\mathbf{4.6}$  using the Tracerlab<sup>TM</sup> FX<sub>FE</sub> synthesis module; NA: Not applicable.

Step	Operations	Process
1	NA	The activity of the target is transferred to vial 1.
2	V5 and V15 open	The solution containing $^{13}\text{N}]\text{NH}_4^+$ , $^{13}\text{N}]\text{NO}_2^-$ and $^{13}\text{N}]\text{NO}_3^-$ is transferred to the cadmium column.
3	V5, V10, V15 and V19 open	The solution containing $^{13}\text{N}]\text{NO}_2^-$ and residual amounts of $^{13}\text{N}]\text{NH}_4^+$ and $^{13}\text{N}]\text{NO}_3^-$ is transferred to the first reactor.
4	V8 up, V10, V15 and V19 open	The cadmium column is rinsed with ultrapure water and the eluate is collected in the first reactor
5	V1, V15 and V19 open	The solution containing 4-iodoaniline, HCl 37%, purified water and MeOH is added to the reactor and the reaction for the formation of the labeled diazonium salt is allowed to occur.
6	V2, V15 and V19 open	The solution containing sodium nitrite, acetic acid and hydrazine monohydrate is added to the reactor and the reaction for the formation of the labeled azide is allowed to occur.
7	V3 and V19 open	The reaction crude is diluted with purified water
8	V9 and V18 open, reactor needle down	The reaction crude is flushed through the C-18 cartridge and the eluate is collected in the waste
9	V4 and V15 open, V6 right	The C-18 cartridge is flushed with purified water and the eluate is collected in the waste. The cartridge is further dried with helium gas.
10	V14 and V15 open, V6 and V13 right, V12 down	The C-18 cartridge is flushed with acetonitrile and the eluate is collected in vial 8. The reaction for the formation of labeled triazole is allowed to occur under heating.
11	V14 and V15 open, V6 and V13 right, V7 left.	The reaction crude is transferred to vial 9 through the filter membrane.
12	V16 left, V17 right	The reaction crude is loaded in the loop and injected into the HPLC system. The radioactive signal is monitored and the desired peak is collected by switching V11.

After completion of the transfer, the venting needle was removed from vial 1 and the solution was transferred to a glass column filled with cadmium to reduce [<sup>13</sup>N]NO<sub>3</sub><sup>-</sup> into [<sup>13</sup>N]NO<sub>2</sub><sup>-</sup> in 1 minute (**step 2**, Table 4.1). The solution was afterwards pushed to a reactor (**step 3**, Table 4.1), and then rinsed with 1.0 mL of ultrapure water, previously loaded in vial 2 (**step 4**, Table 4.1). The acidic solution loaded in vial 3, containing 4-iodoaniline, HCl 37%, purified water and MeOH, was added to the reactor and the reaction for the formation of the labelled diazonium salt was allowed to occur for 30 seconds (**step 5**, Table 4.1). A solution containing a mixture of aqueous sodium nitrite solution, acetic acid and hydrazine monohydrate (Vial 4) was then added to the reactor and the reaction for the formation of labelled azide was allowed to occur for 90 seconds (**step 6**, Table 4.1). After completion of the reaction, ultrapure water (7 mL, Vial 5) was added to the reactor (**step 7**, Table 4.1) and the resulting solution was passed through the C-18 Cartridge to trap the labelled azide (**step 8**, Table 4.1). The cartridge was further rinsed with ultrapure water (2 mL, vial 6) and subsequently dried with helium gas for 1 minute (**step 9**, Table 4.1). The cartridge was rinsed with acetonitrile (1 mL, Vial 7) and the eluate was collected in vial 8, pre-loaded with 4-ethynyl-*N,N*-dimethyl aniline and [(Icy)<sub>2</sub>Cu]PF<sub>6</sub>, and the resulting mixture was allowed to react for 5 min at T=110°C (**step 10**, Table 4.1).

Purification was achieved by semi-preparative HPLC. The reaction mixture was cooled in an ice cold bath, filtered and transferred to vial 9 (**step 11**, Table 4.1). The reaction mixture was finally injected in the HPLC loop (**step 12**, Table 4.1). A RP-C18 column (Mediterranean Sea18, 10x250 mm, 5 µm particle size) was used as the stationary phase and 0.1% TFA in water/acetonitrile (50/50 V/V) was used as the mobile phase with a flow rate of 7ml/min. The desired fraction (retention time = 6.5 min) was collected in the final vial.

Chemical and radiochemical purities of the radiotracer were determined using radio-HPLC, using an Agilent 1200 Series HPLC system with a multiple wavelength UV detector (λ = 254 nm) and a radiometric detector (Gabi, Raytest). A RP-C18 column (Mediterranean Sea18, 4.6x250 mm, 5 µm particle size) was used as stationary phase and 0.1% TFA in water/acetonitrile (40/60 V/V) as the mobile phase. The presence of the desired labelled specie was confirmed by co-elution with reference standard (retention time = 3.4 min).

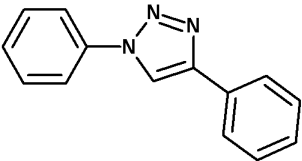
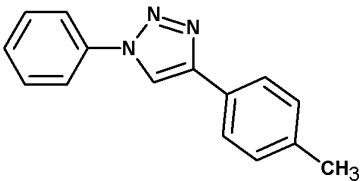
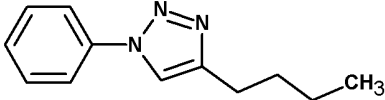
## 4.4. RESULTS AND DISCUSSION

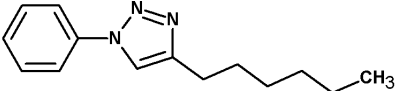
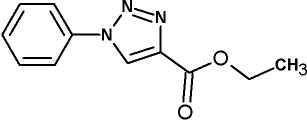
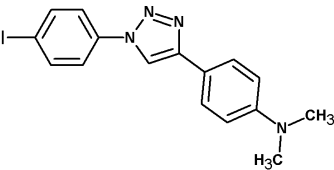
### 4.4.1. Preparation of the reference compounds

Radiochemical reactions carried out under non-carrier added conditions lead to the formation of small amounts of the desired compound in terms of mass. Hence, classical

analytical tools such as NMR cannot be utilised to determine the structure of the labelled compounds. Instead, co-elution of the labelled compounds with reference standard compound using HPLC is widely applied to unambiguously identify the labelled species. Hence, the first step in this work was the preparation of non-radioactive compounds with the same structure as the target compounds. Methodologies previously described in the literature were used. Characterization data obtained by <sup>1</sup>H- and <sup>13</sup>C-NMR as well as mass spectrometry were compared to literature data (see Table 4.2).

**Table 4.2.** Characterization data for compounds 4.1-4.6.

Name / Structure	Characterization data
<p>4.1</p> <p>1, 4-Diphenyl-1H-1, 2, 3-triazole</p> 	<p>White solid.</p> <p><b><sup>1</sup>H NMR</b> (500 MHz, CDCl<sub>3</sub>) δ: 8.23 (s, 1H), 7.94 (d, J=7.2 Hz, 2H), 7.82 (d, J=7.6 Hz, 2H), 7.58 (t, J=8 Hz, 2H), 7.48-7.51 (m, 3H), 7.40 (t, J=7.2 Hz, 1H).</p> <p><b><sup>13</sup>C NMR</b> (125.7 MHz, CDCl<sub>3</sub>) δ: 132.5, 130.3, 129.7, 128.9, 128.7, 128.4, 128.0, 127.8, 125.7, 120.5.</p> <p><b>HRMS</b> Calculated for C<sub>14</sub>H<sub>12</sub>N<sub>3</sub> (MH<sup>+</sup>): 222.257; found: 222.168.</p>
<p>4.2</p> <p>4-Phenyl-1-p-tolyl-1H-1, 2, 3-triazole</p> 	<p>White solid.</p> <p><b><sup>1</sup>H NMR</b> (500 MHz, CDCl<sub>3</sub>) δ: 8.18 (s, 1H), 9.92 (d, J=7.2 Hz, 2H), 7.71 (d, J= 7.6 Hz, 2H), 7.49 (t, J=7.6 Hz, 2H), 7.36-7.41 (m, 3H), 2.47 (s, 3H).</p> <p><b><sup>13</sup>C NMR</b> (125.7 MHz, CDCl<sub>3</sub>) δ:138.8, 134.2, 130.3, 130.2, 128.9, 128.3, 125.8, 120.4, 117.6, 21.1.</p> <p><b>HRMS</b> Calculated for C<sub>15</sub>H<sub>14</sub>N<sub>3</sub> (MH<sup>+</sup>): 236.283; found: 236.186.</p>
<p>4.3</p> <p>1-Phenyl-4-butyl-1, 2, 3-triazole</p> 	<p>White solid.</p> <p><b><sup>1</sup>H NMR</b> (500 MHz, CDCl<sub>3</sub>) δ: 7.76 (s, 1H), 7.65 (d, J= 8Hz, 2H), 7.42 (t, J=8 Hz, 2H), 7.33 (t, J=7.2 Hz, 1H), 2.74 (t, J=7.2 Hz, 2H), 1.65- 1.68 (m, 2H), 1.34-1.37 (m, 2H), 0.90 (t, J=6.4, 3 H);</p> <p><b><sup>13</sup>C NMR</b> (125.7 MHz, CDCl<sub>3</sub>) δ: 136.5, 130.2, 130.0, 129.4, 123.2, 128.8, 30.8, 24.2, 22.2, 13.7;</p> <p><b>HRMS</b> Calculated for C<sub>12</sub>H<sub>16</sub>N<sub>3</sub> (MH<sup>+</sup>): 202.267; found: 202.123.</p>

Name / Structure	Characterization data
<p>4.4</p> <p>1-Phenyl-4-hexyl-1, 2, 3-triazole</p> 	<p>White solid;</p> <p><math>^1\text{H NMR}</math> (500 MHz, <math>\text{CDCl}_3</math>) <math>\delta</math>: 7.77 (s, 1H), 7.34 (d, <math>J=7.6</math> Hz, 2H), 7.49 (t, <math>J=7.2</math> Hz, 2H), 7.40 (t, <math>J=7.2</math> Hz, 1H), 2.79 (t, <math>J=7.2</math> Hz, 2H), 1.70-1.78 (m, 2H), 1.32-1.40 (m, 6H), 0.89 (t, <math>J=6.8</math> Hz, 3H).</p> <p><math>^{13}\text{C NMR}</math> (125.7 MHz, <math>\text{CDCl}_3</math>) <math>\delta</math>: 137.2, 129.6, 128.2, 120.3, 118.8, 31.5, 29.3, 28.9, 25.6, 22.5, 14.7.</p> <p><b>HRMS</b> Calculated for <math>\text{C}_{14}\text{H}_{20}\text{N}_3</math> (<math>\text{MH}^+</math>): 230.320; found: 230.174.</p>
<p>4.5</p> <p>5 - Ethyl 1-phenyl-1, 2, 3-triazole-4-carboxylate</p> 	<p>White solid;</p> <p><math>^1\text{H NMR}</math> (500 MHz, <math>\text{CDCl}_3</math>) <math>\delta</math>: 8.56 (s, 1H), 7.79 (d, <math>J=8.0</math> Hz, 2H), 7.57-7.54 (m, 2H), 7.51-7.48 (m, 1H), 4.46 (dd, <math>J=7.0</math> Hz, 2H), 1.43 (t, <math>J=7.0</math> Hz, 3H).</p> <p><math>^{13}\text{C NMR}</math> (125.7 MHz, <math>\text{CDCl}_3</math>) <math>\delta</math>: 160.42, 140.60, 136.15, 129.78, 129.34, 125.44, 120.62, 61.32, 14.18.</p> <p><b>HRMS</b> Calculated for <math>\text{C}_{11}\text{H}_{11}\text{N}_3\text{O}_2\text{Na}</math> (<math>\text{M}+\text{Na}^+</math>): 240.223; found: 240.124.</p>
<p>4.6</p> <p>4-[1-(4-iodophenyl)-1H-1, 2, 3-triazol-4-yl]-N,N-dimethylaniline</p> 	<p>Pale yellow solid:</p> <p><math>^1\text{H NMR}</math> (500 MHz, <math>(\text{CD}_3)_2\text{CO}</math>) <math>\delta</math>: 8.81 (s, 1H), 7.98 (d, 2H, <math>J=8.9</math> Hz), 7.86-7.73 (m, 4H), 6.84 (d, 2H, <math>J=8.9</math> Hz), 3.02 (s, 6H).</p> <p><math>^{13}\text{C NMR}</math> (500 MHz, <math>(\text{CD}_3)_2\text{CO}</math>) <math>\delta</math>: 150.4, 148.1, 138.4, 136.4, 126.2, 121.6, 121.4, 117.7, 117.3, 112.3, 93.8.</p> <p><b>HRMS</b> Calculated for <math>\text{C}_{16}\text{H}_{15}\text{IN}_4</math> (<math>\text{M}^+</math>), 391.221; found, 391.360.</p>

#### 4.4.2. Preparation of $^{13}\text{N}$ -labelled triazoles ( $^{13}\text{N}$ 4.1- $^{13}\text{N}$ 4.6) in manual mode

The synthesis of triazoles ( $^{13}\text{N}$ 4.1- $^{13}\text{N}$ 4.6) were achieved by reaction of  $^{13}\text{N}$ -labelled aromatic azides with alkyne derivatives and aldehydes (See Figure 4.8).

Nitrogen-13 can be produced in different chemical forms in biomedical cyclotrons and offers a large variety of synthetic possibilities for the preparation of PET radiotracers. In spite of its short half life (10 min.), nitrogen-13 demands for the development of fast, efficient and robust synthetic processes. This was especially significant in the work reported here, because the synthetic strategy was envisioned through a 4-steps process, in addition to one intermediate and one final purification steps.

In our previous work [26], we achieved the synthesis of  $^{13}\text{N}$ -labelled aryl azides by two approaches: (A) Reaction of aniline with sodium nitrite to yield the non-labelled diazonium salt and subsequent reaction with  $^{13}\text{N}$ -labelled azide ion (prepared by reaction of  $^{13}\text{N}[\text{NO}_2]^-$  with hydrazine hydrate in acidic media); and (B) reaction of aniline with  $^{13}\text{N}[\text{NO}_2]^-$  to yield the  $^{13}\text{N}$ -labelled diazonium salt and subsequent reaction with azide ion (prepared by reaction of sodium nitrite with hydrazine hydrate in acidic media). Our results showed that the radiolabel was almost quantitatively transferred to the azide under route (B). Therefore, this route was considered as the most appropriate to achieve optimal results and furthermore the experimental conditions of this part of the reaction were not optimised.

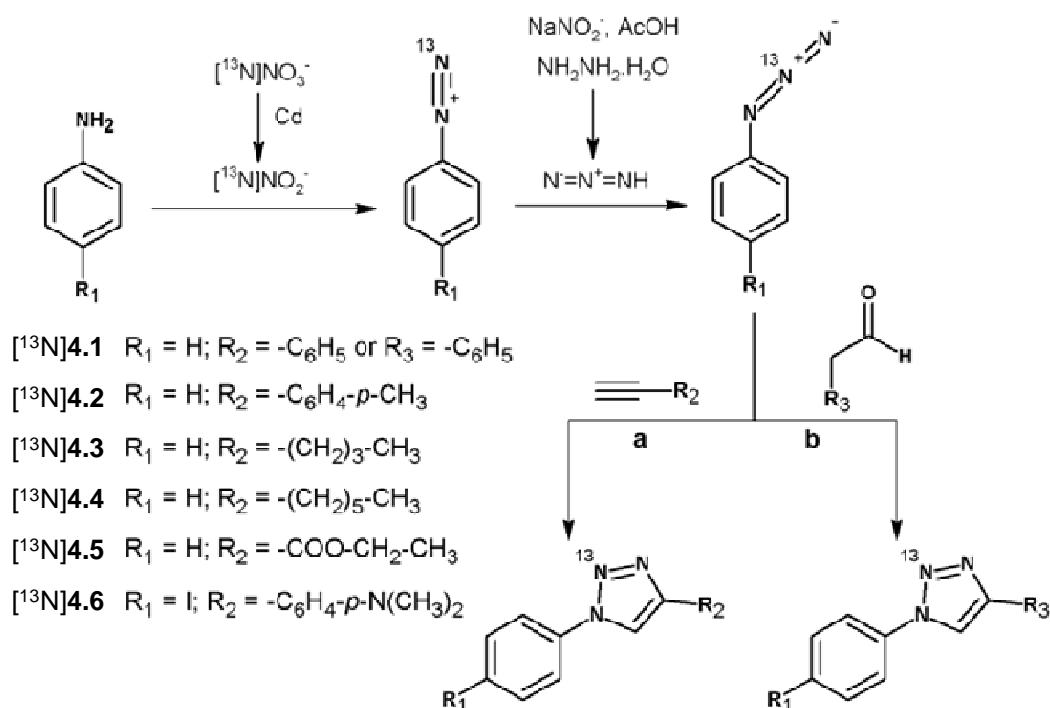


**Figure 4.8.** Scheme of the 4-step synthetic process followed for the preparation of  $^{13}\text{N}$ -labelled substituted triazoles by reaction of  $^{13}\text{N}$ -labelled azides with alkynes (a) and aldehydes (b).

It is worth mentioning that during the preparation of  $^{13}\text{N}$ -labelled azides, it is paramount to work under no-carried-added conditions, in order to achieve the final labelled triazoles in high specific activity (amount of radioactivity per unit mass) values. In other words, the preparation of the labelled diazonium salt had to be conducted without addition of non-radioactive nitrite. This, conclusively, led to the situation in which the labelled specie in the (3+2) Huisgen cycloaddition reaction for the synthesis of  $^{13}\text{N}$ -labelled triazoles is the limiting reagent, as its concentration is much lower than any other reagent. Taking this into account, we first tackled the optimization of the experimental conditions for the

preparation of  $^{13}\text{N}$ -labelled triazoles by reaction of the labelled azides with alkynes (see Figure 4.8). During this process, the work was carried out manually in a lead-shielded hot cell (Manuela, Comecer) especially designed to conduct manual operations to have a better control of the individual steps. In all steps, quality control analysis performed after the reduction step showed that 70-80% of the radioactivity eluted from the cadmium column was due to  $[^{13}\text{N}]\text{NO}_2^-$ ; non-reduced  $[^{13}\text{N}]\text{NO}_3^-$  and  $[^{13}\text{N}]\text{NH}_4^+$  accounted for around 18-28% and 2% of the total radioactivity, respectively. These results are in good agreement with previous data [27-31].

After the preparation of labelled the azides, substantial amount of chemical impurities plus  $[^{13}\text{N}]\text{NH}_4^+$ ,  $[^{13}\text{N}]\text{NO}_3^-$  and unreacted  $[^{13}\text{N}]\text{NO}_2^-$  were present in the reaction mixture. In addition, subsequent reaction for the formation of the labelled triazole should be conducted in non-aqueous media. Because of this, the implementation of an intermediate step to change the solvent was required and we first approached to liquid-liquid extraction with dichloromethane. Radio-HPLC analysis of both the aqueous and organic phases confirmed quantitative extraction of the labelled azide. No peak corresponding to this specie was found in the aqueous phase. Furthermore, no radiochemical impurities (i.e.  $[^{13}\text{N}]\text{NH}_4^+$ ,  $[^{13}\text{N}]\text{NO}_3^-$ ,  $[^{13}\text{N}]\text{NO}_2^-$  or labelled diazonium salt) were observed in the organic phase, although the presence of the starting aniline could be detected. This chemical impurity was anticipated not to interfere in the following copper mediated (3+2) Huisgen cycloaddition step.

In order to set up the (3+2) Huisgen cycloaddition under hot conditions, the reaction was initially carried out using  $^{13}\text{N}$ -labelled phenylazide and phenylacetylene, using  $\text{CuSO}_4 \cdot 5\text{H}_2\text{O}$  as the catalyst, mimicking the reaction conditions used during preparation of the non-radioactive analogues. With that aim, the preparation of  $[^{13}\text{N}]\mathbf{4.1}$  was approached by reaction of  $^{13}\text{N}$ -labelled phenylazide (redissolved in acetonitrile after evaporation of dichloromethane) with phenylacetylene in the presence of the catalyst (2 mg) for 10 min at RT. Unfortunately, the formation of the desired  $^{13}\text{N}$ -labelled triazole could not be detected by radio-HPLC. Similar results were obtained when copper (II) oxide ( $\text{CuO}$ ) and copper (I) iodide were used as the catalyst. In view of this results, we decided to use  $[(\text{Icy})_2\text{Cu}]\text{PF}_6$  as the catalyst. This compound has proven efficient in a wide variety of (3+2) Huisgen cycloaddition reactions [32]. In this case, the reaction at RT for a period of 10 minutes offered radiochemical conversion values (RCC, calculated from radiochromatographic profiles, expressed as the ratio between the area under the peak corresponding to  $^{13}\text{N}$  labelled triazole and the sum of the areas for all the peaks in the chromatogram, in percentage) of  $15 \pm 2\%$  (Table 4.3, entry 1). Further, during the

cycloaddition step the reaction at RT for a period of 20 minutes offered radiochemical conversion values of 50±3% (Table 4.4, entry 1).

**Table 4.3.** Radiochemical conversion values for the preparation of <sup>13</sup>N-labelled triazoles by reaction of <sup>13</sup>N-labelled azides with alkynes or aldehydes at different temperatures.

Entry	Triazole	RT	50°C <sup>a</sup> /60°C <sup>b</sup>
1	[ <sup>13</sup> N]4.1 <sup>a</sup>	15±2	49±8
2	[ <sup>13</sup> N]4.2 <sup>a</sup>	13±3	42±4
3	[ <sup>13</sup> N]4.3 <sup>a</sup>	38±14	92±8
4	[ <sup>13</sup> N]4.4 <sup>a</sup>	10±4	70±8
5	[ <sup>13</sup> N]4.5 <sup>a</sup>	72±3	94±6
6	[ <sup>13</sup> N]4.6 <sup>a</sup>	17±6	38±2
7	[ <sup>13</sup> N]4.1 <sup>b</sup>	23±5	96±2

<sup>a</sup>Reaction of azide with alkyne; <sup>b</sup>reaction of azide with aldehyde; values are expressed as average±standard deviation, n=3; RT: room temperature; reaction time was 10 min in all cases.

After these encouraging results, we decided to extend the methodology by varying alkyne derivatives to the preparation of other functionalized triazoles ([<sup>13</sup>N]4.2-[<sup>13</sup>N]4.6), and different reaction temperatures were assayed. As it can be seen in tables 4.3-4.4, our method enabled the preparation of all <sup>13</sup>N-labelled polysubstituted triazoles. Radiochemical conversion (RCC) values raised with temperature to reach acceptable values (38-94%) when the reaction was carried out at 50°C for a period of 10 minutes (Table 4.3, entries 1-6; see Figures 4.9a and 4.9b for examples of chromatographic profiles corresponding to the synthesis of [<sup>13</sup>N]4.1 at 50°C). Additionally, Radiochemical conversion (RCC) values raised with temperature to reach excellent values (55-99%) when the reaction was carried out at 50°C for 20 minutes (Table 4.4, entries 1-6).

Interestingly, high RCC values were obtained when aliphatic alkynes were used. This result is not in agreement with previous works reported in the literature, as the fact that aliphatic alkynes are well known for their lower reactivity when compared to aromatic ones [33, 34]. However, in these previous works, long reaction times (hours) were used. Additionally, because we conducted all the reactions under no-carrier-added conditions, the intermediate <sup>13</sup>N-labelled azide is the limiting reagent and its concentration is extremely low when compared to that of the alkyne derivative. Despite further investigation would be required, we hypothesize that the low RCC values obtained with aromatic triazoles might be due to the kinetics of the reaction.



**Table 4.4.** Radiochemical conversion values for the preparation of  $^{13}\text{N}$ -labelled triazoles by reaction of  $^{13}\text{N}$ -labelled azides with alkynes or aldehydes at different temperatures.

Entry	Triazole	RT	50°C <sup>a</sup> /60°C <sup>b</sup>
1	[ $^{13}\text{N}$ ]4.1 <sup>a</sup>	50±3	70±8
2	[ $^{13}\text{N}$ ]4.2 <sup>a</sup>	45±4	62±6
3	[ $^{13}\text{N}$ ]4.3 <sup>a</sup>	55±14	98±8
4	[ $^{13}\text{N}$ ]4.4 <sup>a</sup>	12±4	86±8
5	[ $^{13}\text{N}$ ]4.5 <sup>a</sup>	78±5	99±4
6	[ $^{13}\text{N}$ ]4.6 <sup>a</sup>	23±6	55±4
7	[ $^{13}\text{N}$ ]4.1 <sup>b</sup>	39±4	98±2

<sup>a</sup>Reaction of azide with alkyne; <sup>b</sup>reaction of azide with aldehyde; values are expressed as average±standard deviation, n=3; RT: room temperature; reaction time was 20 min in all cases.

In view of the promising results, we decided to expand the scope of our work by tackling the preparation of [ $^{13}\text{N}$ ]4.1 by reaction of the labelled phenylazide with phenylacetaldehyde. In our first attempts, the reaction was carried out between  $^{13}\text{N}$ -labelled phenylazide and phenylacetaldehyde, while [(Icy)<sub>2</sub>Cu]PF<sub>6</sub> was used as the catalyst, but the formation of [ $^{13}\text{N}$ ]4.1 could not be detected by radio-HPLC. The formation of polysubstituted triazoles by reaction of azides with aldehydes has been previously reported in the literature [35]. In this previous work, 1,8-diazabicycloundec-7-ene (DBU) as the catalyst offered excellent results when the reaction was carried out in presence of DMSO as a solvent. In our hands, this catalyst offered good radiochemical conversion (RCC) values (23±5% and 39±4% when the reaction was conducted at room temperature for 10 and 20 minutes, respectively; see Tables 4.3 and 4.4, entry 7). The reaction was almost quantitative at T=60°C (see Figures 4.9c and 4.9d for examples of chromatographic profiles). After these encouraging results, attempts to perform the reaction between  $^{13}\text{N}$ -labelled phenylazide with other commercially available aldehydes under similar conditions were carried out. In this context, the preparation of [ $^{13}\text{N}$ ]4.3 was approached by reaction of  $^{13}\text{N}$ -labelled phenylazide with 1-hexanal in the presence of the DBU as a catalyst for 10 min and 20 min at RT and at T=60°C. Unfortunately, the formation of the desired  $^{13}\text{N}$ -labelled triazole could not be detected in both cases by radio-HPLC. Additionally the preparation of [ $^{13}\text{N}$ ]4.4 was approached by reaction of  $^{13}\text{N}$ -labelled phenylazide with 1-octanal in the presence of the DBU as a catalyst for 10 min and 20 min at RT and at T=60°C. Unfortunately, the formation of the desired  $^{13}\text{N}$ -labelled triazole could not be detected again in both cases by radio-HPLC. Despite further experiments

might be required in order to elucidate the reason of such lack of reactivity, we postulate that aliphatic aldehydes are less reactive than aromatic aldehydes under hot conditions.

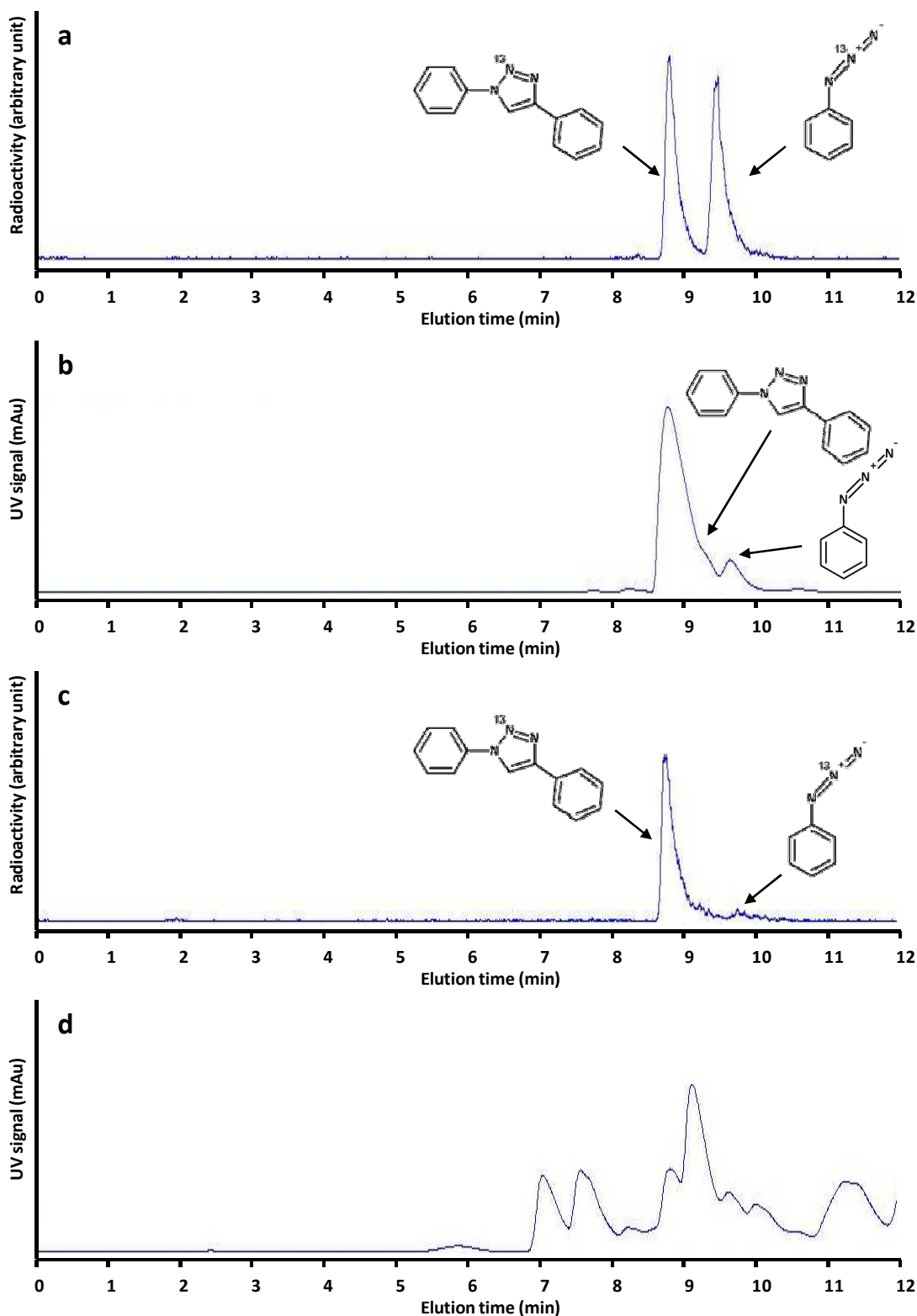


**Figure 4.9.** Chromatographic profiles using radioactive (a, c) and UV (b, d) detection after analysis of the reaction crude corresponding to the synthesis of  $^{13}\text{N}$ **4.1**; (a, b) synthesis by (3+2) cycloaddition using labelled phenylazide with phenylacetylene; (c,d) synthesis by (3+2) cycloaddition using labelled phenylazide with phenylacetaldehyde.

#### 4.4.3. Implementation of an intermediate purification step based on SPE

Liquid-liquid extraction using dichloromethane as an intermediate purification step is a very well established method for reactions that are conducted under non-radioactive conditions. However, such experimental step is quite tedious and sub-optimal in radioactive conditions because automatisation is extremely challenging. Therefore, and moving further towards the development of a fully automated process, other alternatives were explored. In previous works, during the synthesis of <sup>13</sup>N-labelled azo compounds [28], our group has used solid phase extraction cartridges as a suitable tool to switch from aqueous to organic solvent. Here, we anticipated that dilution of the reaction crude with water after formation of the labelled intermediate phenylazide and subsequent elution through a C-18 cartridge would result in quantitative trapping of the labelled intermediate phenylazide. However, first attempts conducted with [<sup>13</sup>N]phenylazide were unsuccessful, and no trapping could be observed. Because the reaction for the formation of the <sup>13</sup>N-labelled phenylazide is carried out under strong acidic conditions, we postulated that the lack of retention might be due to the formation of the protonated form (positively charged) of the azide, which has low affinity for the C-18 cartridge phase. As expected, replacement of water by sodium acetate solution and subsequent elution through the C-18 cartridge resulted in quantitative trapping of the labelled phenylazide, as revealed by radio-HPLC analysis of the eluate. In the case of [<sup>13</sup>N]*p*-iodophenylazide, used in the preparation of compound [<sup>13</sup>N]4.6, dilution with water led to quantitative trapping, probably due to the presence of the iodine atom, which confers a stronger hydrophobic character to the molecule, regardless of the net charge.

Flushing of the C-18 cartridge with helium gas for 1 min was sufficient to remove the majority of the water; subsequent elution of the trapped labelled species with acetonitrile (1mL) and reaction with the corresponding alkyne derivatives under catalytic conditions led to the formation of the desired labelled polysubstituted triazoles ([<sup>13</sup>N]4.1 and [<sup>13</sup>N]4.6) with RCC values equivalent to those shown in table 4.3.

#### Automatisation of the synthetic process for [<sup>13</sup>N] 4.6

Replacement of liquid-liquid extraction by the solid phase extraction process as an intermediate purification step enabled the automatisation of the whole process (including final purification by semi-preparative HPLC) using the Tracerlab™ FX<sub>FE</sub> synthesis module, with appropriate adaptation. The experimental conditions for the preparation of triazole [<sup>13</sup>N]4.6 were further optimized at this step. This triazole was specifically selected for full automatisation process because its non radioactive analogue has shown promising properties to target β-Amyloid aggregates, and therefore it may find application in the

early diagnose or evaluation of response to treatment in Alzheimer's disease [24]. The amount of catalyst, the reaction time and the reaction temperature, for the formation of the labelled triazole were varied (Table 4.5). As it can be seen in the table, the formation of [<sup>13</sup>N]4.6 was not observed when the reaction time was set to 2 min, irrespective of the amount of catalyst (entries 1-3 in Table 4.5). It is worth mentioning the fact that heating of the reaction vial where the reaction is carried out starts at t=0. Hence, 2 min might not be sufficient to reach the desired temperature in the reaction mixture. Higher amount of catalyst, longer reaction times and higher temperature led to higher RCC values, as expected. At optimal reaction temperature (110°C), the reaction time of 10 min and amount of catalyst (10 mg), proved to be less desirable than the 5 min period, because the rise in RCC (approximately 10%, from 85 to 96%, see entries 12 and 13 in Table 4.5) was negligible compared with the short half life of nitrogen-13 (10 min) during the extra 5 min gap (close to 50%). Hence, T=110°C, t=5 min and amount of catalyst=10 mg were established as optimal conditions for [<sup>13</sup>N]4.6 among the investigated scenarios.

**Table 4.5.** Radiochemical conversion values for the preparation of [<sup>13</sup>N]4.6 by reaction of <sup>13</sup>N-labelled 1-azido-4-iodobenzene with 4-ethynyl-*N,N*-dimethylaniline under different experimental conditions, using the automated synthesis box Tracerlab™ FX<sub>FE</sub>

Entry	T (°C)	T (min)	Catalyst (mg)	RCC (%)
1	50	2	2	0
2	50	2	5	0
3	50	2	10	0
4	50	5	2	16±5
5	50	5	5	20±4
6	50	5	10	22±5
7	50	10	2	36±4
8	50	10	5	49±7
9	50	10	10	75±8
10	80	5	10	40±3
11	80	10	10	83±6
12	110	5	10	85±9
13	110	10	10	96±3

Values are expressed as average ± standard deviation, n=3; catalyst: [(Icy)<sub>2</sub>Cu]PF<sub>6</sub>; RCC: Radiochemical conversion.

These optimised experimental conditions were applied for the fully automated preparation of pure  $^{13}\text{N}$ 4.6.

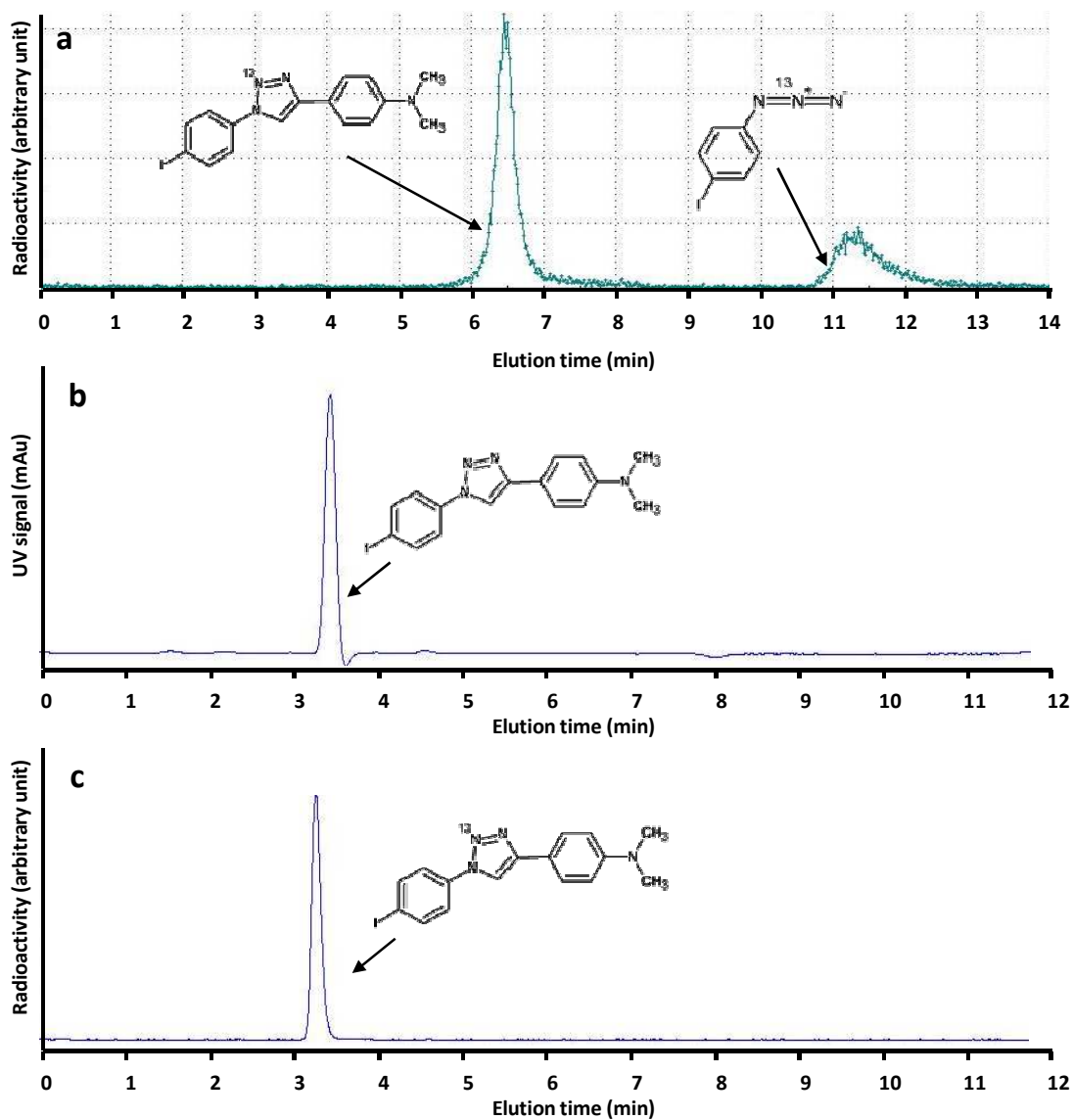


**Figure 4.10.** (a) Chromatographic profile (radioactive detector) corresponding to the purification of  $^{13}\text{N}$ 4.6. Two radioactive peaks, corresponding to  $^{13}\text{N}$ 4.6 and unreacted  $^{13}\text{N}$ -labelled 1-azido-4-iodobenzene, were found; (b,c) Chromatographic profiles (UV-Vis and radioactive detectors, respectively) corresponding to the analysis of purified  $^{13}\text{N}$ 4.6. No chemical nor radiochemical impurities were detected.

After purification by semi-preparative HPLC (see Figure 4.10a for example of chromatographic profile) isolated radiochemical yields of  $11 \pm 2\%$ , related to the starting amount of  $^{13}\text{N}$  produced in the cyclotron and decay corrected to the end of the irradiation process, were obtained in overall production times of 25 min (non-decay corrected radiochemical yield =  $2 \pm 0.4\%$ ). Specific activities at the end of the synthesis were  $4.6 \pm 0.2$

GBq/μmol, and radiochemical purity was >99% (Figure 4.10b) in all cases, as determined by radio-HPLC. No further chemical impurities were detected by HPLC (Figure 4.10c). Despite non-decay corrected radiochemical yields are low, an irradiation of 4 μAh yields around 6.6 GBq of <sup>13</sup>N in the cyclotron target. Therefore, around 130 MBq (3.6 mCi) of pure radiotracer could be obtained at the end of the preparation process. Typical injected doses in rats and mice are around 500 and 100 μCi, respectively. Hence, the here reported methodology should enable subsequent *in vitro* or *in vivo* studies in small animal species.

#### 4.5. SUMMARY AND CONCLUSIONS

In conclusion, we present here an unprecedented and fully automated methodology for the preparation of chemically and radiochemically pure <sup>13</sup>N-labelled polysubstituted triazoles by reaction of <sup>13</sup>N-labelled azides with alkynes *via* (3+2) Huisgen cycloaddition. The methodology could be extended to the preparation of triazoles in the (3+2) cycloaddition step using aromatic aldehydes and DBU as the catalyst. After optimization of the experimental conditions, sufficient amount of radiotracer to approach subsequent *in vitro* and *in vivo* studies in small animal species could be obtained. Radiolabelling using <sup>13</sup>N may find interesting applications, especially in those instances in which incorporation of other positron emitters into the target molecule is not feasible, or to tackle the incorporation of the label in different positions to enable accurate metabolic studies.

#### 4.6. REFERENCES

1. Ferreira, S., et al., *Synthesis, Biological Activity, and Molecular Modeling Studies of 1H-1,2,3-Triazole Derivatives of Carbohydrates as α-Glucosidases Inhibitors*. Journal of Medicinal Chemistry, 2010. **53**(6): p. 2364-2375.
2. Bourne, Y., et al., *Freeze-frame inhibitor captures acetylcholinesterase in a unique conformation*. Proceedings of the National Academy of Sciences of the United States of America, 2004. **101**(6): p. 1449-1454.
3. Whiting, M., et al., *Inhibitors of HIV-1 protease by using in situ click chemistry*. Angewandte Chemie - International Edition, 2006. **45**(9): p. 1435-1439.
4. Pagliai, F., et al., *Rapid synthesis of triazole-modified resveratrol analogues via click chemistry*. Journal of Medicinal Chemistry, 2006. **49**(2): p. 467-470.
5. Pirali, T., et al., *Estrogenic analogues synthesized by click chemistry*. ChemMedChem, 2007. **2**(4): p. 437-440.
6. Briguglio, I., et al., *Benzotriazole: An overview on its versatile biological behavior*. European Journal of Medicinal Chemistry, 2015. **97**(1): p. 612-648.

7. Huisgen, R., *1,3-Dipolare Cycloadditionen Rückschau und Ausblick*. Angewandte Chemie, 1963. **75**(13): p. 604-637.
8. Tornøe, C.W., C. Christensen, and M. Meldal, *Peptidotriazoles on solid phase:[1, 2, 3]-triazoles by regiospecific copper (I)-catalyzed 1, 3-dipolar cycloadditions of terminal alkynes to azides*. The Journal of organic chemistry, 2002. **67**(9): p. 3057-3064.
9. Rostovtsev, V.V., et al., *A stepwise huisgen cycloaddition process: copper (I)-catalyzed regioselective "ligation" of azides and terminal alkynes*. Angewandte Chemie, 2002. **114**(14): p. 2708-2711.
10. Rostovtsev, V., et al., *Scheme 7. Deuterium-labeling experiments*. Angew. Chem, 2002. **114**: p. 2708-2711.
11. Zhang, L., et al., *Ruthenium-catalyzed cycloaddition of alkynes and organic azides*. Journal of the American Chemical Society, 2005. **127**(46): p. 15998-15999.
12. Boren, B.C., et al., *Ruthenium-catalyzed azide-alkyne cycloaddition: scope and mechanism*. Journal of the American Chemical Society, 2008. **130**(28): p. 8923-8930.
13. Smith, C.D. and M.F. Greaney, *Zinc mediated azide-alkyne ligation to 1, 5-and 1, 4, 5-substituted 1, 2, 3-triazoles*. Organic letters, 2013. **15**(18): p. 4826-4829.
14. Glaser, M. and E.G. Robins, *'Click labelling'in PET radiochemistry*. Journal of Labelled Compounds and Radiopharmaceuticals, 2009. **52**(10): p. 407-414.
15. Gill, H.S., et al., *A modular platform for the rapid site-specific radiolabeling of proteins with  $^{18}\text{F}$  exemplified by quantitative positron emission tomography of human epidermal growth factor receptor 2*. Journal of medicinal chemistry, 2009. **52**(19): p. 5816-5825.
16. Ramenda, T., et al., *Radiolabelling of proteins with fluorine-18 via click chemistry*. Chemical Communications, 2009(48): p. 7521-7523.
17. Marik, J. and J.L. Sutcliffe, *Click for PET: rapid preparation of [ $^{18}\text{F}$ ] fluoropeptides using CuI catalyzed 1, 3-dipolar cycloaddition*. Tetrahedron Letters, 2006. **47**(37): p. 6681-6684.
18. Glaser, M. and E. Årstad, *"Click labeling" with 2-[ $^{18}\text{F}$ ]fluoroethylazide for positron emission tomography*. Bioconjugate chemistry, 2007. **18**(3): p. 989-993.
19. Inkster, J.A., et al., *Radiosynthesis and bioconjugation of [ $^{18}\text{F}$ ]FPy5yne, a prosthetic group for the  $^{18}\text{F}$  labeling of bioactive peptides*. Journal of Labelled Compounds and Radiopharmaceuticals, 2008. **51**(14): p. 444-452.
20. Hausner, S.H., et al., *In vivo positron emission tomography (PET) imaging with an  $\alpha\beta 6$  specific peptide radiolabeled using  $^{18}\text{F}$ -"click" chemistry: evaluation and*

- comparison with the corresponding 4- $^{18}\text{F}$ fluorobenzoyl- and 2- $^{18}\text{F}$  fluoropropionyl-peptides. *Journal of medicinal chemistry*, 2008. **51**(19): p. 5901-5904.
21. Li, Z.-B., et al., *Click chemistry for  $^{18}\text{F}$ -labeling of RGD peptides and microPET imaging of tumor integrin  $\alpha_v\beta_3$  expression*. *Bioconjugate chemistry*, 2007. **18**(6): p. 1987-1994.
  22. Sirion, U., et al., *An efficient F-18 labeling method for PET study: Huisgen 1, 3-dipolar cycloaddition of bioactive substances and F-18-labeled compounds*. *Tetrahedron Letters*, 2007. **48**(23): p. 3953-3957.
  23. Moorhouse, A.D. and J.E. Moses, *Microwave enhancement of a 'one-pot'tandem azidation-'click'cycloaddition of anilines*. *Synlett*, 2008. **2008**(14): p. 2089-2092.
  24. Qu, W., et al., *Quick assembly of 1, 4-diphenyltriazoles as probes targeting  $\beta$ -amyloid aggregates in Alzheimer's disease*. *Journal of medicinal chemistry*, 2007. **50**(14): p. 3380-3387.
  25. Kaboudin, B., R. Mostafalu, and T. Yokomatsu,  *$\text{Fe}_3\text{O}_4$  nanoparticle-supported Cu (II)- $\beta$ -cyclodextrin complex as a magnetically recoverable and reusable catalyst for the synthesis of symmetrical biaryls and 1, 2, 3-triazoles from aryl boronic acids*. *Green Chemistry*, 2013. **15**(8): p. 2266-2274.
  26. Joshi, S.M., et al., *Synthesis of radiolabelled aryl azides from diazonium salts: experimental and computational results permit the identification of the preferred mechanism*. *Chemical Communications*, 2015. **51**(43): p. 8954-8957.
  27. Gómez-Vallejo, V., et al., *Efficient system for the preparation of  $^{13}\text{N}$  labeled nitrosamines*. *Bioorganic & medicinal chemistry letters*, 2009. **19**(7): p. 1913-1915.
  28. Gómez-Vallejo, V., et al., *Fully automated synthesis of  $^{13}\text{N}$ -labeled nitrosothiols*. *Tetrahedron Letters*, 2010. **51**(22): p. 2990-2993.
  29. Gaja, V., et al., *Synthesis and Evaluation of  $^{13}\text{N}$ -Labelled Azo Compounds for  $\beta$ -Amyloid Imaging in Mice*. *Molecular Imaging and Biology*, 2014. **16**(4): p. 538-549.
  30. Gómez-Vallejo, V., J.I. Borrell, and J. Llop, *A convenient synthesis of  $^{13}\text{N}$ -labelled azo compounds: A new route for the preparation of amyloid imaging PET probes*. *European journal of medicinal chemistry*, 2010. **45**(11): p. 5318-5323.
  31. Gaja, V., et al., *Synthesis of  $^{13}\text{N}$ -labelled radiotracers by using microfluidic technology*. *Journal of Labelled Compounds and Radiopharmaceuticals*, 2012. **55**(9): p. 332-338.
  32. Díez-González, S. and S. Nolan, *Scheme 3. Catalytic Aerobic Oxidation of Benzyl Alcohol*. *Angew. Chem., Int. Ed*, 2008. **47**: p. 8881.
  33. Krasinski, A., V.V. Fokin, and K.B. Sharpless, *Direct synthesis of 1, 5-disubstituted-4-magnesio-1, 2, 3-triazoles, revisited*. *Organic letters*, 2004. **6**(8): p. 1237-1240.



34. Meng, X., et al., *Zn/C-Catalyzed Cycloaddition of Azides and Aryl Alkynes*. *European Journal of Organic Chemistry*, 2010. **2010**(28): p. 5409-5414.
35. Ramachary, D.B., A.B. Shashank, and S. Karthik, *An Organocatalytic Azide-Aldehyde [3+ 2] Cycloaddition: High-Yielding Regioselective Synthesis of 1, 4-Disubstituted 1, 2, 3-Triazoles*. *Angewandte Chemie International Edition*, 2014. **53**(39): p. 10420-10424.



## **5. Synthesis of $^{13}\text{N}$ -labelled tetrazoles**



## 5. NEW HETEROGENEOUS CATALYSTS: APPLICATION TO THE SYNTHESIS OF $^{13}\text{N}$ -LABELLED TETRAZOLES

### 5.1. INTRODUCTION

Tetrazoles are heterocyclic compounds with molecular formula  $\text{CH}_2\text{N}_4$ , having a five-membered ring with four nitrogen atoms and one carbon atom, and are unknown in nature. Tetrazoles are quite strong acids and readily form salts with transition metal ions. They emit toxic oxides of nitrogen fumes when heated to decomposition. Tetrazole salts are quite often heat- and shock- sensitive and therefore tetrazoles can be used as explosives or detonators. Tetrazoles exist in two tautomeric forms (Figures 5.1a and 5.1b), of which the 1H form (Figure 5.1 a) is dominant.

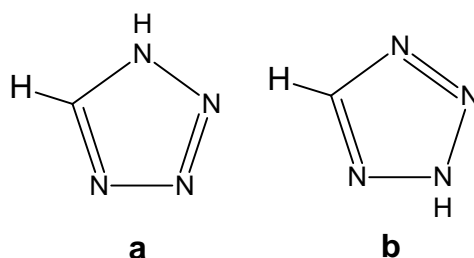


**Figure 5.1.** Chemical structure of 1H-tetrazole in the two different tautomeric forms.

Tetrazoles were first discovered in 1885 by J. A. Bladin [1] and can be prepared using different routes (see Table 5.1 for most relevant routes). Among tetrazoles, 5-substituted-1H-tetrazoles have been an interesting field of study over the past few years, as various substituted tetrazoles are used as surrogates for carboxylic acids in pharmaceutically active agents, having higher lipophilicities and improved metabolic resistance [2]. They also find application in a variety of fields including materials sciences, information recording systems, rocket propellants, ligands, and precursors of a variety of nitrogen containing heterocycles in coordination chemistry [3-5]. Recently, tetrazole moieties were used for binding aryl thiotetrazolylacetanilides with HIV-1 reverse transcriptase [6].

Several strategies for the synthesis of 5-substituted tetrazoles have been reported. The most common approach is the addition of the azide anion to nitrile or cyanamide groups in the presence of an acid catalyst [7]. However, this procedure has several drawbacks including the use of expensive and toxic metal organic azides [8] and strong Lewis acids [9]. An innovative and safe method for the synthesis of tetrazoles based on the addition of sodium azide to nitriles using stoichiometric amount of Zn(II) salts in water or dimethylformamide (DMF) as the solvent was later described [10]. However, this

approach requires the tedious and time-consuming removal of zinc salts from the acidic products.

**Table 5.1.** Production of tetrazoles

Route	Scheme
First synthesis described: Reaction of anhydrous hydrazoic acid with hydrogen cyanide under pressure [11].	$\text{HN}_3 + \text{H}-\text{C}\equiv\text{N} \longrightarrow \text{C}_2\text{H}_2\text{N}_4$
(3 + 2) cycloaddition using inorganic azides (instead of hydrazoic acid) with benzonitrile [12].	$\text{C}_6\text{H}_5\text{C}\equiv\text{N} + \text{NaN}_3 \xrightarrow[\text{DMF}]{\text{NH}_4\text{Cl}} \text{C}_6\text{H}_5\text{C}_2\text{H}_2\text{N}_4$
Replacement of $\text{NaN}_3$ by $\text{TMSN}_3$ . Formation of tetrazoles by reaction of $\text{TMSN}_3$ with nitriles [13].	$\text{R}-\text{C}\equiv\text{N} + \text{TMSN}_3 \xrightarrow[\text{DMF/MeOH, 100 }^\circ\text{C}]{\text{Cu}_2\text{O}} \text{R}-\text{C}_2\text{H}_2\text{N}_4 \quad \text{R} = \text{Ar, alkyl}$
Reaction of amines and triethyl orthoformate with sodium azide under catalytic conditions [14].	$\text{R-NH}_2 + \text{EtO-CH(OEt)-OEt} + \text{NaN}_3 \xrightarrow[\text{CH}_3\text{OC}_2\text{H}_4\text{OH, 100 }^\circ\text{C}]{\text{Yb(OTf)}_3} \text{R}-\text{C}_2\text{H}_2\text{N}_4 \quad \text{R} = \text{Ar}$
Reaction of alkenes, NBS, nitriles and $\text{TMSN}_3$ under catalytic conditions to form various 1, 5-disubstituted tetrazoles [15].	$\text{R}_1\text{-CH=CH-R}_2 \xrightarrow[\text{R}_3\text{CN, 23 }^\circ\text{C}]{\text{Zn(OTf)}_2, \text{NBS, TMSN}_3} \text{R}_1\text{-CH(R}_2\text{)-C}_2\text{H}_2\text{N}_4\text{-R}_3$ <p style="text-align: right;"><math>\text{R}_1, \text{R}_2 = \text{alkyl, Ar, H}</math> <math>\text{R}_3 = \text{alkyl, Ar}</math></p>
Reaction of aryl diazonium salts with 2,2,2-trifluorodiazethane under mild conditions in the presence of a silver catalyst [16].	$\text{C}_6\text{H}_5\text{-N}_2^+ \text{BF}_4^- + \text{CF}_3\text{CHN}_2 \longrightarrow \text{C}_6\text{H}_4(\text{CF}_3)\text{-N}_2\text{C}_2\text{H}_2\text{N}_4$

Pizzo and co-workers also reported an efficient method for synthesis of tetrazoles by the reaction of nitriles with  $\text{TMSN}_3$  (TMS=trimethylsilyls) in the presence of tetra-n-butylammonium fluoride (TBAF) as the catalyst [17]. Since then, various homo- and heterogeneous catalysts have been investigated including Brønsted acids, Lewis acids ( $\text{BF}_3\cdot\text{OEt}_2$ ), metal chlorides ( $\text{AlCl}_3$ ,  $\text{CdCl}_2$ ), metal oxides ( $\text{Cu}_2\text{O}$ ,  $\text{ZnO}$ ,  $\text{Sb}_2\text{O}_3$ ,  $\gamma\text{-Fe}_2\text{O}_3$ ), clay and modified clay, Cu-incorporated ordered hexagonal mesoporous silicates (Cu-MCM-41),  $\text{FeCl}_3/\text{SiO}_2$ ,  $\text{BaWO}_4$ ,  $\text{ZnS}$ , and natural natrolite zeolite [5, 9, 12, 18-20]. Although most of these methods are efficient, they have common drawbacks. Homogeneous catalytic processes require expensive metal catalysts and hydrazoic acid, which is toxic and

explosive. Additionally, refluxing for a prolonged period of time and difficulty in separation and recovery of the catalyst result in tedious workup [21]. On the other hand, heterogeneous catalytic processes require a large excess of sodium azide, and long reaction times (24-96h) are usually needed to achieve acceptable reaction yields [22]. These reaction times are clearly too long for application to the preparation of  $^{13}\text{N}$ -labelled tetrazoles.

Reaction times can be shortened by using microwave (MW) technology [5], and this could aid in the translation of the synthetic routes into the radiochemical field. Surprisingly, only a few works on the synthesis of 5-substituted tetrazoles using heterogeneous catalysts under microwave irradiation conditions have been reported to date. One of the first works was based on the treatment of nitriles with sodium azide and ammonium chloride using DMF as the solvent in a closed vessel [23]. Under this experimental setting, isolated yields between 40 and 96% could be achieved (depending on the substrates) in short reaction times (10-25 min). The use of other heterogeneous catalysts such as Montmorillonite K-10 clay and platinum nanoparticles decorated on activated carbon (Pt NPs@AC) has recently been reported [24, 25]. Microwave reactions have also been assayed using different homogeneous catalysts, e.g. triethyl ammonium chloride in nitrobenzene [26], nitriles in ionic liquids [27],  $\text{ZnCl}_2$  [28, 29], and  $\text{ZnBr}_2$  [30]. However, as it has been mentioned above, the use of homogeneous catalysts poses several drawbacks in terms of purification, recovery of the catalyst and reusability.

In this scenario, it is clear that the development of cheap, environment friendly, recyclable and efficient heterogeneous catalysts for the synthesis of tetrazoles under microwave assisted conditions is extremely challenging. In order to be useful in  $^{13}\text{N}$ -radiochemistry, the reaction for the formation of the tetrazoles should be completed in just a few minutes.

## 5.2. AIM AND OBJECTIVES

As it has been described in previous chapters, this PhD thesis initially focused in the development of radiolabelling strategies for the preparation of  $^{13}\text{N}$ -labelled azides and triazoles. After achieving the initial goals, we decided to expand the range of applications of Nitrogen-13 by working on the development of synthetic strategies for the preparation of  $^{13}\text{N}$ -labelled tetrazoles with the radioactive atom placed in the heterocycle. Despite tetrazoles have been labelled with Nitrogen-15 [31], the synthesis of  $^{13}\text{N}$ -labelled tetrazoles is still unprecedented. After literature search, it was found that already described reactions under conventional heating required very long reaction times, which were not compatible with the short half-life of Nitrogen-13. Hence, the feasibility of other

alternatives such as microwave heating was explored. Indeed, we found that there are very few reports in the literature concerning the preparation of tetrazoles under microwave conditions using heterogeneous catalyst, and hence we decided to take advantage of the experience and knowledge of one of our collaborators, Dr. Chandrashekhar V. Rode (National Chemical Laboratory, Pune, India) to develop novel heterogeneous catalyst which may enable the conversion of azides into tetrazoles in a fast and efficient fashion.

Based on the experience of our collaborator, the main goal was the development of nanostructured, copper based catalyst to assist in the production of tetrazoles *via* [3+2] cycloaddition involving the corresponding nitriles and sodium azide. The ultimate objective was to apply the newly developed catalysts to the production of one selected <sup>13</sup>N-labelled tetrazole as a model reaction. To achieve these general objectives, the following specific objectives were established:

1. To prepare and characterize nanostructured copper-based catalysts.
2. To develop a synthetic strategy for the preparation of a small library of tetrazoles by the reaction of sodium azide with nitriles using the copper-based nanostructured heterogeneous catalysts (developed in Objective 1) *via* (3+2) Huisgen cycloaddition.
3. To apply the best heterogeneous catalyst to the preparation of one <sup>13</sup>N-labelled tetrazole by the reaction of <sup>13</sup>N-labelled azide with nitrile *via* (3+2) Huisgen cycloaddition.

### 5.3. MATERIALS AND METHODS

#### 5.3.1. General Information

Copper(II) nitrate trihydrate, aluminium nitrate nonahydrate, potassium carbonate, ammonium chromate and ammonium dichromate AR were purchased from Loba Chemie. Aluminium oxide was purchased from Chem-Labs. Benzonitrile (99%), 4-chlorobenzonitrile, 4-(trifluoromethyl)benzonitrile (99%), *p*-tolunitrile (98%), 4-methoxybenzonitrile (98%), (4-chlorophenyl)acetonitrile (96%), copper(I) oxide (>99.9%), zinc oxide (ACS reagent, >99.9%), Celite® S (filter aid, dried, untreated), silica, ammonia solution (28-30%), potassium carbonate (>99%), *N*-methylpyrrolidine (97%), *N,N*-dimethylformamide (>99%), methanol (anhydrous, >99.8%), dimethyl sulfoxide (anhydrous, >99.9%) and hydrochloric acid (37%, extrapure, Ph. Eur.) were purchased from Sigma-Aldrich and used without further purification. Hexane (synthesis grade), ethyl acetate (synthesis grade), dichloromethane (synthesis grade), acetonitrile (HPLC grade)



and diethyl ether (extra pure) were purchased from Scharlab. Ultrapure water (Type I water, ISO 3696) was obtained from a Milli-Q® purification system (Merck Millipore).

### 5.3.2. Preparation of the catalysts

The nano structured Cu–Al catalyst (50% content in Copper; named in the current PhD 50%Cu-Al) was prepared by a simultaneous co-precipitation and digestion method with co-addition of an equimolar (0.05 M) mixture of an aqueous solution (250 mL) of  $\text{Cu}(\text{NO}_3)_2 \cdot 3\text{H}_2\text{O}$  (9.06 g),  $\text{Al}(\text{NO}_3)_3 \cdot 9\text{H}_2\text{O}$  (14.06 g) and 0.2 M aqueous  $\text{K}_2\text{CO}_3$  (20.7 g in 250 mL), in a round bottom flask having 5–10 mL of water at room temperature. After complete addition, the precipitate was digested further for 4–5 h and then filtered and washed with deionized water to remove the traces of potassium. The precipitate was dried in an oven at 100 °C for 5–8 h.

Cu-Al catalysts with chromium as a promoter having molar composition of 30%Cu, 39%Al and 31%Cr (named in the current PhD 30%Cu-Cr-Al) was prepared following a co-precipitation method. The ammonium chromate solution was prepared by adding 15 mL of 30% aqueous ammonia solution to 100 mL aqueous ammonium dichromate solution (18.63 g). This was added under stirring in a thin stream to nitrate solution of metal precursors prepared by dissolving 18.12 g of  $\text{Cu}(\text{NO}_3)_2 \cdot 3\text{H}_2\text{O}$  and 36.38 g of  $\text{Al}(\text{NO}_3)_3 \cdot 9\text{H}_2\text{O}$  in 130 mL water. After complete addition, a reddish brown precipitate was obtained which was then filtered and dried at 100°C for 8 h.

The last catalyst, named 20%Cu/SiO<sub>2</sub> in the current PhD thesis, was prepared by a wet impregnation method. In brief, silica (3.2 g) was added to a solution of  $\text{Cu}(\text{NO}_3)_2 \cdot 3\text{H}_2\text{O}$  (3.04 g) in water (50 mL), and the slurry was stirred for 12 h. Excess water was then removed by rotavaporation and the residue was oven-dried at 100°C. All the three prepared catalysts were calcined at 400°C for 3 h prior to use.

### 5.3.3. Characterization of the catalysts

Powder X-ray diffraction patterns were recorded on a P Analytical PXRD system (Model X-Pert PRO-1712), using Ni filtered Cu K radiation ( $\lambda = 0.154$  nm) as an X-ray source at 30 mA and 40 kV connected with an X-accelerator detector.

Transmission electron microscopy (TEM) analyses were performed on a Jeol Model JEM 1200 electron microscope operated at an accelerating voltage of 120 kV. A small amount of the sample was prepared by ultrasonically suspending the powder sample in ethanol. A drop of the suspension was deposited on a carbon coated copper grid and dried at room temperature before analysis.

Ammonia temperature programmed desorption (NH<sub>3</sub>-TPD) measurements were carried out on a Micromeritics-2720 (Chemisoft TPx) instrument. In order to evaluate the acidity of the catalysts, ammonia TPD measurements were carried out by (i) pre-treating the samples from room temperature to 473K under helium flow (25 mL min<sup>-1</sup>) for 2 h; (ii) adsorption of ammonia at 323K; and (iii) desorption of ammonia with a heating rate of 283K min<sup>-1</sup> starting from the adsorption temperature to 973K. The total amount of NH<sub>3</sub> desorbed was calculated by measuring the area of desorption peaks in both low and high temperature regions.

### 5.3.4. Synthetic procedures: chemistry

Six different tetrazoles (**5.1-5.6**) were prepared (see Figure 5.2).

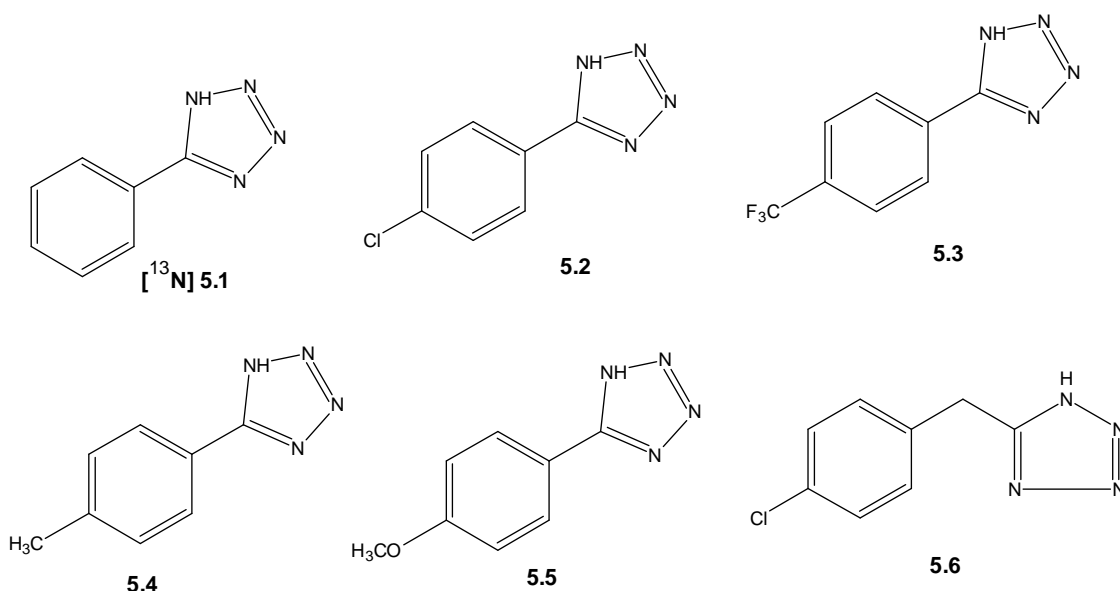


**Figure 5.2.** Tetrazoles prepared in this PhD thesis using the newly developed catalysts. Compound **5.1** was also labelled with Nitrogen-13.

The preparation of compounds **5.1-5.6** was carried out following a previously published method [32]. In brief, to a solution of anhydrous 30%Cu-Cr-Al (17mg) in NMP (1 mL) were added NaN<sub>3</sub> (94.66 mg, 1.4563 mmol) and the corresponding nitrile (0.9708 mmol). The reaction mixture was stirred for 1 min at room temperature and was subsequently irradiated in a single-mode microwave instrument (Biotage Initiator 2.5) at 230°C for 3-20 min. The reaction was monitored by TLC. The reaction crude was poured into 10 mL of H<sub>2</sub>O and the pH was adjusted to 1.0 with concentrated HCl (Caution: gas evolution). The mixture was cooled in an ice bath, the precipitate was collected by filtration and washed thoroughly with cold 1M HCl to yield the desired tetrazole. Characterization was

performed using <sup>1</sup>H-NMR, <sup>13</sup>C-NMR and Mass Spectrometry and data was compared to literature [13, 32].

### 5.3.5. Radiochemistry: Synthesis of [<sup>13</sup>N]5.1

#### 5.3.5.1. General

All procedures were carried out under EU standards in terms of radioprotection and following internal procedures.

#### 5.3.5.2. Production of the primary labelling agent

The whole synthetic procedure for the preparation of the labelled [<sup>13</sup>N]NO<sub>2</sub><sup>-</sup> was carried out using same procedure followed in the chapters 3 and 4 (see above).

#### 5.3.5.3. Synthesis of <sup>13</sup>N-labelled tetrazoles [<sup>13</sup>N]5.1

The solution containing [<sup>13</sup>N]NO<sub>2</sub><sup>-</sup> was added drop-wise to a second solution containing acetic acid (102 μL, 1.79 mmol) and hydrazine monohydrate solution (65 μL, 1.34 mmol) and the reaction for the formation of <sup>13</sup>N-labelled azide was allowed to occur for 5 min. at room temperature (RT). The <sup>13</sup>N-labelled azide was then added to a second solution containing benzonitrile (23 mg, 0.22 mmol), 30%Cu-Cr-Al Catalyst (4 mg of catalyst in 0.3 mL of NMP) and the reaction was allowed to occur for 20 minutes at 200°C under conventional oil bath heating. After quenching the reaction by dilution with 0.1% TFA in water, chromatographic yield was determined by radio-HPLC, using an Agilent 1200 Series HPLC system with a multiple wavelength UV detector (λ = 254 nm) and a radiometric detector (Gabi, Raytest). A RP-C18 column (Mediterranean Sea18, 4.6x250 mm, 5 μm particle size) was used as the stationary phase and 0.1 % TFA in water (A)/ 0.1 % TFA in acetonitrile (B) was used as the mobile phase, with the following gradient: t=0 min, 90%A/10%B; t=10 min, 20%A/80%B; t=12 min, 20%A/80%B; t=15 min, 90%A/10%B. The retention time for the labelled tetrazole was 7.4 min.

## 5.4. RESULTS AND DISCUSSION

### 5.4.1. Synthesis of tetrazoles (5.1-5.6) using Copper based heterogeneous catalysts

In this work, we explored the microwave assisted synthesis of 5-substituted 1*H*-tetrazole derivatives using copper-based nanostructures catalysts *via* [3+2] cycloaddition involving the corresponding nitriles and sodium azide in *N*-Methyl-2-pyrrolidone (NMP) as the solvent (Figure 5.3).

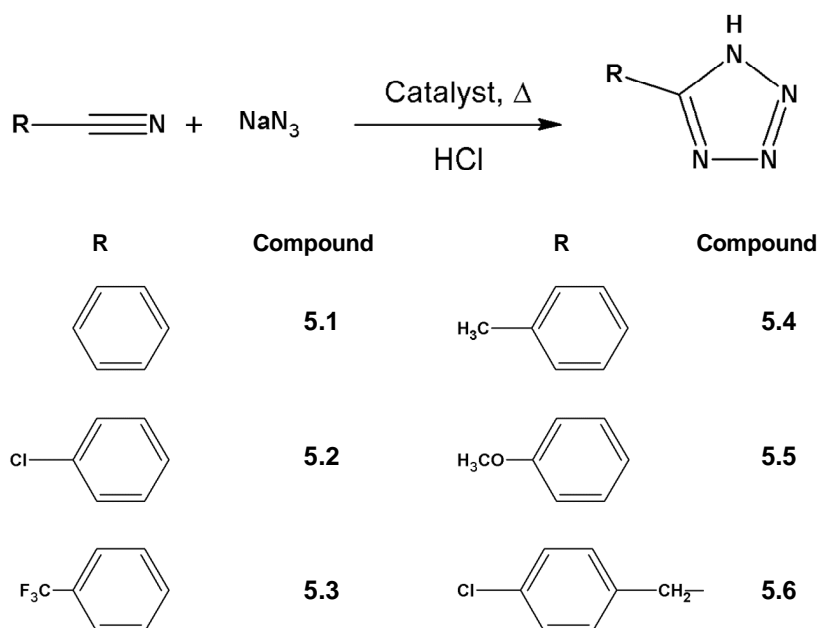


**Figure 5.3.** Synthesis of 5-substituted 1*H*-tetrazoles by reaction of sodium azide with nitriles.

#### 5.4.2. Preparation and characterization of the catalysts

Three different Copper based catalysts (named 20%Cu/SiO<sub>2</sub>, 50%Cu-Al, and 30%Cu-Cr-Al) were prepared and evaluated for the synthesis of 5-substituted 1*H*-tetrazoles by reacting the corresponding benzonitriles with sodium azide using NMP as the solvent. Before approaching the chemical reactions, the catalysts were thoroughly characterized by X-Ray diffraction (XRD), transmission electron microscopy (TEM) and NH<sub>3</sub>-temperature-programmed desorption (NH<sub>3</sub>-TPD) in order to investigate the copper oxidation state, particle size and the acidity of the catalysts, respectively.

In Figure 5.4, the XRD patterns of the catalysts after calcinations are shown. As it can be seen, 20%Cu/SiO<sub>2</sub> catalyst showed narrow and high intensity peaks at  $2\theta$  values of 35.5 ( $\bar{1}11$ ), 38.7 (111) and small peaks centred at the 32.5° (110), 48.6° ( $\bar{2}02$ ) 53.3° (020), 58.1° (202), 61.4° (113), 66.3° ( $\bar{3}11$ ), 68.1° (220), 72.4° (311), and 75.1° ( $\bar{2}22$ ) corresponding to CuO phase (PCPDF win no. 80-1917). The appearance of such sharp peaks was mainly due the impregnation method followed for the preparation of the catalyst. 30%Cu-Cr-Al catalyst showed CuO ( $2\theta = 35.5^\circ$ ) phase together with broad, low intensity peaks at  $2\theta$  values of 37.3° (222), 18.2° (111), 30.4° (220), 43.3° (400), 57.2° (511), and 63.1° (440) corresponding to CuCr<sub>2</sub>O<sub>4</sub> phase (PCPDF win no. 26-0509). However, 50%Cu-Al catalyst showed amorphous nature with a very small, broad peak at  $2\theta = 35.5^\circ$  ( $\bar{1}11$ ) corresponding to CuO phase. The lack of distinct peaks corresponding to CuO phase in 50%Cu-Al catalyst indicates the presence of small CuO particles. However, crystalline nature of the 20%Cu/SiO<sub>2</sub> catalyst points to the formation of larger Cu crystallites and/or particles

compared to that of Cu-Al and Cu-Cr-Al catalysts. In all cases, Cu was present in Cu(II) state, which is known to act as a Lewis acid and activates the nitrile group *via* coordination in tetrazole synthesis [33].

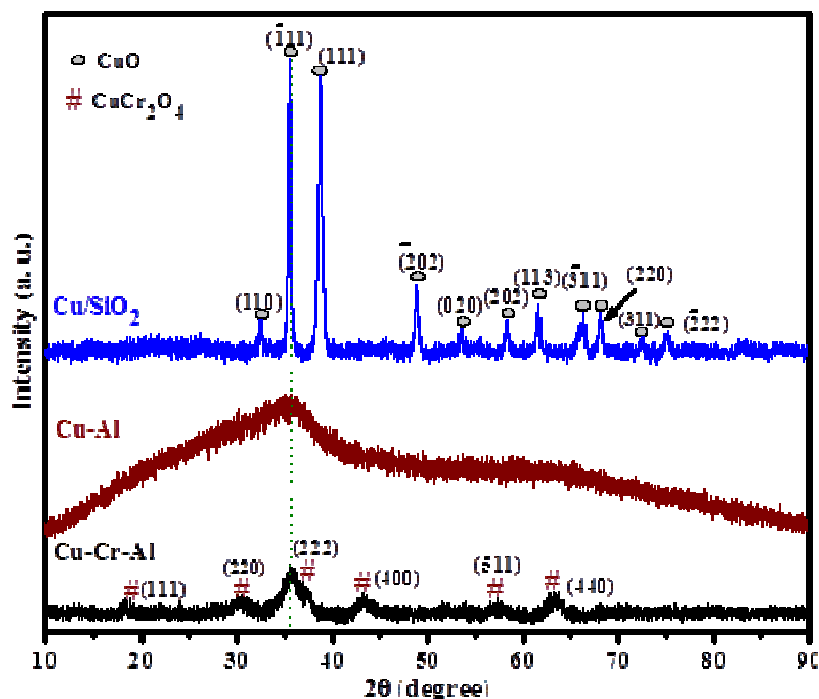


**Figure 5.4.** X-ray diffraction patterns of the Cu based catalysts.

These results were supported by the HR-TEM images (Figure 5.5). Images acquired with 50%Cu-Al and 30%Cu-Cr-Al catalysts showed dispersed, small and spherical particles with sizes in the ranges of 4-5 and 5-8 nm, respectively (Figures 5.5a, b, c, and d). The rod-like shape evidenced in TEM images for 30%Cu-Cr-Al catalyst was associated with the boehmite phase of alumina (Figure 5.5a) [34]. However, slight aggregations with larger particles (17-28 nm) could be observed in the case of 20%Cu/SiO<sub>2</sub> catalyst (Figures 5.5e and f).

The acidity of the catalysts plays a pivotal role in the synthesis of tetrazoles. Because of this, the acidity and acid strength was investigated using NH<sub>3</sub>-TPD analysis (Figure 5.6). All the catalysts showed an NH<sub>3</sub> desorption peak at approximately 90°C, which was due to desorption of physisorbed ammonia. The catalyst 20%Cu/SiO<sub>2</sub> showed very less acidity with a small hump like peak at approximately 350°C, corresponding to moderate acid sites. The TPD profile of 50%Cu-Al catalyst showed peak maxima at 377.5°C and 502°C, and a high intensity peak at 652.8°C, confirming the presence of moderate and strong acid sites [35]. Similarly, 30%Cu-Cr-Al catalyst also showed the peaks corresponding to the

moderate and strong acid sites. However,  $\text{NH}_3$  desorption peak intensity at  $652.8^\circ\text{C}$  of 50%Cu-Al catalyst was much higher compared to that of the 30%Cu-Cr-Al catalyst, indicating higher acidic strength of the 50%Cu-Al catalyst. Acidic strength values calculated based on total desorbed  $\text{NH}_3$  were  $0.554 \text{ mmol g}^{-1}$  for 50%Cu-Al,  $0.446 \text{ mmol g}^{-1}$  for 30%Cu-Cr-Al, and  $0.0684 \text{ mmol g}^{-1}$  for 20%Cu/ $\text{SiO}_2$ . Such difference in acidity was responsible for the difference in catalytic activity as discussed below.

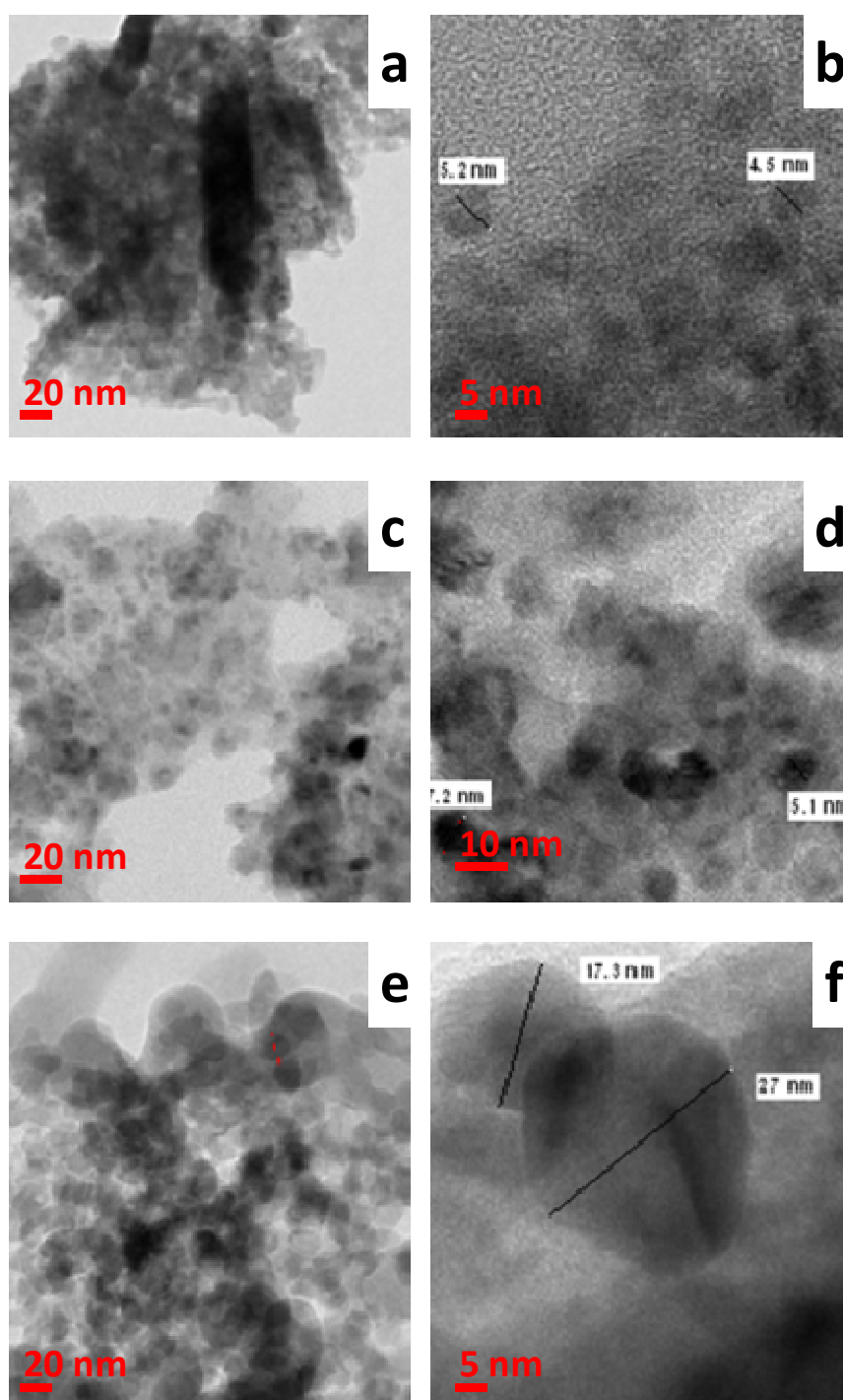


**Figure 5.5.** HR-TEM images of (a,b) Cu-Cr-Al, (c,d) Cu-Al and (e,f) Cu/ $\text{SiO}_2$  catalysts.

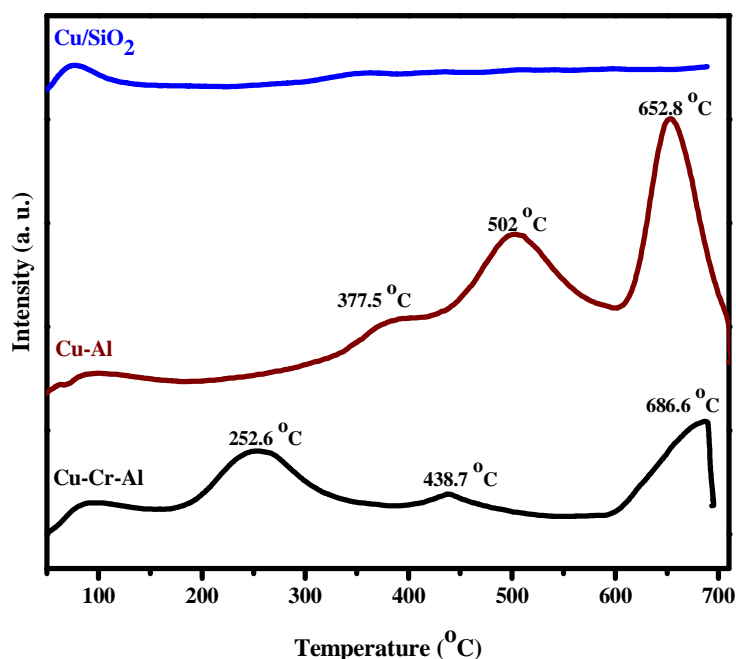


**Figure 5.6.**  $\text{NH}_3$ -TPD profiles of Cu-based catalysts.

### 5.4.3. Catalytic activity

Copper based catalysts have been explored in the production of 5-substituted 1*H*-tetrazoles by reaction of sodium azide and nitriles. As the solvent is known to play a pivotal role in tetrazole synthesis [36], various solvents were initially evaluated in the presence and absence of catalyst and under different temperature conditions for compound **5.1** (see Table 5.2). Without the presence of the catalysts, no formation of the corresponding tetrazole could be observed, irrespective of the solvent (see Table 5.2, entries 1-4). Under catalytic conditions, none of the catalysts led to the formation of the desired tetrazole when the reaction was conducted in water or DMF/MeOH(9:1) as the solvent (Table 5.2, entries 5, 6, 9, 10 and 13), except 30%Cu-Cr-Al which resulted in 60% isolated yield (Table 5.2, entry 16). Interestingly, the three Cu-based catalysts showed excellent results in polar, aprotic solvents such as DMSO and NMP, both at 200 $^{\circ}\text{C}$  and 230 $^{\circ}\text{C}$  (Table 5.2, entries 7 and 8 for 20%Cu/SiO<sub>2</sub>; entries 11 and 12 for 50%Cu-Al; entries 17-19 for 30%Cu-Cr-Al). The enhanced catalytic properties of the catalysts in these media might be due to the high dipole moment of DMSO and the high nucleophilicity of NMP [2]. However, the time required to achieve maximum tetrazole formation was different for the three catalysts. When NMP was used as the solvent, 91% yields could be achieved with 30%Cu-Cr-Al catalyst in 7 min reaction (Table 5.2, entry 18), while at the same temperature 15 minutes of reaction were required to achieve yields of 78 and 81% when

20%Cu/SiO<sub>2</sub> and 50%Cu-Al were used, respectively. The yield obtained for 30%Cu-Cr-Al catalyst is significantly higher than that achieved with cuprous oxide and ZnO under identical experimental conditions (74% and 30%, respectively; see Table 5.2, entries 20 and 21).

**Table 5.2:** Synthesis of 5-phenyl-1H-tetrazole (**5.1**) in the presence of different Cu and Zn catalyst under different experimental conditions.<sup>a</sup>

Entry	Catalyst	Solvent	Time (min)	T (°C)	Yield <sup>b</sup> (%)
1	None	Water	30	100	-
2	None	DMF/MeOH(9:1)	30	180	-
3	None	DMSO	30	200	-
4	None	NMP	30	230	-
5	Cu-SiO <sub>2</sub>	Water	30	100	-
6	Cu-SiO <sub>2</sub>	DMF/MeOH(9:1)	30	180	-
7	Cu-SiO <sub>2</sub>	DMSO	25	200	84
8	Cu-SiO <sub>2</sub>	NMP	15	230	78
9	Cu-Al	Water	30	100	-
10	Cu-Al	DMF/MeOH(9:1)	30	180	-
11	Cu-Al	DMSO	15	200	77
12	Cu-Al	NMP	15	230	81
13	Cu-Cr-Al	Water	30	100	-
14	Cu-Cr-Al	MeOH	30	100	30
15	Cu-Cr-Al	DMF	30	140	48
16	Cu-Cr-Al	DMF/MeOH(9:1)	30	140	60
17	Cu-Cr-Al	DMSO	15	200	75
18	Cu-Cr-Al	NMP	7	230	91
19	Cu-Cr-Al	NMP	7	200	77
20	Cu <sub>2</sub> O	NMP	7	230	74
21	ZnO	NMP	7	230	30

<sup>a</sup> Reaction conditions: 0.97 mmol nitrile, 1.46 mmol NaN<sub>3</sub>, 17 mg catalyst, and 1.0 mL NMP; microwave heating at 230 °C. <sup>b</sup> Isolated yield.

The lowest activity of 20%Cu/SiO<sub>2</sub> with respect to 30%Cu-Cr-Al can be explained by the larger particle size (17-28 nm), which ultimately results in lower surface area (see Figure 5.5). Interestingly, 50%Cu-Al catalyst shows higher acidity than 30%Cu-Cr-Al, but lower yields were obtained with the first under equivalent experimental conditions. This result suggests that moderate acid sites and addition of Cr to the catalyst contribute to enhance the catalytic activity.

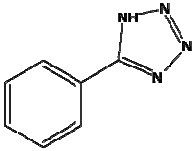
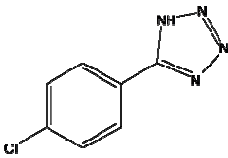
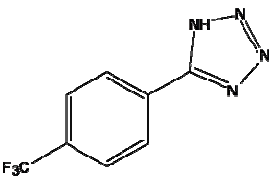
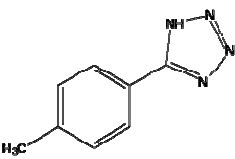
The effect of the reaction temperature on the catalytic activity of 30%Cu-Cr-Al was also investigated. When the temperature was decreased to 200°C, lower yield was achieved (77%; Table 5.2, entry 19). Optimal results were obtained with NMP as the solvent. Hence,

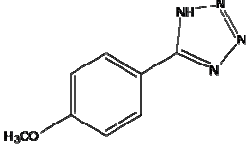
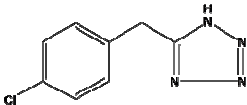


NMP was the solvent of choice to explore the application of the catalyst to the preparation of other tetrazoles (5.2-5.6).

In order to check the scope of the prepared 30%Cu-Cr-Al catalyst for the synthesis of 5-substituted 1H tetrazoles, different substituted nitriles were explored to prepare compounds 5.1-5.6 (see table 5.3 for characterization of the isolated tetrazoles).

**Table 5.3:** Characterization of compounds 5.1-5.6.

	Name / Structure	Characterization data
5.1	5-Phenyl-1H-tetrazole 	<sup>1</sup> H NMR (400 MHz, DMSO-d <sub>6</sub> ) δ 7.55-7.60 (m, 3H, aromatic), 8.01-8.05 (m, 2H, aromatic); <sup>13</sup> C NMR (125 MHz, DMSO-d <sub>6</sub> , δ, ppm): 154.5 (tetrazole ring), 131.0, 130.2, 127.2, 124.4; LCMS: calculated for C <sub>7</sub> H <sub>6</sub> N <sub>4</sub> (MH <sup>+</sup> ): 147.149; found: 147.054.
5.2	5-(4'-Chlorophenyl) -1H-tetrazole 	<sup>1</sup> H NMR (400 MHz, DMSO-d <sub>6</sub> ) δ 8.02 (d, J = 8.4 Hz, 2H, aromatic), 7.65 (d, J = 8.4 Hz, 2H, aromatic); <sup>13</sup> C NMR (125 MHz, DMSO-d <sub>6</sub> ): d = 155.6, 135.2, 129.5, 128.2, 124.4; LCMS calculated for C <sub>7</sub> H <sub>5</sub> ClN <sub>4</sub> (MH <sup>+</sup> ): 181.594; found: 181.006.
5.3	5-(4'-(Trifluoromethyl)phenyl)-1H-tetrazole 	<sup>1</sup> H NMR (400 MHz, DMSO-d <sub>6</sub> ) δ 8.21(d, J = 8.1 Hz, 2H, aromatic), 7.92 (d, J = 8.1 Hz, 2H, aromatic); <sup>13</sup> C NMR (125 MHz, DMSO-d <sub>6</sub> ): d = 155.2, 131.2, 128.3, 127.6, 126.2, 123.7; LCMS calculated for C <sub>8</sub> H <sub>5</sub> F <sub>3</sub> N <sub>4</sub> (MH <sup>+</sup> ): 215.147; found: 215.021.
5.4	5-(4'-Tolyl) -1H-tetrazole 	<sup>1</sup> H NMR (400 MHz, DMSO-d <sub>6</sub> ) δ 7.96(d, J = 8.0 Hz, 2H, aromatic), 7.48 (d, J = 8.0 Hz, 2H, aromatic), 2.30 (s, 3H, CH <sub>3</sub> ); <sup>13</sup> C NMR (125 MHz, DMSO-d <sub>6</sub> , δ, ppm): 154.8, 139.4, 130.4, 126.6, 121.4, 21.1; LCMS calculated for C <sub>8</sub> H <sub>8</sub> N <sub>4</sub> (MH <sup>+</sup> ): 161.175; found: 161.067.

Name / Structure	Characterization data
<p>5.5</p> <p>5-(4'-Methoxyphenyl)-1H-tetrazole</p> 	<p><b><sup>1</sup>H NMR</b> (400 MHz, DMSO-d<sub>6</sub>) δ 7.94 (d, J = 9.0 Hz, 2H, aromatic), 7.13 (d, J = 9.0 Hz, 2H, aromatic), 3.82 (s, 3H, CH<sub>3</sub>).</p> <p><b><sup>13</sup>C NMR</b> (125 MHz, DMSO-d<sub>6</sub>, δ, ppm): 161.6, 154.4, 128.4, 116.4, 114.6, 55.2;</p> <p><b>LCMS</b> calculated for C<sub>8</sub>H<sub>8</sub>N<sub>4</sub>O(MH<sup>+</sup>): 177.175; found: 177.053.</p>
<p>5.6</p> <p>5-((4'-Chlorophenyl)methyl)-1H-tetrazole</p> 	<p><b><sup>1</sup>H NMR</b> (400 MHz, DMSO-d<sub>6</sub>) δ 7.36 (d, J = 8.4 Hz, 2H, aromatic), 7.27 (d, J = 8.4 Hz, 2H, aromatic), 4.36 (s, 2H, CH<sub>2</sub>);</p> <p><b><sup>13</sup>C-NMR</b> (125 MHz, DMSO-d<sub>6</sub>, δ, ppm): 154.4, 134.5, 131.2, 130.2, 128.2, 27.4;</p> <p><b>LCMS</b> calculated for C<sub>8</sub>H<sub>7</sub>ClN<sub>4</sub> (MH<sup>+</sup>): 195.620; Found: 195.508.</p>

The results (Table 5.4) show that all nitriles explored in this work react efficiently with sodium azide, and excellent yields within 3-20 min could be obtained, depending on the reactivity of the substrate. Nitriles having electron-withdrawing groups at the *p*- position (compounds **5.2-5.4**, Table 5.4, entries 2-4) gave excellent yields in very short reaction times when compared to nitriles containing electron-donating groups on the same position (Table 5.4, compound **5.5**, entry 5), which required prolonged reaction time [25]. This was an expected result, as the presence of electron-withdrawing groups increases the polarity of the cyanide group inductively, favouring thus the reaction. 4-Chlorophenyl acetonitrile (precursor for **5.6**), was the less reactive precursor and required a reaction time of 20 min to yield the corresponding tetrazole in moderate yield (Table 5.4, entry 6).

**Table 5.4:** Preparation of tetrazoles **5.1-5.6** mediated by the Cu-Cr-Al catalyst.<sup>a</sup>

Entry	Compound	Time (min)	Yield <sup>b</sup> (%)	TON	TOF (h <sup>-1</sup> )
1	<b>5.1</b>	7	91	17.26	148.02 592.08 <sup>c</sup>
2	<b>5.2</b>	4	93	17.30	259.52
3	<b>5.3</b>	3	82	15.96	319.20
4	<b>5.4</b>	6	85	16.04	160.4
5	<b>5.5</b>	15	88	16.91	67.64
6	<b>5.6</b>	20	77	14.26	42.78

<sup>a</sup> Reaction conditions: 0.97 mmol nitrile, 1.46 mmol NaN<sub>3</sub>, 17 mg Cu-Cr-Al, and 1.0 mL NMP; microwave heating at 230°C. <sup>b</sup>Isolated yield. <sup>c</sup>TOF after fourth recycle; TON: Turn-over number, calculated as the molar ratio between desired product and catalyst; TOF: turn-over frequency, calculated as TON/reaction time.

X-ray diffraction analyses revealed that copper was present in all catalysts mainly in the (II) oxidation state. This oxidation state is required to activate the nitrile group *via* coordination (see Figure 5.7 for a proposed reaction mechanism) [33]. This accelerates the cyclization step (**a** in the Figure 5.7) by enhancing the electrophilic character of the cyanide group, which reacts with sodium azide to form the intermediate compound **b**. (see Figure 5.7) Further protonation of **b** during the acid treatment results in the formation of a more stable tetrazole in tautomeric form (see Figure 5.7).

One of the major advantages of heterogeneous catalysts arises from their recyclability. In order to proof the recyclability of our catalyst, five consecutive reactions were carried out. Between runs, the 30%Cu-Cr-Al catalyst was separated by centrifugation (5000 rpm) and washed twice with ultra pure water (5 mL). The catalyst was further dried by rotary evaporation and reused. With the fresh catalyst, the preparation of **5.1** could be achieved in 91% isolated yield when the reaction was conducted at 230°C for 7 min under MW heating. Under identical experimental conditions, isolated yields of 90%, 90%, 88% and 87% were obtained in the second, third, fourth and fifth uses, respectively (Figure 5.8). These results suggest that the catalytic activity remains unaltered over the synthetic cycles, while the slight decrease in yield might be due to minor loss of the catalyst during the recycling process.

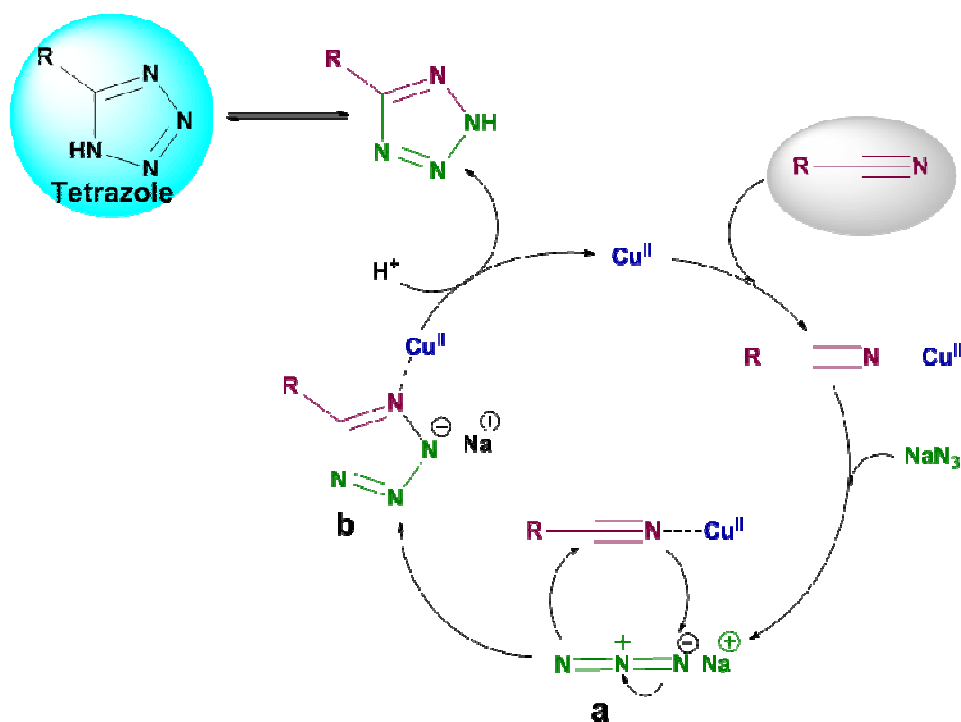


Figure 5.7. Plausible mechanism for the formation of tetrazoles.

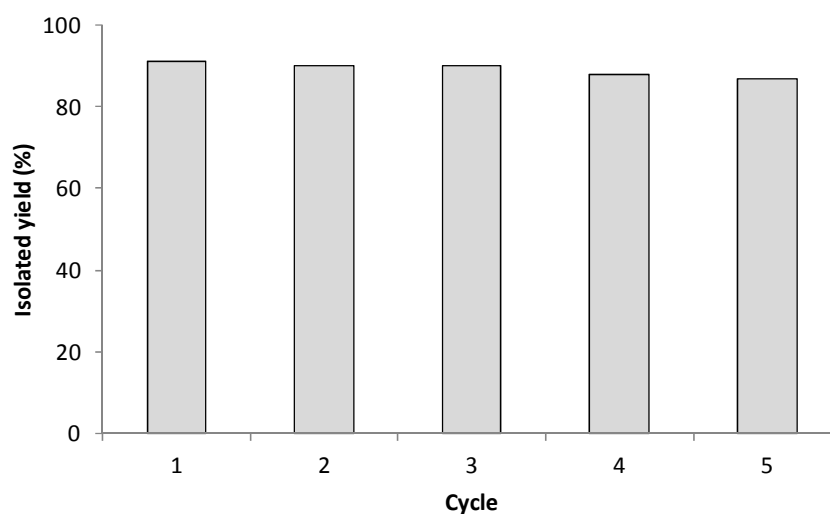


Figure 5.8. Reusability of the 30%Cu-Cr-Al catalyst for the synthesis of 5.1.

#### 5.4.4. Radiochemistry: Synthesis of $^{13}\text{N}$ 5.1

The results obtained in non-radioactive conditions encouraged us to investigate the suitability of the catalyst to prepare  $^{13}\text{N}$ -labelled tetrazoles. However, the current configuration of our dependencies does not permit the application of microwave heating within the radiation controlled facilities. Because of this, the catalyst was assayed under

conventional heating using the automated synthesis modules currently available in our labs.

When the reaction for the formation of the azide was conducted for 5 min, the presence of the desired labelled tetrazole could be identified after 20 min reaction under conventional heating (see Figure 5.9) with chromatographic yield of  $20\pm 4\%$ . The product could be isolated by using semi-preparative HPLC. Despite the overall radiochemical yield after isolation was low (approximately 1%, not decay corrected) our experiments show the first example of  $^{13}\text{N}$ -labelled tetrazole. Implementation of microwave heating in the radiation-controlled facility, full automation of the process and utilisation of the newly developed outstanding catalysts should lead to the formation of sufficient amount of labelled compound to approach in vivo imaging studies in small animals.

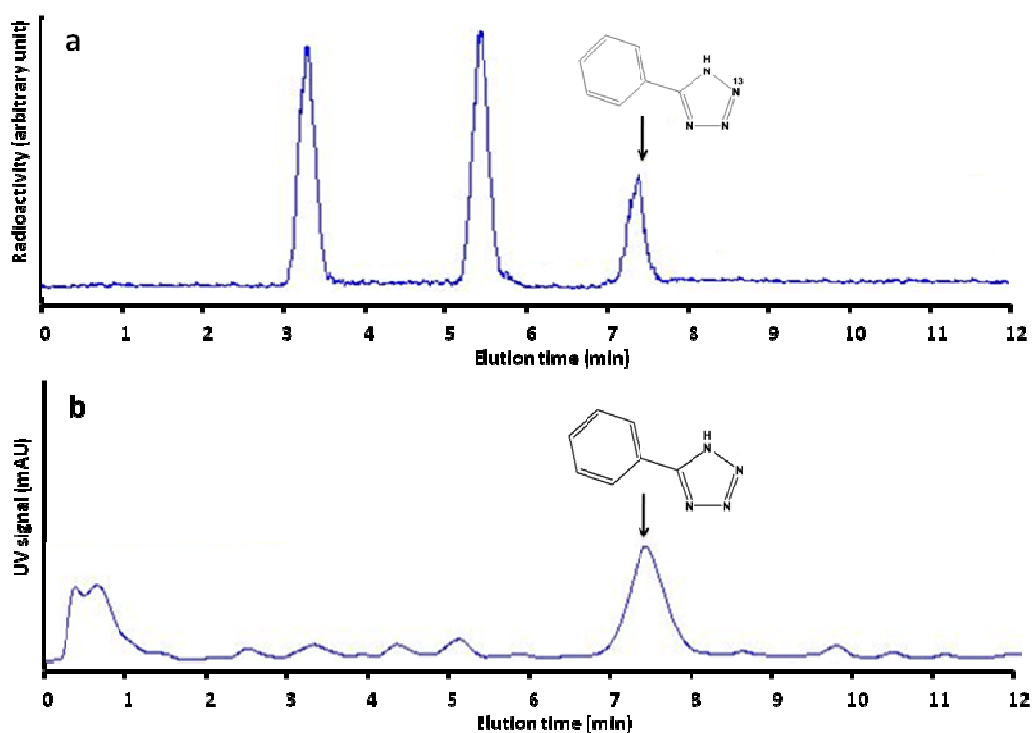


**Figure 5.9.** Chromatographic profiles for the synthesis of  $[^{13}\text{N}]5.1$  using radioactivity (a) and UV (b) detectors. Reaction time for the formation of the tetrazole: 20 min.

## 5.5. SUMMARY AND CONCLUSIONS

In conclusion, we have prepared copper-based heterogeneous catalysts for the synthesis of 5-substituted 1H-tetrazoles from nitriles and sodium azide *via* (3+2) Huisgen cycloaddition. This nano-sized heterogeneous catalyst showed excellent activity for the preparation of different tetrazoles in short reaction time in the range 3-20 min at  $230^\circ\text{C}$ . Catalyst-recycling studies confirmed that 30%Cu-Cr-Al can be reused up to five

consecutive runs without significant loss of catalytic activity. The high catalytic efficiency of the newly developed catalyst enabled the preparation of one selected <sup>13</sup>N-labelled tetrazole even under conventional heating. Translation of the experimental conditions to microwave heating should result in improved radiochemical yields, and hence the <sup>13</sup>N-labelled compounds may find application in the field of *in vivo* imaging using Positron Emission Tomography.

## 5.6. REFERENCES

1. Bladin, J., *Ueber von dicyanphenylhydrazin abgeleitete verbindungen*. European Journal of Inorganic Chemistry, 1885. **18**(1): p. 1544-1551.
2. Cantillo, D., B. Gutmann, and C.O. Kappe, *Mechanistic Insights on Azide-Nitrile Cycloadditions: On the Dialkyltin Oxide- Trimethylsilyl Azide Route and a New Vilsmeier- Haack-Type Organocatalyst*. Journal of the American Chemical Society, 2011. **133**(12): p. 4465-4475.
3. Butler, R., et al., *Comprehensive heterocyclic chemistry*. Katritzky, AR, Rees, CW, Scriven, EFV, Eds, 1996.
4. Myznikov, L., A. Hrabalek, and G. Koldobskii, *Drugs in the tetrazole series.(Review)*. Chemistry of Heterocyclic Compounds, 2007. **43**(1): p. 1-9.
5. Roh, J., K. Vávrová, and A. Hrabálek, *Synthesis and Functionalization of 5-Substituted Tetrazoles*. European Journal of Organic Chemistry, 2012. **2012**(31): p. 6101-6118.
6. Ali, M.A.E.A.A., E. Remaily, and S.K. Mohamed, *Eco-friendly synthesis of guanidinyltetrazole compounds and 5-substituted 1H-tetrazoles in water under microwave irradiation*. Tetrahedron, 2014. **70**(2): p. 270-275.
7. Gutmann, B., et al., *Synthesis of 5-Substituted 1H-Tetrazoles from Nitriles and Hydrazoic Acid by Using a Safe and Scalable High-Temperature Microreactor Approach*. Angewandte Chemie International Edition, 2010. **49**(39): p. 7101-7105.
8. Curran, D.P., S. Hadida, and S.-Y. Kim, *Tris (2-perfluorohexylethyl) tin azide: A new reagent for preparation of 5-substituted tetrazoles from nitriles with purification by fluorous/organic liquid-liquid extraction*. Tetrahedron, 1999. **55**(29): p. 8997-9006.
9. Kumar, A., R. Narayanan, and H. Shechter, *Rearrangement reactions of (hydroxyphenyl) carbenes*. The Journal of organic chemistry, 1996. **61**(13): p. 4462-4465.

10. Himo, F., et al., *Mechanisms of tetrazole formation by addition of azide to nitriles*. Journal of the American Chemical Society, 2002. **124**(41): p. 12210-12216.
11. HARVILL, E.K., et al., *The Synthesis of 1, 5-disubstituted tetrazoles*. The Journal of organic chemistry, 1950. **15**(3): p. 662-670.
12. Finnegan, W.G., R.A. Henry, and R. Lofquist, *An improved synthesis of 5-substituted tetrazoles*. Journal of the American Chemical Society, 1958. **80**(15): p. 3908-3911.
13. Jin, T., et al., *Copper-catalyzed synthesis of 5-substituted 1H-tetrazoles via the [3+ 2] cycloaddition of nitriles and trimethylsilyl azide*. Tetrahedron Letters, 2008. **49**(17): p. 2824-2827.
14. Su, W.K., et al., *A Facile Synthesis of 1-Substituted-1H-1, 2, 3, 4-Tetrazoles Catalyzed by Ytterbium Triflate Hydrate*. European Journal of Organic Chemistry, 2006. **2006**(12): p. 2723-2726.
15. Hajra, S., D. Sinha, and M. Bhowmick, *Metal triflate catalyzed reactions of alkenes, NBS, nitriles, and TMSN<sub>3</sub>: synthesis of 1, 5-disubstituted tetrazoles*. The Journal of organic chemistry, 2007. **72**(5): p. 1852-1855.
16. Chen, Z., et al., *Silver-catalyzed regioselective [3+ 2] cycloaddition of arene-diazonium salts with 2, 2, 2-trifluorodiazoethane (CF<sub>3</sub>CHN<sub>2</sub>): a facile access to 2-aryl-5-trifluoromethyltetrazoles*. Chemical Communications, 2015. **51**(92): p. 16545-16548.
17. Amantini, D., et al., *TBAF-catalyzed synthesis of 5-substituted 1 H-tetrazoles under solventless conditions*. The Journal of organic chemistry, 2004. **69**(8): p. 2896-2898.
18. HERBST, R.M. and K.R. WILSON, *Apparent Acidic Dissociation of Some 5-Aryltetrazoles<sup>1</sup>*. The Journal of organic chemistry, 1957. **22**(10): p. 1142-1145.
19. Mihina, J.S. and R.M. Herbst, *The reaction of nitriles with hydrazoic acid: Synthesis of monosubstituted tetrazoles*. The Journal of organic chemistry, 1950. **15**(5): p. 1082-1092.
20. Venkateshwarlu, G., et al., *Cadmium Chloride as an Efficient Catalyst for Neat Synthesis of 5-Substituted 1 H-Tetrazoles*. Synthetic Communications®, 2009. **39**(24): p. 4479-4485.
21. Khalafi-Nezhad, A. and S. Mohammadi, *Highly efficient synthesis of 1-and 5-substituted 1 H-tetrazoles using chitosan derived magnetic ionic liquid as a*

- recyclable biopolymer-supported catalyst*. RSC Advances, 2013. **3**(13): p. 4362-4371.
22. Akhlaghinia, B. and S. Rezazadeh, *A novel approach for the synthesis of 5-substituted-1H-tetrazoles*. Journal of the Brazilian Chemical Society, 2012. **23**(12): p. 2197-2203.
23. Alterman, M. and A. Hallberg, *Fast microwave-assisted preparation of aryl and vinyl nitriles and the corresponding tetrazoles from organo-halides*. The Journal of organic chemistry, 2000. **65**(23): p. 7984-7989.
24. Marvi, O., A. Alizadeh, and S. Zarrabi, *Montmorillonite K-10 clay as an efficient reusable heterogeneous catalyst for the solvent-free microwave mediated synthesis of 5-substituted 1H-tetrazoles*. Bull. Korean Chem. Soc, 2011. **32**(11): p. 4001.
25. Erken, E., et al., *A rapid and novel method for the synthesis of 5-substituted 1 H-tetrazole catalyzed by exceptional reusable monodisperse Pt NPs@ AC under the microwave irradiation*. RSC Advances, 2015. **5**(84): p. 68558-68564.
26. Roh, J., et al., *Practical synthesis of 5-substituted tetrazoles under microwave irradiation*. Synthesis, 2009. **2009**(13): p. 2175-2178.
27. Schmidt, B., D. Meid, and D. Kieser, *Safe and fast tetrazole formation in ionic liquids*. Tetrahedron, 2007. **63**(2): p. 492-496.
28. Myznikov, L., et al., *Tetrazoles: LI. Synthesis of 5-substituted tetrazoles under microwave activation*. Russian Journal of Organic Chemistry, 2007. **43**(5): p. 765-767.
29. Zhao, Z., et al., *Discovery of 2, 3, 5-trisubstituted pyridine derivatives as potent Akt1 and Akt2 dual inhibitors*. Bioorganic & medicinal chemistry letters, 2005. **15**(4): p. 905-909.
30. Shie, J.-J. and J.-M. Fang, *Microwave-assisted one-pot tandem reactions for direct conversion of primary alcohols and aldehydes to triazines and tetrazoles in aqueous media*. The Journal of organic chemistry, 2007. **72**(8): p. 3141-3144.
31. Wentrup, C. and C. Thétaz, *<sup>15</sup>N Labelling: Potassium azide, tetrazoles and imidazoles*. Helvetica Chimica Acta, 1976. **59**(1): p. 256-259.
32. Cantillo, D., B. Gutmann, and C.O. Kappe, *An Experimental and Computational Assessment of Acid-Catalyzed Azide-Nitrile Cycloadditions*. The Journal of organic chemistry, 2012. **77**(23): p. 10882-10890.
33. Ghorbani-Choghamarani, A., L. Shiri, and G. Azadi, *The first report on the eco-friendly synthesis of 5-substituted 1 H-tetrazoles in PEG catalyzed by Cu (ii)*



- immobilized on  $\text{Fe}_3\text{O}_4@\text{SiO}_2@l$ -arginine as a novel, recyclable and non-corrosive catalyst.* RSC Advances, 2016. **6**(39): p. 32653-32660.
34. Bai, X., et al., *Efficient and tuneable photoluminescent boehmite hybrid nanoplates lacking metal activator centres for single-phase white LEDs.* Nature communications, 2014. **5**.
35. Cai, F., W. Zhu, and G. Xiao, *Promoting effect of zirconium oxide on  $\text{Cu-Al}_2\text{O}_3$  catalyst for the hydrogenolysis of glycerol to 1, 2-propanediol.* Catalysis Science & Technology, 2016.
36. Lang, L., et al., *Mesoporous  $\text{ZnS}$  nanospheres: A high activity heterogeneous catalyst for synthesis of 5-substituted 1H-tetrazoles from nitriles and sodium azide.* Chemical Communications, 2010. **46**(3): p. 448-450.



## **6. Concluding Remarks**



## 6. CONCLUDING REMARKS

1.  $^{13}\text{N}$ -labelled aryl azides can be efficiently prepared by reaction of the  $^{13}\text{N}$ -labelled aryl-diazonium salt with *in situ* generated hydrazoic acid.
2. The experimental data combined with computational calculations support a stepwise mechanism *via* acyclic zwitterionic intermediates.
3. The preparation of chemically and radiochemically pure  $^{13}\text{N}$ -labelled polysubstituted triazoles can be achieved by reaction of  $^{13}\text{N}$ -labelled azides with alkynes *via* (3+2) Huisgen cycloaddition. The same methodology can be applied to the preparation of triazoles using aromatic aldehydes and DBU as the catalyst, although this reaction does not work under radioactive conditions for aliphatic aldehydes.
4. Automatisation of the radiosynthetic process described above enables the preparation of  $^{13}\text{N}$ -labelled triazoles in sufficient amount of radioactivity to approach putative *in vivo* studies in small animals.
5. Copper based, nanostructured heterogeneous catalyst can be efficiently used for the preparation of 5-substituted 1H-tetrazoles by (3+2) Huisgen cycloaddition using nitriles and sodium azide under microwave heating in short reaction times. Isolated yields are higher than those obtained using conventional catalysts.
6. The high catalytic efficiency of the copper-based nanostructured heterogeneous catalysts enabled the preparation of one selected  $^{13}\text{N}$ -labelled tetrazole under conventional heating.



## ABBREVIATIONS

ATP	Adenosine triphosphate
CT	Computerised tomography
DEAD	Diethyl azodicarboxylate
DFT	Density functional theory
DMF	Dimethylformamide
DMSO	Dimethylsulfoxide
GC	Gas chromatography
GC-MS	Gas chromatography mass spectrometry
BOC	Tert-butyloxycarbonyl
MW	Microwave
GSH	Glutathione
GMP	Good manufacturing practices
HPLC	High-performance liquid chromatography
HRMS	High-Resolution Mass Spectrometry
LC-MS	Liquid chromatography–mass spectrometry
MRI	Magnetic resonance imaging
MRS	Magnetic resonance spectroscopy
MS	Mass spectrometry
NBS	N-Bromosuccinimide
NMP	N-Methyl-2-pyrrolidone
OI	Optical imaging
PET	Positron emission tomography
RT	Room temperature
SN <sup>2</sup> Ar	Aromatic nucleophilic substitution bimolecular
SPE	Solid phase extraction
SPECT	Single photon emission computerised tomography
TDP	Temperature programmed desorption
TEM	Transmission electron microscopy
TFA	Trifluoroacetic acid
THF	Tetrahydrofuran
TLC	Thin layer chromatography
US	Ultra sound
UV	Ultraviolet

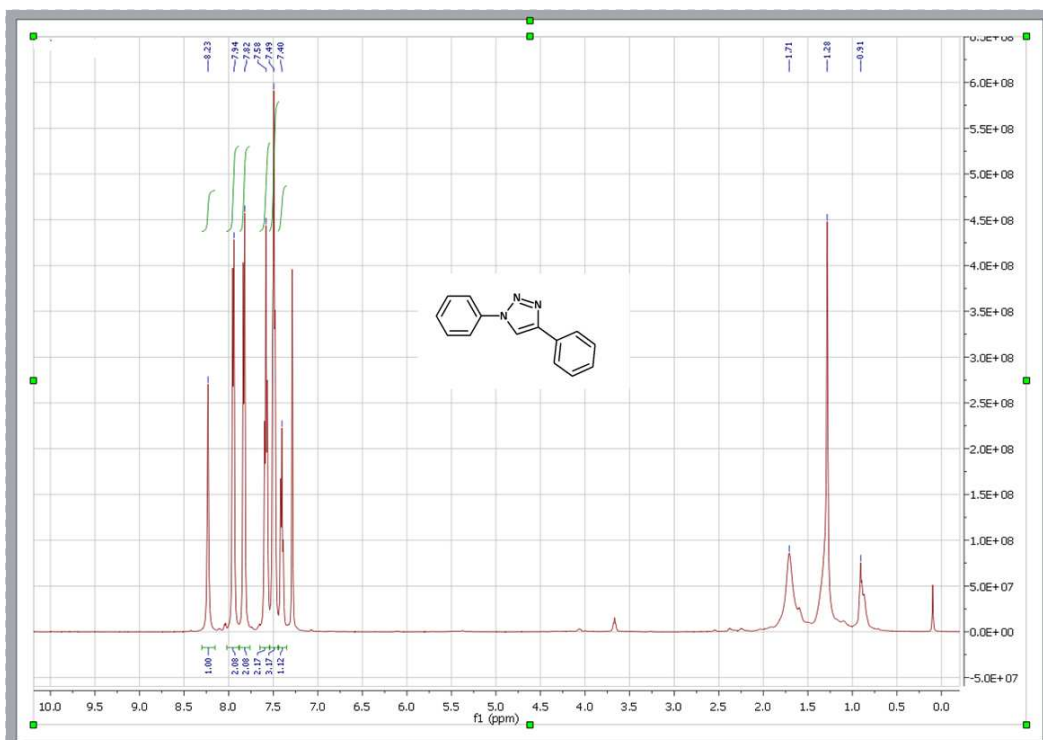




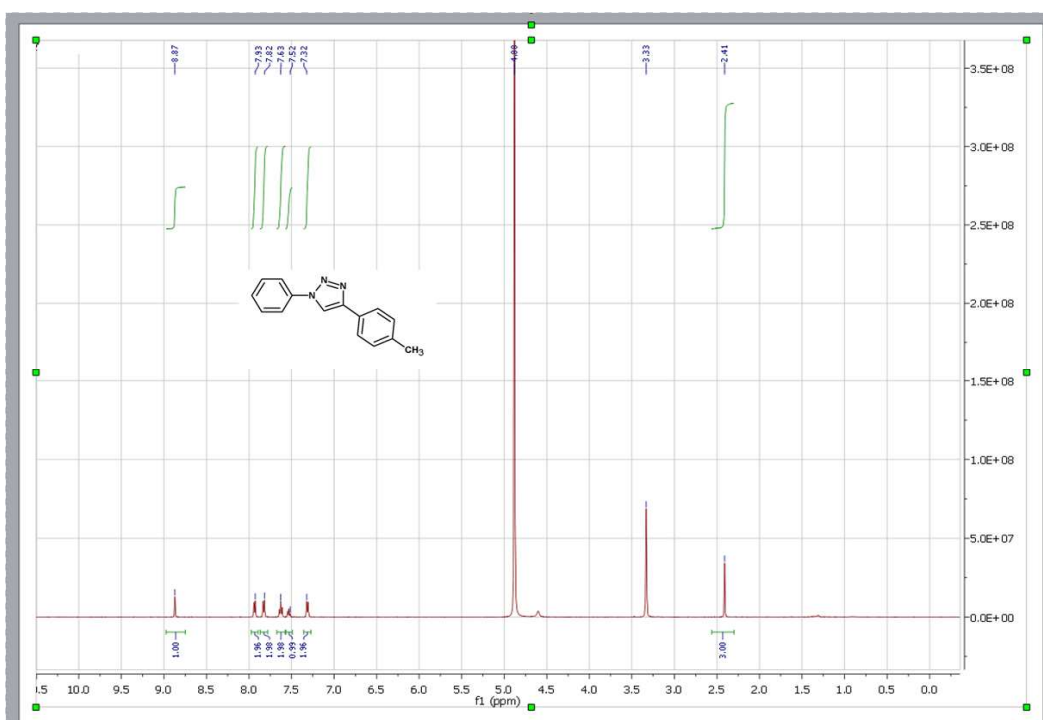
## **Selected $^1\text{H}$ NMR spectra**



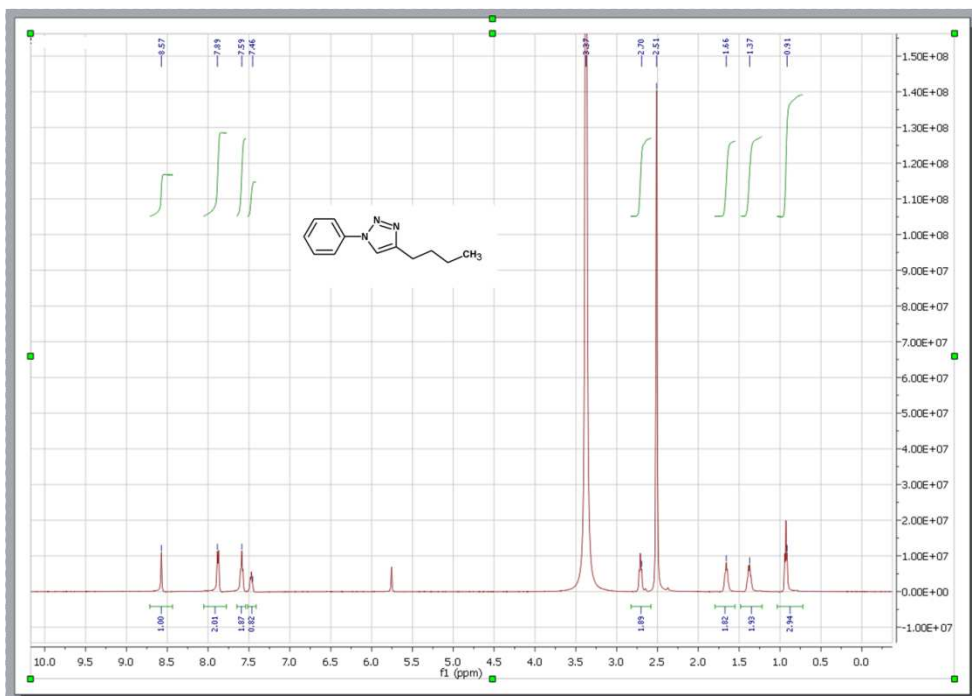
### 1, 4-Diphenyl-1H-1,2,3-triazole (4.1)



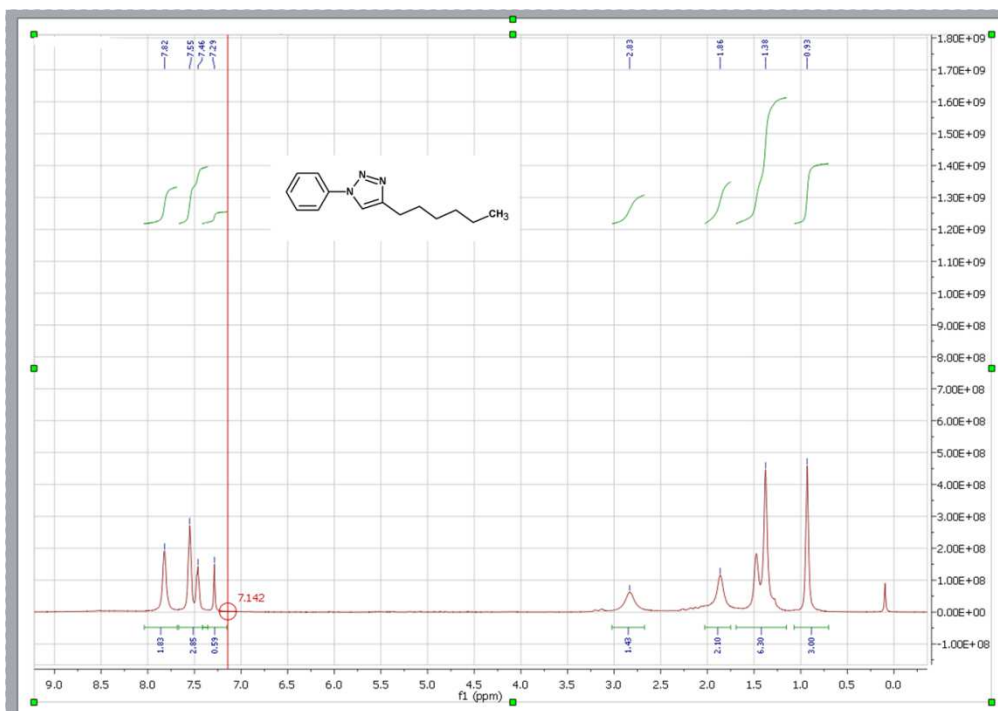
### 4-Phenyl-1-p-tolyl-1H-1,2,3-triazole (4.2)



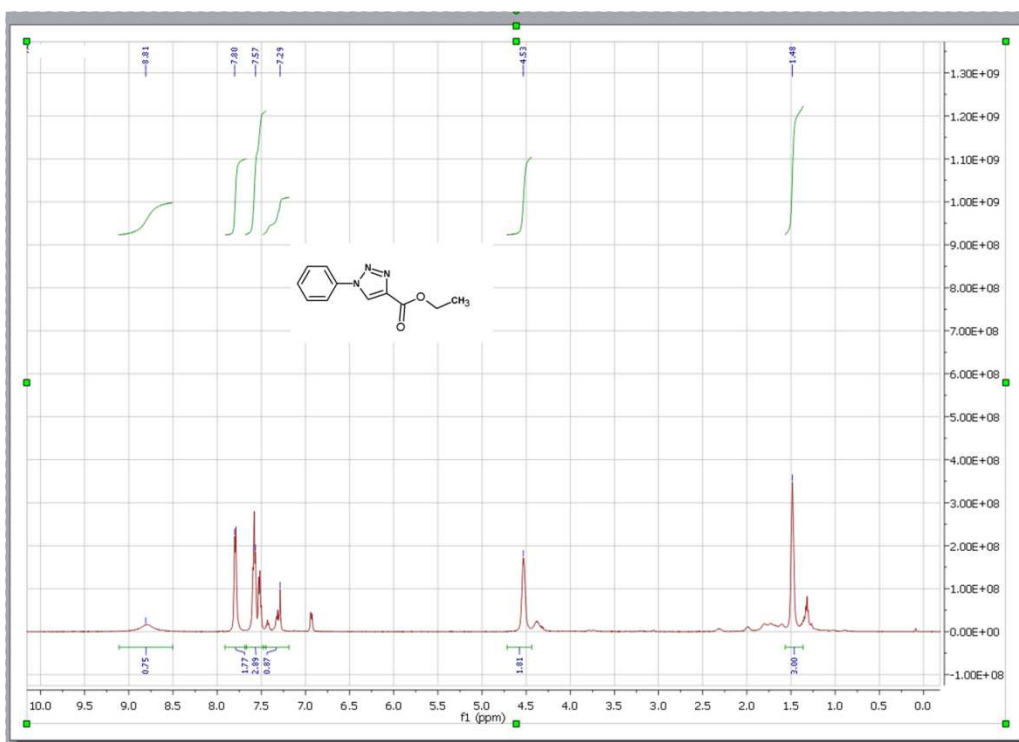
### 3 - 1-Phenyl-4-butyl-1,2,3-triazole (4.3)



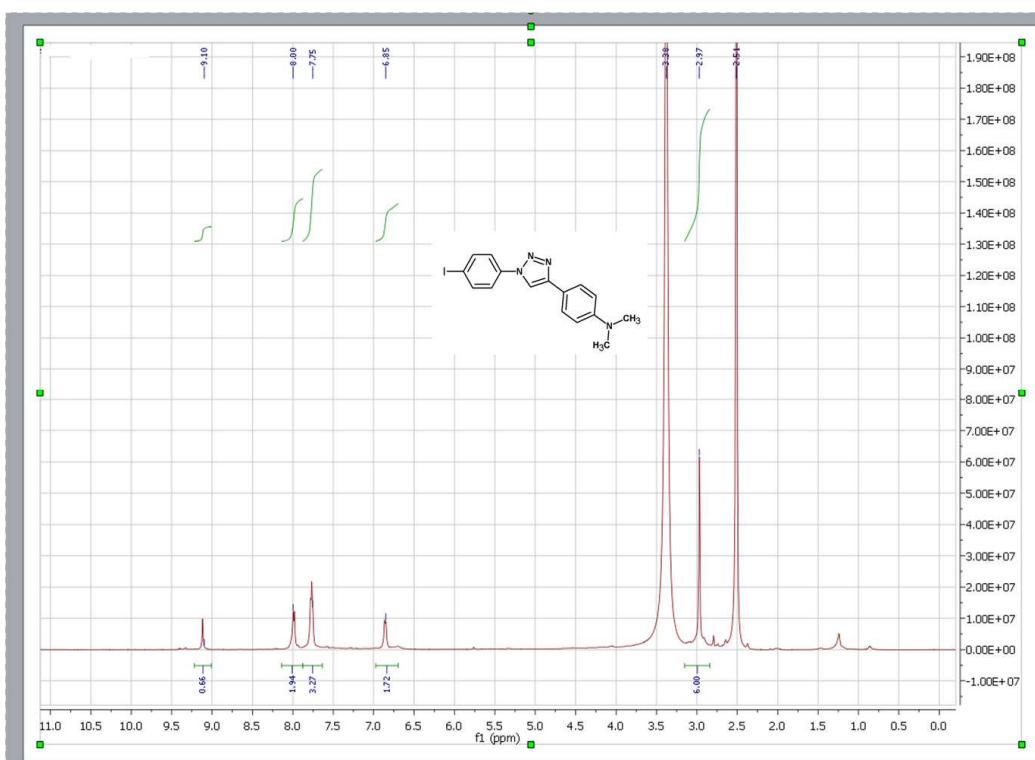
### 1-Phenyl-4-hexyl-1,2,3-triazole (4.4)



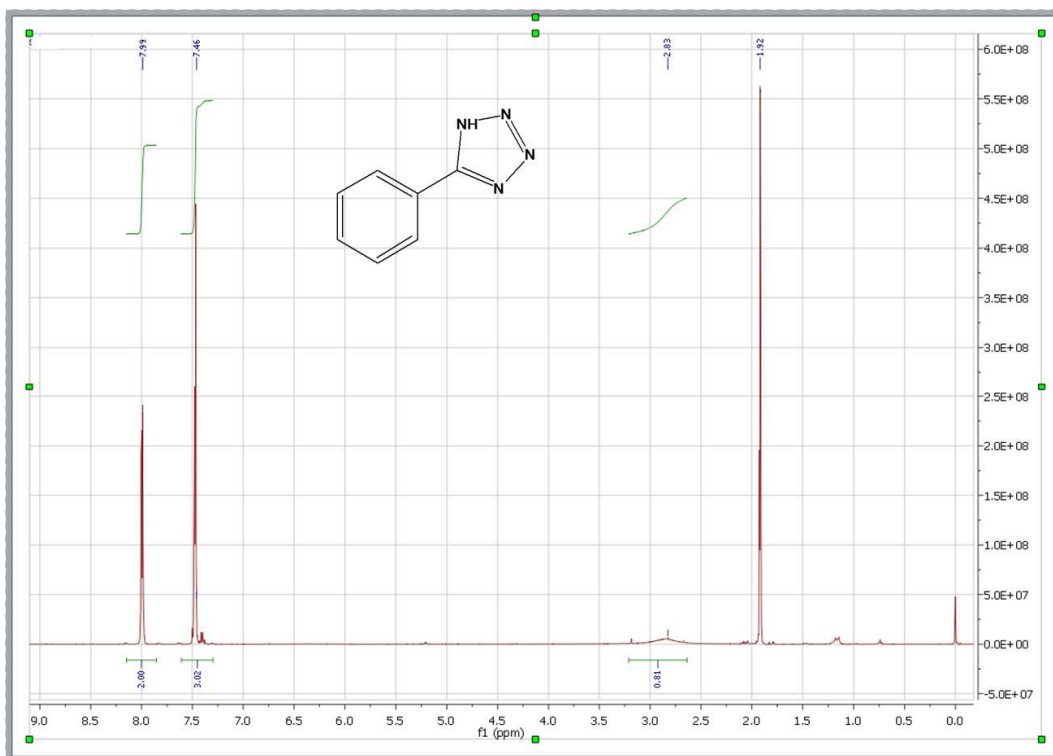
### 5 - Ethyl 1-phenyl-1,2,3-triazole-4-carboxylate (4.5)



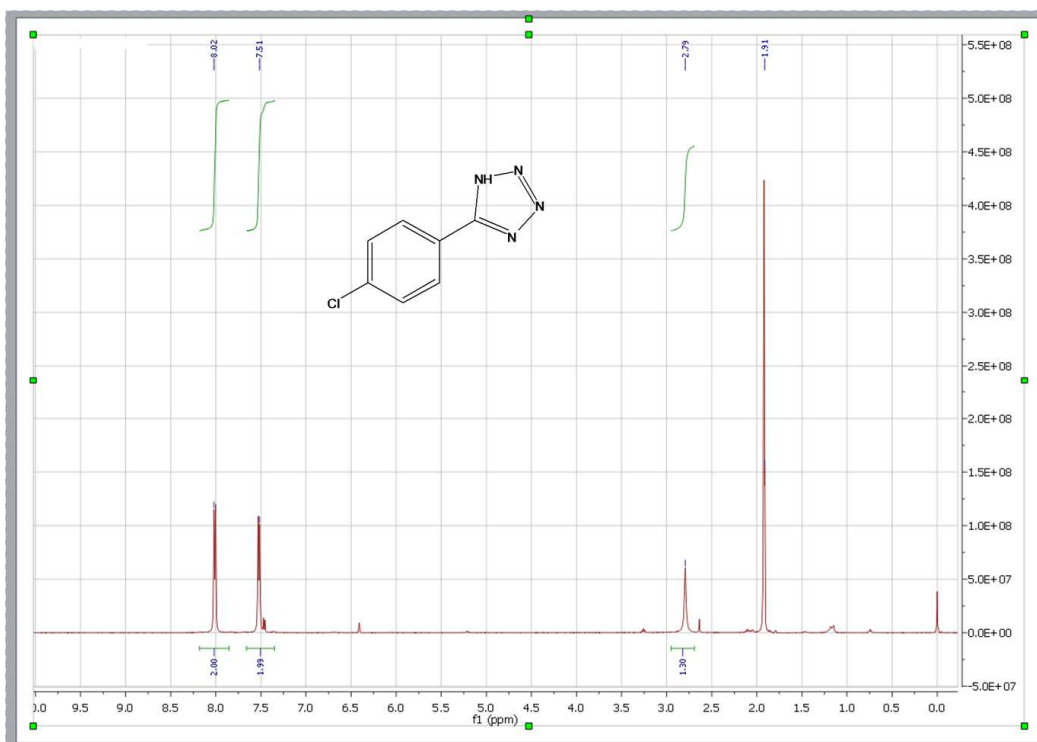
### 4-[1-(4-iodophenyl)-1H-1,2,3-triazol-4-yl]-N,N-dimethylaniline (4.6)



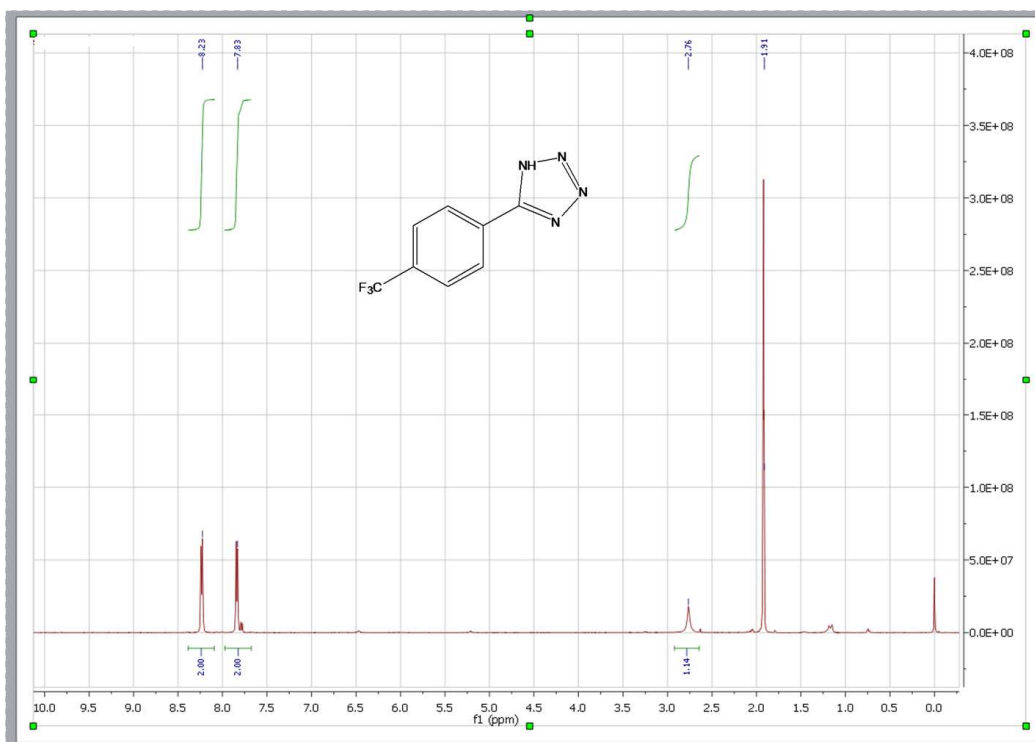
### 5-Phenyl-1H-tetrazole (5.1)



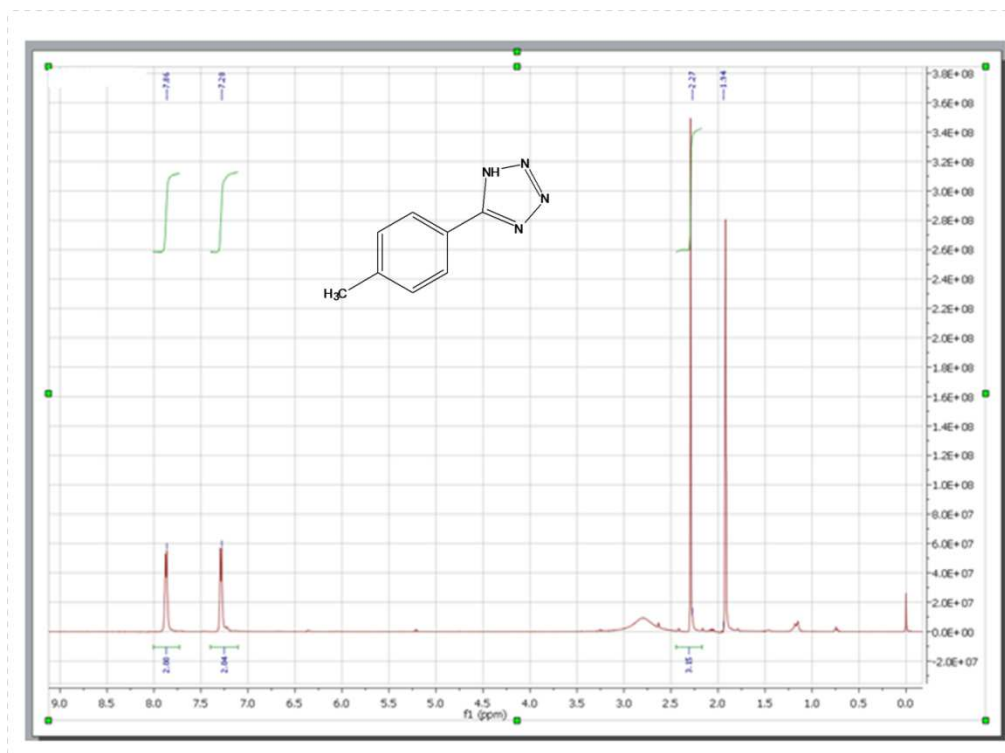
### 5-(4'-Chlorophenyl) -1H-tetrazole (5.2)



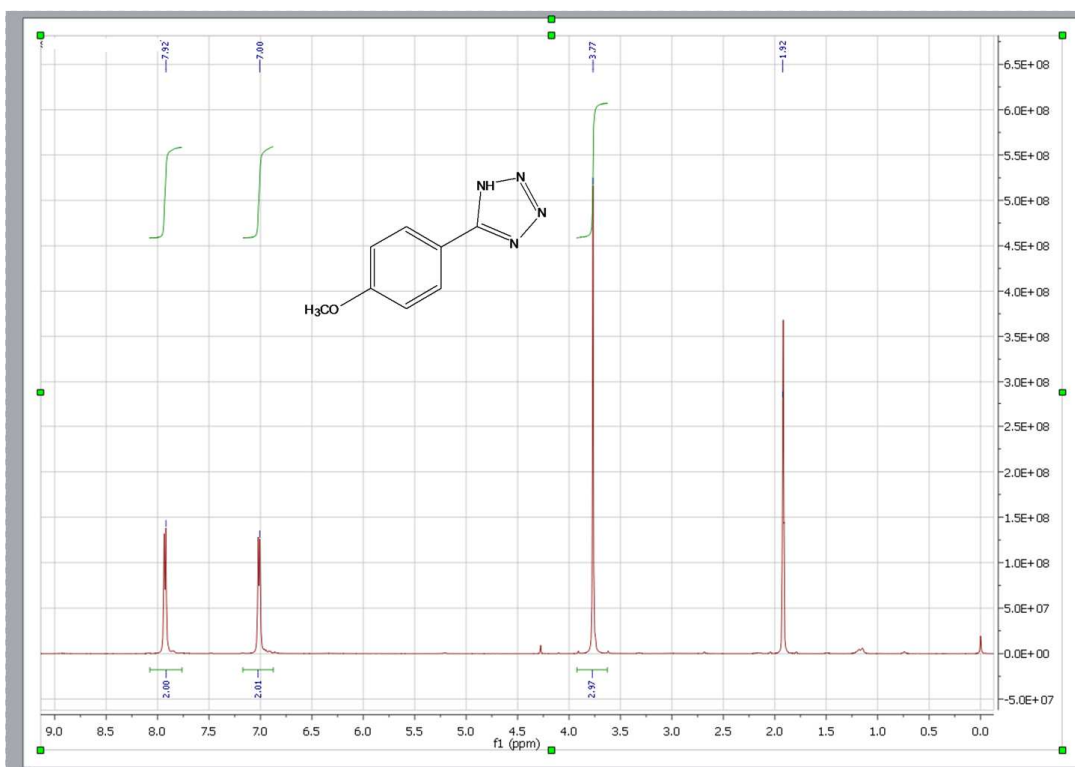
### 5-(4'-(Trifluoromethyl)phenyl)-1H-tetrazole (5.3)



### 5-(4'-Tolyl)-1H-tetrazole (5.4)



### 5-(4'-Methoxyphenyl)-1H-tetrazole (5.5)



### 5-((4'-Chlorophenyl)methyl)-1H-tetrazole (5.6)

